

Recycling Fibres Recovered from Composite Materials using a Fluidised Bed Process

by
Jonathan Kennerley
BSc

Thesis submitted to the University of Nottingham
for the degree of Doctor of Philosophy, May 1998.

Table of Contents

ABSTRACT.

ACKNOWLEDGEMENTS.

GLOSSARY.

NOMENCLATURE.

1 INTRODUCTION.

1.0 Introduction	1
1.1 The composites market.	1
1.2 Thermoset composites in automotive applications.	2
1.3 Thermoset composites recycling.	4
1.4 Thermoset composite recycling at the University of Nottingham.	6
1.5 Theme of this work.	7

2 LITERATURE SURVEY.

2.0 Introduction.	9
2.1 Reuse of thermoset composite recycle.	9
2.1.1 Reuse of reground composite materials.	9
2.1.2 Reuse of material recovered during thermal processing.	12
2.1.3 Economics of recycling thermoset composites.	12
2.1.4 Discussion.	12
2.2 The properties of glass fibres.	13
2.2.1 Composition.	13
2.2.2 Structure.	13
2.2.3 The strength of glass.	14
2.2.4 The Young's modulus of glass fibres.	17
2.3 The effect of heat on the mechanical properties of glass fibres.	17
2.3.1 Fibre strength.	17
2.3.2 Fibre modulus.	23
2.4 Enhancement of glass fibre reinforcement potential.	23
2.4.1 Reduction of flaw severity.	23

2.4.2 Alignment of fibres.	24
2.4.3 Sizing.	24
2.5 Carbon fibre manufacture and properties.	24
2.5.1 Manufacture.	24
2.5.2 Properties.	25
2.5.3 Effect of heat.	26
2.6 Conclusions.	26

3 HEAT CLEANED GLASS CLOTH AS COMPOSITE REINFORCEMENT.

3.0 Introduction.	27
3.1 Experimental details	27
3.1.1 Preform preparation.	27
3.1.2 Moulding details.	28
3.1.3 Testing.	29
3.2 Results and discussion.	29
3.2.1 Laminate tensile strength.	30
3.2.2 Laminate flexural strength.	36
3.2.3 Laminate tensile modulus.	37
3.2.4 Laminate flexural modulus.	37
3.2.5 Laminate strain at failure.	41
3.3 Conclusions.	41

4 RECOVERED FIBRE CHARACTERISATION.

4.0 Introduction.	43
4.1 Fluidised bed processing rig.	43
4.2 Feed materials.	45
4.3 The strength of recovered fibres.	46
4.3.1 The Weibull distribution.	47
4.3.2 Experimental method.	47
4.3.3 Reproducibility.	48
4.3.4 Effect of processing conditions on recovered fibre strength.	50
4.3.5 Comparison of rotating screen and cyclone collection systems.	52
4.3.6 The strength of fibres recovered from FW pipe.	54
4.3.7 The strength of recovered carbon fibres.	55

6.2.2 Discussion.	93
6.3 Veil wet strength.	94
6.3.1 Method.	95
6.3.2 Results.	95
6.3.3 Discussion.	97
6.4 Veil strength.	98
6.4.1 Method.	99
6.4.2 Results.	100
6.4.3 Discussion.	102
6.5 Veil permeability.	102
6.5.1 Method.	102
6.5.2 Results.	105
6.5.3 Discussion.	106
6.6 Veil as corrosion inhibitor.	106
6.7 Conclusions.	107

7 USE OF RECOVERED FIBRES IN A DOUGH MOULDING COMPOUND.

7.0 Introduction.	108
7.1 Dough moulding compounds.	108
7.2 Laboratory trial.	108
7.2.1 Preparation of the recovered fibre.	108
7.2.2 DMC processing.	109
7.2.3 DMC testing.	111
7.2.4 Discussion.	115
7.3 Pilot plant trial.	116
7.3.1 Method.	116
7.3.2 Results.	116
7.3.3 Discussion.	118
7.4 Conclusions.	119

8 CONCLUSIONS AND FURTHER WORK.

8.0 Introduction.	120
8.1 Conclusions.	120
8.1.1 Heat treated glass cloth as reinforcement in a thermoset composite.	120

8.1.2 Properties of recycled glass fibres.	121
8.1.3 Reinforcement potential of recycled glass fibres.	121
8.1.4 Use of recycled glass fibres in a veil material.	122
8.1.5 Use of recycled glass fibres in a dough moulding compound.	123
8.2 Original aspects of this investigation.	123
8.3 Further work.	124
8.3.1 Properties of recycled glass fibres.	124
8.3.2 Reinforcement potential of recycled glass fibres.	124
8.3.3 Use of recycled glass fibres in a veil material.	124
8.3.4 Use of recycled glass fibres in a dough moulding compound.	125
8.3.5 Properties of recycled carbon fibres.	125
REFERENCES.	126
APPENDICES.	136

Abstract

This work is concerned with the characterisation and reuse of fibres recovered from end of life thermoset composites by fluidised bed thermal processing. Emphasis is placed on the properties of recovered glass fibres and their reuse in a dough moulding compound and a tissue product.

The need for a recycling process is demonstrated by a survey of the market for thermoset composites with particular consideration given to the potential growth in automotive applications. A study of processes developed to recycle such materials and the effect on the structural properties of composites containing such recyclate shows that a process capable of generating recyclate of greater value is required, particularly for the case of contaminated materials. A review of investigations into the effect of prior heat treatment on the mechanical properties of glass fibres shows that their strength will be reduced by a deterioration of the fibre surface during fluidised bed thermal recovery but that their stiffness is likely to be unaffected. The implications of these effects on possible applications for the recovered fibres are described.

Tests are reported on the structural properties of laminates containing heat treated glass cloth which show that there is a strength reduction which is both time and temperature dependent but that modulus is not significantly affected. Strength loss increases with up to 20 minutes heating but then remains constant. In some cases the strength loss can be reduced by resizing the cloth.

Measurement of the properties of fibres recovered using the fluidised bed process shows that the recovered fibre strength decreases with increasing processing temperature. Glass and carbon fibres recovered at 450°C retain approximately 50% and 80% of their virgin strengths respectively. The Young's modulus of the recovered fibres is shown to be largely unaffected by the process for both glass and carbon fibres. Investigation of the lengths of the recovered glass fibres by image analysis techniques suggests that their distribution depends on the structure of the composite and the method of size reduction. A weighted mean fibre length of 3.5 mm to 5.5 mm is possible with the apparatus described in this

thesis. The reduced reinforcement potential of the recovered fibres is confirmed by experiment.

Recovered glass fibres are used to displace virgin fibres in a dough moulding compound. At replacement levels of up to 50% there is no significant effect on the mechanical properties of a compression moulded plate. Above this level, tensile, flexural and impact strengths are reduced and with complete replacement the reduction is by approximately 40%, 50% and 70% respectively. These results are confirmed on a pilot plant scale.

Recovered glass fibres can be successfully incorporated with virgin fibres into a veil. Replacement of virgin fibres reduces both wet and dry strength because the recovered fibres are both shorter and weaker. The permeability of the veil is found to depend on its porosity and not its recovered fibre content. The experimental veils can be used to protect and improve the surfaces of mouldings.

Acknowledgements

Thank you:

to Dr SJ Pickering and Professor CD Rudd for their helpful guidance.

to DTI, EPSRC, Alcan Chemicals, DSM Resins, Balmoral Group, BIP Plastics, British Plastics Federation, Cray Valley, Croxton & Garry, Dow Chemical Company, Filon Products, Ford Motor Company (including Jaguar Cars), GKN Technology, Laminated Profiles, Owens-Corning Fiberglas, Permali, Rover Group and Scott Bader for their financial and technical support.

to members of the Department of Mechanical Engineering for their time.

to Neal Fenwick and Richard Kelly, my co-workers on the RRECOM project, who recovered the fibres.

to Hil and Han.

Glossary

ASR	Automotive Shredder Residue.
ASTM	American Society for Testing Materials.
BMC	Bulk Moulding Compound.
BS	British Standard.
Calcining	Modification of a material by high temperature heating.
CCTV	Close Circuit Television.
CF	Carbon Fibre.
CFRM	Continuous Filament Random Mat.
CFRP	Carbon Fibre Reinforced Plastic.
CS	Chopped Strands.
DMC	Dough Moulding Compound.
EDS	Energy Dispersive Spectral.
ELV	End of Life Vehicle.
FBPR	Fluidised Bed Processing Rig.
FW	Filament Wound.
GRP	Glass Reinforced Plastic.
HEC	Hydroxy Ethyl Cellulose.
HLU	Hand Lay Up.
IRC	Interdisciplinary Research Centre.
LVDT	Linear Variable Differential Transformer.
MEKP	Methyl Ethyl Ketone Peroxide.
MSW	Municipal Solid Waste.
OCF	Owens Corning Fiberglas.
PAN	Polyacrylonitrile.
PC	Personal Computer.
PVC	Polyvinyl Chloride.
ROI	Region Of Interest.
RTM	Resin Transfer Moulding.
SAE	Society of Automotive Engineers.
SEM	Scanning Electron Microscope.
SMC	Sheet Moulding Compound.
RRECOM	Recycling and Recovery from Composite Materials.
WCS	Wet Chopped Strands.

Nomenclature

a	Asymptotic proportion of retained strength	.
A	Area	(m ²).
b	Strength loss constant	.
B	Breaking load	(N).
c	Rate of strength loss	(minute ⁻¹).
C	Linear density	(kgm ⁻¹).
D	Cross sectional diameter	(μm).
E	Young's modulus	(GPa).
f _i	Frequency of resonant mode i	(Hz).
f _s	Frictional sliding force	(N).
F	Force per unit width	(Nm ⁻¹).
g	Acceleration due to gravity	(ms ⁻²).
G	Shear modulus	(GPa).
I	Moment of inertia	(m ⁴).
k	Hydrodynamic permeability	(m ⁻²).
k _i	Constant for resonant mode i	(m ⁻¹).
L	Fibre length	(mm).
L _b	Breaking length	(km).
L _c	Critical length	(μm).
L _n	Number average length	(mm).
L _w	Weight average length	(mm).
m	Mass	(g).
N	Number of fibres	.
P	Porosity	.
P(σ)	Weibull probability density function	.
Q	Volumetric flow rate	(mls ⁻¹).
r	Cross sectional radius	(μm).
R	Half interfibre spacing	(mm).
Ra	Average surface roughness	(μm).
S	Areal density	(gm ⁻²).
t	Time	(minutes).

T	Temperature	(°C).
T _g	Glass transition temperature	(°C).
U	Surface energy	(Jm ⁻²).
v/v	Proportion by volume	.
V	Volume fraction	.
V _b	Density bottle volume	(cm ⁻³).
w	Weibull shape parameter	.
w/w	Proportion by weight	.
W	Width	(mm).
x	Interatomic spacing	(nm).
β	Shear-lag length factor	(m ⁻¹).
Δp	Pressure drop	(Pa).
ε	Laminate strength ratio	.
η _l	Fibre length factor	.
η _θ	Fibre orientation factor	.
Λ	Sample length	(mm).
μ	Dynamic fluid viscosity	(cP).
ρ	Density	(kgm ⁻³).
ρ _b	Bulk density	(kgm ⁻³).
σ	(Fibre) Tensile strength	(MPa).
σ _{um}	Matrix stress at fibre failure strain	(MPa).
σ ₀	Weibull scale parameter	(GPa).
τ	Interfacial strength	(MPa).
χ ²	Chi squared value	.

subscripts:

c	composite.
f	fibre.
m	matrix.
i,j	summation terms.

Chapter 1.

Introduction.

1.0 Introduction

Thermoset composites are very useful engineering materials. Amongst their most attractive properties for engineering applications are their high strength and stiffness allied to their low density. For these reasons they are particularly suitable for transport uses where the substitution of composite materials for the traditional engineering metals leads to weight reduction and fuel savings in operation. However, the presence of two or more phases makes recycling more difficult than for monolithic materials.

This chapter will introduce the size of the scrap thermoset composite problem, recycling processes that have already been developed and will outline the work to be presented in this thesis.

1.1 The composites market.

Plastics usage.

The consumption of plastics materials in western European countries has been growing steadily and in 1995 stood at over 28 million tonnes [1]. In the USA, the rate of growth of the plastics market has been averaging 10.3% over the period 1968-98 [2]. World consumption of plastics in 1994 was estimated to be around 130 million tonnes [1].

Most plastics are quickly discarded. Western Europeans were generating approximately 11 million tonnes of plastic waste per year by 1990 [2], 73% of which was arising in municipal solid waste (MSW). In the same year, 13 million tonnes of plastic waste, over half the total consumption, was generated in the USA, of which only 1% was recycled [2]. Meanwhile, the Japanese were discarding 5 million tonnes of plastics, 65% of which was incinerated, 23% landfilled and 5% recycled [2].

Polymer composites usage.

Composites have become an area of assured growth for the plastics industry though they

still represent a small fraction of the total plastics market. Use of reinforced plastics in Europe increased by 100% between the years 1982 and 1988 [3] and the total consumption of thermoset composites in western Europe stood at over 1 million tonnes in 1995 [1], the major applications being transportation, construction and electrical. In 1994, annual reinforced plastics production in the USA was 1.4 million tonnes [4]. These figures represent only 4% of total plastics production in the USA. Of this figure, 11% [5] was SMC and only 2% was high performance prepreg [2], highlighting the move into high volume applications [1].

Glass fibres are the most popular form of reinforcement for composite materials. Estimates of western European glass fibre consumption in 1995 were 481,000 tonnes [1]. This compares with global estimates for the year 1993 of 1.2 million tonnes of glass fibre reinforcement used in the manufacture of 3.5 million tonnes of composite materials [6].

1.2 Thermoset composites in automotive applications.

The material value of a thermoset composite is generally much higher than that of steel or aluminium [7]. However, there are many benefits to be gained from their use in automotive applications: thermoset composite components can be manufactured under temperatures and pressures much lower than those required to form steel which means that less expensive tooling is required [8]; the use of plastics leads to weight savings and opportunities for parts consolidation (Chrysler found that one SMC windshield wiper cowl plenum replaced 11 steel parts welded together in their minivan [9]); replacing the steel bumpers on a car can lead to a saving in weight of 2.7 kg which, in turn, can lead to an estimated fuel saving of 24 litres over a 150,000 km lifetime [10]. Weight savings gained from the use of thermoset composites can also lead to secondary weight savings. For example, a lightweight car can be powered by a small engine and does not require a heavy duty drivetrain or brakes. The General Motors Ultralite concept vehicle is hand made from carbon fibre composites and achieved 100 miles per gallon at 50 miles per hour [11]. For these reasons, the proportion of plastics in cars is growing and in 1994 was estimated to be between 10% [12] and 13% [13].

Approximately 56% of all the composite materials in the average car manufactured in the

USA in 1993 had thermosetting matrices [2] and their use was predicted to double from 110,000 tonnes in 1990 to approximately 200,000 tonnes in 1995 [14], SMC accounting for 46% of this total [2]. However, to date, thermoset composite materials have been restricted to semi-structural applications in low volume vehicles. For example the General Motors Trans Am contains nearly 23 kg of SMC in its hatch and spoiler assemblies [11], but it has been suggested [2] that in the future a composite intensive vehicle could be manufactured in which half the vehicle weight could be non metallic. Despite the benefits there are many immediate barriers to the widespread use of composite materials in vehicles including cost and production worries [15]. Recyclability is seen as a long term barrier to their use [15].

End of life vehicles (ELVs).

When an automobile is no longer required it is sold to a vehicle dismantler [12]. Here, useful components are removed for resale and the remaining hulk is sold to a shredder operator. The car hulk is reduced to fist sized pieces in a hammer mill [12], the metals are then extracted and the remainder, known as automotive shredder residue (ASR) is sent to landfill. The ASR consists of rubber, plastics, glass and other non-metallic materials [12]. It is in this form that any composite materials used in a car arise for recycling.

In the UK approximately 1.3 million vehicles, weighing 1.4 million tonnes in total, are scrapped every year. Of this weight, 0.35 million tonnes, or 25%, is sent to landfill, the remainder is successfully recycled [12]. As the proportion of non-metallic components in cars increases the revenue that the scrap yard can earn from the sale of the recovered metals is reduced and this is compounded by the fact that more ASR has to be disposed of at ever increasing cost.

At the present time a satisfactory process for recycling contaminated composites does not exist and this type of waste is landfilled. However, the number of landfill sites is diminishing worldwide as they reach their capacity (in 1979 there were 18,000 sites in the USA [16] but this had fallen to 5,400 in 1990 and is predicted to fall to around 1235 by 2006 [14]) and it has become socially unacceptable to dispose of scrap in this way. In the UK in 1996, a landfill tax was introduced as a penalty against landfill use and to generate

money to investigate alternative disposal options [17]. Thermoset composites are classed as inactive waste and attract a levy of £2 tonne⁻¹ [17] but in Germany, where landfill is heavily discouraged, the landfill tax rate is about seven times what it is in the UK [18]. The European Commission has also decided to act to limit the amount of waste being disposed of by landfill. It has targeted ASR by adopting a proposal for a council directive on ELVs [19] to decrease the proportion of an ELV going to landfill from the present level of 25 % to 15 % by 2005 and 5 % by 2015.

In addition to government legislation, some companies are bidding for environmental leadership within their markets. Ford Motor Company has set a goal of 25% post consumer content in its recycled plastics and rubbers [5]. With some high glass content composite materials this might be achieved by using recycled A-glass [20] as reinforcement but with a SMC component this goal requires the use of post consumer SMC recyclate. In fact, in 1990 the automobile industry announced to the SMC industry that unless the SMC industry could prove recyclability on a production scale, SMC would no longer be specified for parts [21]. To safeguard the use of thermoset composites in automotive applications a recycling process to deal with end-of-life components is required.

1.3 Thermoset composites recycling.

Several methods of recycling thermoset composite materials have been developed over the period 1978-98. Some of them have been designed to deal with relatively clean factory scrap whilst others have been designed for contaminated or mixed product post consumer scrap. A small number have been investigated as methods of recycling uncured materials.

Size reduction.

Thermoset composite components can be reduced in size by careful grinding [14] to produce different grades of recyclate ranging from filler grades to high aspect ratio reinforcing grades. One such processor operating successfully in Germany is Ercom [21]. A mobile shredder reduces the volume of the scrap at source and transports it back to the recycling plant. Here it is circulated through a series of metal separation, hammer milling, drying and air separation stages until the desired particle shape and size is produced. A

range of products including fibrous and filler grades are produced. The Ercom plant in Germany has a 6000 tonnes year⁻¹ capacity and in 1994 was processing approximately 2000 tonnes year⁻¹ [21]. A similar operation in Canada, Phoenix [22], ceased trading in April 1996.

As part of the RRECOM [23] project, researchers at Brunel University developed a novel compounding technology based on twin screw extrusion for the integration of recycle size reduction, treatment and recombination with thermoplastic and thermosetting polymers [24].

Size reduction processes are best suited to relatively pure industrial scrap. Ercom requires their waste feed to be guaranteed free of impurity by the moulder [21] and this allows them to produce a well characterised and carefully controlled product.

Thermal processing.

In a process known as pyrolysis, thermoset composites are heated in the absence of oxygen. This causes the organic polymer matrix to break down into shorter chain hydrocarbons. In this way, the composite material can be converted into three products: a gas, a liquid and a solid residue [11, 14]. Decomposition starts at around 300°C [14] but pyrolysis plants more commonly operate in the range 750°C to 1000°C [14] and the exact proportions of the three products varies with processing temperature. The gas product has a heat content similar to that of natural gas [25], burns cleanly and can be used to sustain the process [11, 14]. The liquid product is similar to heavy crude oil and can be used as a hydrocarbon feed stock [14]. The solid residue consists of the inorganic part of the feed material. By careful control of the pyrolysis temperature useful fibres can be recovered and 500°C has been found to be the upper limit for the recovery of useful, clean carbon fibres [26].

Scrap printed circuit boards are a valuable source of copper and often contain approximately 50% by weight of glass fibre in an epoxy matrix. A process [27] has been developed in which printed circuit boards, from which the copper has been recovered, are calcined at approximately 500°C to remove the organic content leaving useful glass fibres

as an end product.

Two other thermal treatments which have been investigated as means of recovering value from thermoset composites are reverse gasification [4] and catalytic conversion at approximately 60°C [28]. Both these processes convert the scrap composites to clean fibres and fuel gases at relatively low temperatures. Thermal processes can be more tolerant of contamination than size reduction processes.

Other methods.

Scrap thermoset composite materials can be disposed of in a cement kiln [29] where the polymer is burnt and is a source of process heat and the inorganic parts become part of the cement product. Highly filled composites containing large quantities of calcium carbonate can be burnt in coal fired boilers [29, 30] where the energy content of the polymer is used and the calcium carbonate can lessen sulphur dioxide emissions.

Solvent separation methods have been investigated for uncured SMC scrap [31] and useful fibres have been recovered using this technique.

1.4 Thermoset composite recycling at the University of Nottingham.

Since the 1960s there has been a research group at the University of Nottingham investigating the processing of thermoset composites. One particular aim has been to speed up the manufacturing cycle time so that thermoset composite components would be attractive to motor manufacturers for high volume models (greater than 100,000 units per year) [32-36]. For around ten years, the problem of what to do with end of life composite parts has also been investigated with a view to securing their future use in automotive applications.

Among the processes investigated for recycling thermoset composites were disposal in a cement kiln [29], incineration followed by use as an agricultural liming agent [37] and combustion with coal to restrict sulphur dioxide pollution [30].

All of the preceding three disposal routes can be used to deal with waste materials.

However, the heat energy in a thermoset composite is not the main source of value and the reuse of the filler in any application can only be the source of limited income to the recycler because filler materials are inherently cheap. The majority of the value in a scrap thermoset composites lies in the reinforcement and any process capable of reclaiming it stands a better chance of economic viability.

1.5 Theme of this work.

Investigation of the sulphur absorbing properties of scrap composites was carried out using a fluidised bed based boiler at the University's Sutton Bonnington site [30]. During these investigations the scrap composite was burnt in the fluidised bed and the heat energy recovered. However, once the polymer had been degraded the glass fibres were liberated and carried out in the fluidising gas stream. A recovery process based on fluidised bed combustion would be able to recover the heat energy of the organic components of ASR and the more valuable reinforcing fibres from any thermoset composite present. Following on from these trials, a pilot scale fluidised bed combustion rig was designed and built in the Department of Mechanical Engineering at the University of Nottingham. Fibres have been successfully recovered from scrap thermoset composites using this rig.

It has been shown that the present market size, and hence the waste disposal problem, for thermoset composites is small compared to that for plastics in general. However, it has also been demonstrated that thermoset composites are attractive engineering materials with the potential to be used in large quantities in the future. The example of the automotive industry has been used to illustrate the form in which scrap composite materials might arise, ie as contaminated, mixed waste. Such material is landfilled at the present time but factors which will limit this option have been presented.

This thesis is concerned with the characterization, enhancement and reuse of the fibrous reinforcement recovered from scrap thermoset composites by the fluidised bed process. Several types of thermoset composites have been processed in the fluidised bed rig and both glass and carbon fibres recovered from these materials have been studied. Characterization of the recovered fibres will include the effect of processing on the strength, stiffness and length of recovered fibres. These properties will determine the

likely effectiveness of the recovered fibres when they are recompounded into a thermoset composite and hence their value.

Recovered fibres are likely to have undergone some physical damage. Chemical strengthening of the recovered fibres will be investigated.

Investigations into the effect of using heat cleaned glass cloth as reinforcement in a thermoset composite were carried out before recovered material became available and the results of this work will be included.

The ultimate aim has been to find a reuse for the recovered fibres. A veil or tissue product is one application for glass fibres in which they are used in monofilament form. Glass fibre veil commonly consists of a random web of discontinuous E or C glass fibres held together by a binding resin. The areal density of the veil is usually between 50 gm^{-2} and 150 gm^{-2} and the binder accounts for typically 20% of the mass of the veil. Glass veil is used as a backing material to improve the dimensional stability of wall and floor coverings and roof shingles and in glass reinforced plastic (GRP) manufacture to improve surface appearance and to improve the chemical resistance of the surface [38]. The reuse of recovered glass fibres in a veil will be investigated.

Dough moulding compounds are made at high volumes on Z-blade mixers which require very little labour and hence they are relatively low cost materials [39]. Their low fibre contents make them ideal for small, thick section components where strength is not critical [39] and they can be processed by compression, transfer and injection moulding techniques [40] which makes them very versatile engineering materials. The opportunities for replacing virgin glass by recovered glass fibres will be studied.

The thesis will conclude with a summary and suggestions for further work.

Chapter 2.

Literature Survey.

2.0 Introduction.

The first aim of this literature survey is to review the use of recyclate in thermoset composites and its effect on composite properties. This will indicate the minimum performance that the fluidised bed recyclate must achieve. The second part will review the properties of reinforcing fibres and the likely effect on glass fibre properties of processing at high temperatures in a fluidised bed. This review will concentrate mainly on glass fibres since they are the most common form of reinforcement used in composites.

2.1 Reuse of thermoset composite recyclate.

Investigations into several processes by which valuable materials might be recovered from scrap thermoset composites have been described in Chapter 1. The aim of these recycling processes should be to produce recyclate that can be used in parts comparable in quality to those being recycled [21]. This is known as primary recycling. Schaeffer [21] has calculated that a recyclate content of 25% in an SMC formulation is required in order for the process to be sustainable.

2.1.1 Reuse of reground composite materials.

The effects of replacing the fibre and filler in thermoset composites with various grades of regrind have been investigated by several researchers. Grinding scrap thermoset composites leads to a loss of fibre length, polymer degradation and disruption of the interface [41]. Consequently there is often a reduction in properties when they are used in a composite. Figures 2.1 and 2.2 show the results of experiments [42-44] into the effect of replacing calcium carbonate filler with ground SMC and BMC on the properties of SMC and BMC mouldings. It can be seen that regardless of the grade of recyclate used, a decrease in both flexural strength and modulus is observed as the replacement level increases. Similar effects are seen with other properties.

Figure 2.1 Effect of replacing calcium carbonate filler by ground SMC and BMC on the flexural strengths of SMC and BMC mouldings. (See Table 2.1). Filled symbols represent use in SMC, open symbols represent use in BMC.

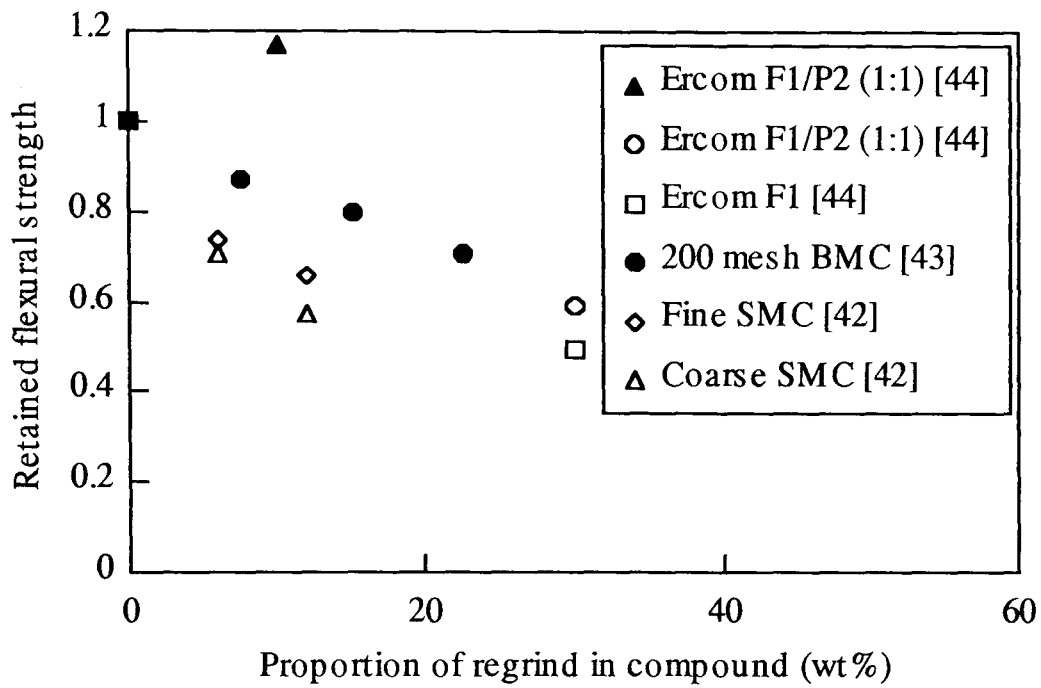


Figure 2.2 Effect of replacing calcium carbonate filler by ground SMC and BMC on the flexural moduli of SMC and BMC mouldings. (See Table 2.1). Filled symbols represent use in SMC, open symbols represent use in BMC.

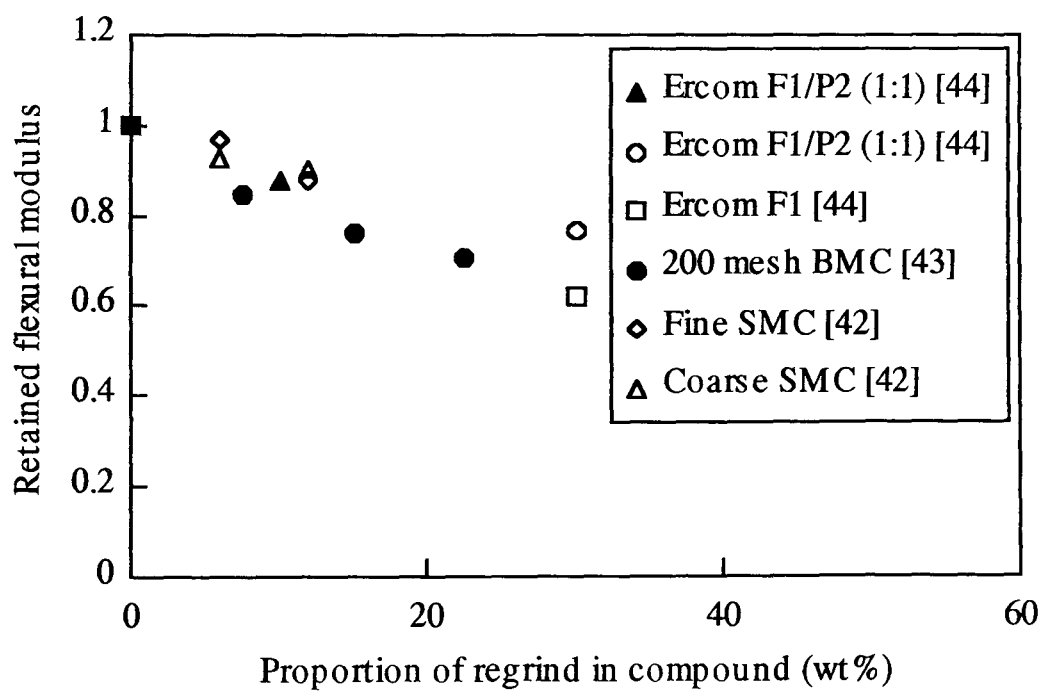


Table 2.1 Notes on Figures 2.2 and 2.3.

Identification	Description
F1	Ercom fibrous SMC fraction up to 500 μm in length.
P2	Ercom powdered SMC fraction size 200 μm to 1 mm.
200 mesh BMC	mean particle size 30 μm .
Fine SMC	45% less than 200 μm .
Coarse SMC	24% less than 200 μm .

Similarly, a DMC moulding in which all the 6.4 mm chopped strand fibre and calcium carbonate filler was replaced by ground SMC (45% < 200 μm) [43] had tensile strength reduced by 10%, tensile modulus by 40% and notched impact strength by 70%. A coarser grade (24% < 200 μm) gave a lower tensile strength (40% reduction), similar modulus but an improved impact strength (only 50% reduction). With a 10% addition of ground SMC, such as might be obtained if 50% of the calcium carbonate filler of a typical DMC were replaced, a surface finish visually indistinguishable from a control sample can be achieved [42, 44, 45].

One advantage of the use of regrind in SMC and BMC is that there is often a reduction in material density [22, 44].

The regrinding technologies, and Ercom in particular, have led the way in getting thermoset composite recyclate reused in production materials. SMC containing regrind has been used to manufacture an Audi spare wheel well, a BMW sun roof frame [21] and several other items on a production scale. However, there are still some problems to be overcome in the use of the longer, fibrous recyclate fraction including wet out and distribution in an SMC [46]. One use of this fibrous fraction is in RTM where Priest [47] found that up to 10% of the virgin glass fibre in a preform could be replaced with little effect on the properties of subsequent mouldings.

The use of ground material in concrete mortar, gypsum [45], asphalt and insulation boards [14] has also been investigated and found to be promising.

2.1.2 Reuse of material recovered during thermal processing.

Woven glass fibre patches recovered from printed circuit boards by a calcining process operating at between 450°C and 550°C [27] were laminated with a polyester resin to give a fibre weight fraction of 15% [27]. Tensile and flexural strengths of the experimental moulding were comparable to one containing virgin fibres of approximately half the length of the recovered fibres. When the recovered fibres were compounded with polypropylene at 20% w/w, the resulting material had a strength approximately half that of a virgin fibre control specimen. The recovered fibres were found to give reinforcement comparable to that of virgin glass fibres when compounded with a nylon matrix [27]. These results are encouraging since the fluidised bed can also recover fibres within this range of temperatures.

Solid residue from the pyrolysis of scrap SMC mouldings was ground into a filler material (size approximately 10 μm) and used at a level of 30% w/w in an SMC formulation [14]. No effect on mechanical properties, processing or final moulding surface was observed. There was a slight rise in the viscosity of the moulding compound. It can be concluded that the solid residue was not suitable for reuse before grinding. Any fibres would have been destroyed during the size reduction stage.

2.1.3 Economics of recycling thermoset composites.

Curcuras [14] calculated the cost of producing filler by grinding scrap SMC. A cost of \$0.03 per lb was calculated assuming no transport or collection costs, ie that the recycling was performed at the moulding facility. This figure is competitive with other filler materials eg calcium carbonate filler at \$0.04 per lb [48]. The cost of pyrolysing SMC was also calculated [14]. Profit or loss was found to be very dependent on the resale price of the pyrolysis solid residue. The range investigated was \$0.06 per lb (loss) to \$0.11 per lb (profit). For pyrolysis to be economical, the reinforcement potential of the solid residue must be improved so that it can command a higher price.

2.1.4 Discussion.

It has been shown that size reduction processes exist for recycling uncontaminated thermoset composites. However, the recyclate does not perform as well as calcium

carbonate in a composite and can only be produced at about the same price. For contaminated composites where size reduction is unsuitable a different process is required and for it to be economically viable it should concentrate on recovering the valuable reinforcement from the composite. The fluidised bed process can do this but the quality of the recovered fibres will be of prime concern. The next part of the literature review will focus on the likely effect of fluidised bed processing on the reinforcing fibres.

2.2 The properties of glass fibres.

2.2.1 Composition.

The properties of a glass depend on its composition. Four common glass compositions are given in Table 2.2 [49].

Table 2.2 The compositions of four common glasses.

	SiO ₂	Al ₂ O ₃	Fe ₂ O ₃	CaO	MgO	Na ₂ O	K ₂ O	B ₂ O ₃	BaO	Other
A	72.0	0.6	0	10.0	2.5	14.2	0	0	0	0.7
C	64.6	4.1	0	13.2	3.3	7.7	1.7	4.7	0.9	0
E	54.3	15.2	0	17.2	4.7	0.6	0	8.0	0	0
S	64.2	24.8	0.21	0.01	10.27	0.27	0	0.01	0.2	0

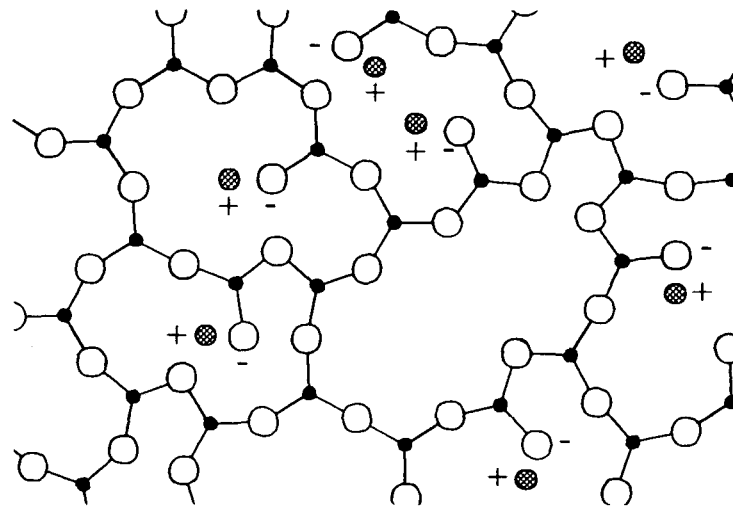
Each of these compositions was developed to provide certain desired properties. A-glass is resistant to alkali environments; C-glass has extremely good chemical resistance; E-glass was originally developed to be a good electrical insulator and S-glass has a high tensile strength [50]. E-glass has become the composition most commonly used for reinforcing thermoset composites because it has good all round physical properties and is easy to draw into fibres and so can be manufactured cheaply.

2.2.2 Structure.

One way to visualize the structure of a silicate glass is as an irregular three dimensional network of silicon atoms linked together by oxygen atoms [51]. Strong covalent bonds exist between the silicon and the oxygen atoms. Some of the oxygen atoms present in the glass do not form links between silicon atoms but are attached only to one silicon atom

(Figure 2.3). These non bridging oxygen atoms act as centres of unbalanced negative charge and will form an ionic bond with the metal cations, such as Ca^{2+} , K^+ etc., that are present. Ion location in the glass structure affects the physical properties of the glass.

Figure 2.3 A two dimensional representation of the three dimensional structure of a silicate glass [60]. \circ oxygen, \bullet silicon, \odot metal cation.



The glass surface.

The surface of a glass fibre is very important since it will be shown that it is at the surface where the strength controlling features of the fibre are situated and it is also where the interface between the organic resin and the inorganic glass is formed in a composite material. This interface is vital to the properties of the composite material. When the molten glass fibres cool the silicon-oxygen bonds on the glass surface are highly strained and so are susceptible to attack. Molecules of water in the size spray or in the atmosphere break the silicon-oxygen bonds and react to form surface silanol groups [52] and a layer of adsorbed water molecules is built up on the glass surface.

2.2.3 The strength of glass.

Theory.

An approximate value for the theoretical strength of a material can be calculated by relating the strain energy in a stressed sample to the energy of the two new surfaces created when it breaks [7].

$$\sigma \approx \sqrt{\frac{U E}{x}} \quad 2.1$$

where strength (σ), surface energy (U), Young's modulus (E) and interatomic spacing (x) are known. The theoretical strength varies for different materials but in every case it is much higher than the strength commonly measured in experiments.

In the 1920s, Griffith conducted a series of experiments to investigate this discrepancy [53]. He chose glass as a model material because its surface energy is quite easily measured and it breaks by simple brittle failure. The theoretical strength of his glass samples was calculated to be over 10 GPa. Griffith tested a series of glass rods and found that the measured strength increased as the rod diameter decreased. Extrapolation of his results to zero rod diameter gave a figure close to his calculated theoretical strength.

Griffith then applied the idea of stress concentration by cracks to explain his glass fibre strength measurements. For example, a crack of two microns depth and 1 Å tip radius magnifies the stress in the body of the material by just over 200 times in the molecules adjacent to the crack tip [7] and so would reduce the strength of a piece of glass from 10 GPa to 50 MPa ie from theoretical strength levels to commonly measured levels. Such a crack would not be visible with an optical microscope and would be very difficult to see with a scanning electron microscope (SEM).

Observations.

Many investigators also found that fibre strength was related to fibre diameter. Otto [54] investigated this phenomena but by careful control of all the processing conditions during the manufacture of his glass fibres was able to show that "when fibres of different diameter are formed under controlled, nearly identical conditions, the breaking strengths are identical within the experimental limits and there is no effect of diameter as such". Thomas [55] in 1960 also showed that fibre strength was independent of fibre diameter for carefully made fibres.

Bartenev and Izmailova [56] obtained glass fibres with surfaces free from microcracks.

These fibres had a strength of approximately 3 GPa, which was independent of fibre diameter and gauge length (up to 100 mm), and the scatter of the strength test results was very low. When a surface layer of 50 Å depth was removed by etching with hydrofluoric acid, the strength was found to be reduced. This result was used as evidence for a tempered surface layer which is responsible for the high strength in defect free glass fibres.

Three strength levels were described for industrially produced glass fibres. A high strength of around 3 GPa was measured in defect free glass fibres and over short (2 mm to 3 mm) lengths of industrial fibres. A lower strength of below 1 GPa was measured in defective fibres. If a thin layer of glass was etched from the high strength fibres the strength was reduced to around 2 GPa. If a layer was etched from the surface of a defective fibre the strength was increased to this same figure. A greater depth had to be removed from the weak fibres to increase their strengths than had to be removed from the strong fibres to reduce their strengths. For a weak fibre, more material had to be removed to erase all traces of cracks. Bartenev and Izmailova proposed that 2 GPa was the stable strength of the inner region of the glass fibre and that this strength is determined by the structure of the original glass and depends primarily on its chemical composition. This work provided proof that the strength controlling defects in a glass fibre are on the fibre surface.

Metcalf and Schmitz [57] investigated the effect of test gauge length on the measured strengths of glass fibres. They attempted to use the Weibull statistical theory of failure based on randomly distributed flaws of random severity [58] to describe the distribution of flaws on the surface of glass fibres. Testing both E and S-glass fibres over a range of gauge lengths from 0.25 mm to 300 mm they discovered that two types of flaw were present in the virgin glass fibres. One type was described as severe with wide spacing and governed the failure of long fibres. The second type was less severe and more narrowly spaced and governed the failure of shorter fibres.

In summary, the strength of a glass fibre is controlled by defects on the fibre surface. These fundamental cracks have never been observed [59] but overwhelming evidence for their existence exists. The experimental evidence presented indicates that size effects in

glass fibres appear to be slight and strengths in bulk glass can be obtained which approach recorded strengths for fibres closely. This implies that thermal history and molecular orientation can only have a slight influence on fibre strength [59].

2.2.4 The Young's modulus of glass fibres.

In carbon and aramid fibres there is often a high degree of molecular alignment introduced by the manufacturing process [60]. However, there is little or no change in molecular orientation due to the glass fibre forming process and the properties of a glass fibre are largely isotropic [50]. Thus the Young's modulus is essentially the same both in fibrous and bulk form. The value for a silicate glass is very sensitive to packing density [61]. When an external load is applied, there are three main mechanisms for deformation: rotation of the SiO_4 tetrahedrons; bond angle distortion and elongation of Si-O bonds [61]. Rotation of SiO_4 tetrahedra can occur quite easily in silicate glasses due to the low packing density and this is the main reason for the low stiffness of E-glass fibres compared to other forms of reinforcement.

2.3 The effect of heat on the mechanical properties of glass fibres.

2.3.1 Fibre strength.

There have been numerous investigations into the effect of heating on the tensile strength of glass fibres. Several mechanisms have been proposed to explain the loss in strength that is commonly measured. As has already been shown, the strength of glass is governed by the defects in the glass surface and so the effect of heat on the strength of glass fibres is best explained by surface phenomena.

In 1957, Sakka investigated the effect of reheating on the strength of glass fibres [62]. Samples of fibre were heated for one hour at temperatures of up to 750°C . Some of the heated fibres were then etched with hydrofluoric acid. Tensile strength measurements showed that heating the fibres weakened them and the retained strength was reduced as the temperature of the heat treatment was increased. Heating at 550°C for one hour led to a reduction in fibre strength of 50%. At temperatures below 660°C the original fibre strength could be completely recovered by etching away a thin surface layer from the fibres. For temperatures above 660°C the fibre surface became irregularly etched by the

hydrofluoric acid, which was ascribed to the formation of an inhomogeneous structure at the surface caused by the high temperature. The original fibre strength could not be recovered. No mechanism for the observed strength loss was presented. Later work by Hara [63] also showed the effect of heating on the strength of glass and its subsequent recovery by etching with hydrofluoric acid. Hara measured the strengths of glass plates containing well characterised and reproducible flaws introduced into the glass surface by a diamond pyramid indenter. As the glass surface was etched and the severity of the flaw was reduced, the strength of the sample increased but the original site of the flaw was always the point at which the sample failed. Etched samples which were subsequently heat treated had reduced strength and in many cases the fracture did not start at the etch pit, suggesting that some new, randomly introduced flaw had been introduced.

Brearley and Holloway [64] also investigated the effect of heat treatment on the breaking strength of glass. Soda lime silica glass rods (diameter 300 μm to 900 μm), with an initial breaking strength of 3.2 GPa when tested in torsion, were given various heat treatments and their strengths remeasured. After treatment at temperatures as low as 50°C there was a reduction in fibre strength and an increase in the scatter. When the fibres that had undergone heat treatment for one hour at 50°C and 125°C were stored in air at 85% humidity there was some recovery of strength. There was a complete recovery of the original fibre strength if the same fibres were stored in water after heating. As before, hydrofluoric acid etching of the fibres heated at 400°C and 530°C led to complete strength recoveries. Flaws created on the fibre surface during heating below 125°C could be reduced to a negligible severity by the corrosive attack of the water. A similar reduction in flaws generated at a higher temperature could only be achieved with a more corrosive medium.

Another series of fibres were heated in dry nitrogen to determine whether moisture in the atmosphere during the heating cycle had limited the strength loss in the fibres. Fibres heated in dry nitrogen were found to be weakened to the same extent as fibres heated in air. Storage of heat treated fibres in dry nitrogen inhibited the recovery of fibre strength. The authors confirmed that the strength loss occurred during the heat treatment and not, for example, as a result of the cooling process.

These effects were explained by postulating that changes in breaking strength during heat treatment, even at relatively low temperatures, were due to the bonding of contaminating particles to the glass surface and that the bound particles subsequently acted as stress concentrators. Strongly bonded particles which could not be removed by direct mechanical manipulation were observed after heating at temperatures as low as 125°C. Study of the fibre fracture surfaces of cleanly broken samples with an optical microscope showed that the fracture had been initiated by a surface bonded particle. These researchers could not rule out other weakening processes since in the course of the fracture of some fibres a clean surface was not created.

However, evidence against the theory of the dust particles weakening the glass fibres during heat treatment was presented by Cameron [65] who heated glass fibres for up to one hour at temperatures up to 280°C. The fibres were weakened by this treatment and the same strength loss occurred if the fibres were heated in air or high purity argon. The results cast doubt on the dust particle theory proposed by Brearley and Holloway because the high purity argon had a significantly lower dust concentration than laboratory air and so would not be expected to lead to the same degree of strength loss as that measured in the fibres treated in air. A structural change in the glass was suggested as the cause of the weakening.

In a series of experiments on soda-lime-silica glass rods, Ward et al [66] noted that heating at 350°C led to maximum strength loss after only ten minutes and that the residual strength decreased with increasing temperature up to 350°C, after which there was little further decrease. Storing the treated samples in water led to a complete recovery of strength. Samples heated at 350°C for one hour recovered their original strengths after storage in water for one month. The loss in strength was attributed to the formation of flaws and cracks as a result of molecular and structural rearrangements. It has been shown that glass surfaces are covered with an adsorbed surface layer of water up to 20 molecules thick as soon as they are created [52]. This layer can be completely removed by heating at temperatures over 250°C [66] and it was proposed that cracks form in this hydrated layer as it dries which are responsible for the loss of fibre strength.

By comparing the tensile and flexural strengths of heat treated silica fibres, Piggott and Yokom [67] found that the intrinsic strength of the fibres (as measured by the bending test where only a very small gauge length is under test) increased with heat treatment up to 200°C but that the tensile strength was reduced by heating at the same temperatures. Treatment at higher temperatures reduced strength in both bending and tension.

In a later paper, Cameron [68] once again investigated the effect of heating on the strength of E-glass fibres. He investigated treatment temperatures of up to 273°C and treatment times of up to seventy hours. The measured weakening due to heating was not consistent and he postulated that other variables were operating. He suggested that one such variable could be the airborne dust density in the furnace and his results provided some evidence of this.

Figures 2.4 and 2.5 show the measured effect on the strengths of E-glass fibres of heating as measured by Cameron [68] and Thomas [55]. It can be seen that heating at temperatures as low as 200°C can significantly reduce the strength of glass fibres. Strength loss increases with time until a plateau is reached. This steady state strength decreases as the treatment temperature increases.

Figure 2.4 Effect of heating on glass fibre strength.

Reference: Cameron [68].

Glass: E-glass.

Diameter: 6 - 17 μm .

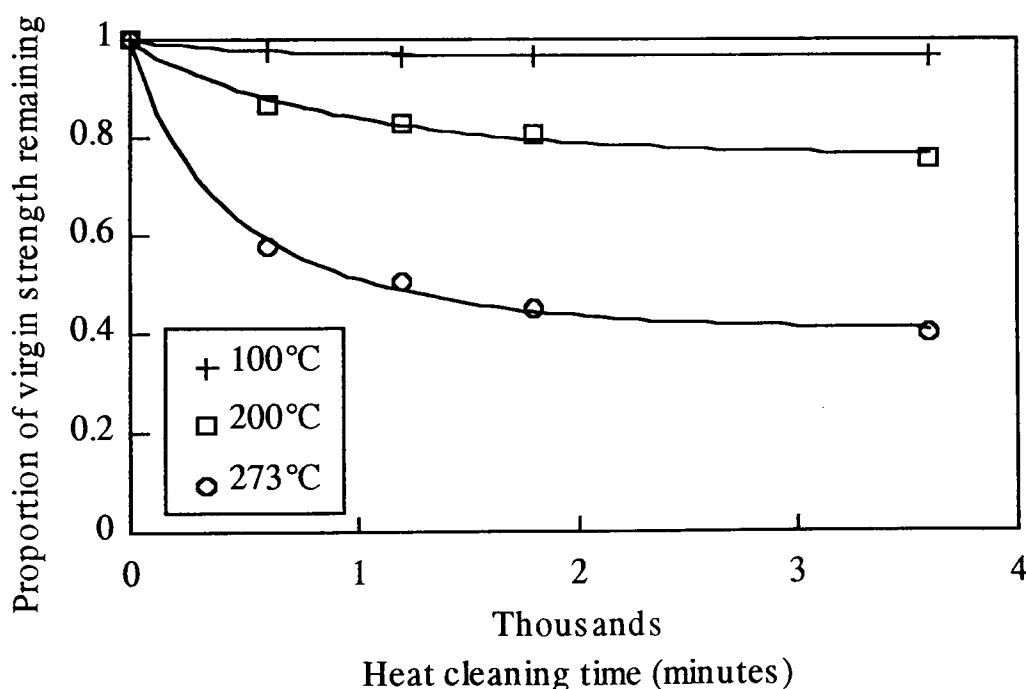
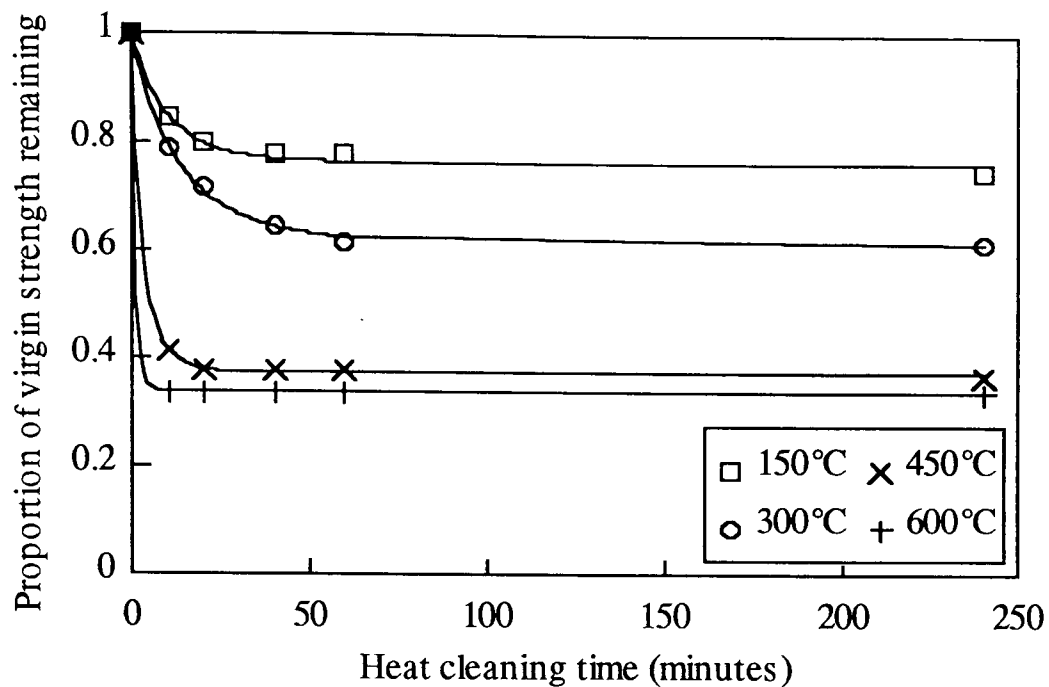


Figure 2.5 Effect of heating on glass fibre strength.

Reference: Thomas [55].

Glass: E-glass.

Diameter: 13 μm .



Glass fibres which are to be woven into a fabric are sized with a weaving size when they are formed. Unfortunately this size is not compatible with the resins used in thermoset composite manufacture and would interfere with the bond between resin and fibre which is vital for optimum composite properties. For this reason, the weaving size is removed from the fibres once the weaving has been completed and a new, resin compatible size is applied [69]. Most of the interest in the effect of heat on the properties of glass fibres has been as a result of the need to heat clean glass cloth without causing excessive damage. There are two common cycles for heat cleaning glass cloth. The low temperature cycle involves slowly heating a roll of glass cloth in a large circulating air oven to around 300°C to 350°C over 72 hours [69]. In the high temperature cycle, the roll of cloth is unwound through an oven where it is heated to about 700°C for 5 to 20 seconds [70]. Adams et al [71] investigated the effect of heat cleaning time and temperature on the strength of a glass cloth, finding that at 650°C only 50% of the original strength was retained after heating for only 4 seconds but that a similar degree of strength loss took 83 minutes to occur at a temperature of 371°C. Heat cleaned glass has a high surface alkalinity which Adams et al attributed to the migration of sodium ions to the surface during heat treatment. It has been reported that Na^+ ions can be removed from glass in contact with water by an ion exchange mechanism where H^+ ions diffuse into the glass to preserve the electrical

neutrality [71] and that the sodium hydroxide thus formed can attack the glass, causing it to be weakened. They suggested that the loss of strength was due to the partial exchange of Na^+ ions for smaller H^+ ions creating a tensile stress at the fibre surface which could promote the formation of surface cracks. They postulated that the source of the H^+ ions could be hydroxyl groups present on the fibre surface (even at heat cleaning temperatures), water generated by the thermal degradation of the weaving size or from combustion products of the heating fuel. The researchers applied an excess of Na^+ ions in the form of sodium nitrate to glass cloth and heat cleaned it. They reported that the strength loss was much reduced and that this suggested that the ion exchange mechanism had dominated over any corrosive attack by sodium hydroxide.

Jarvela [72] used a looped bending test to investigate the strength of E-glass fibres under different atmospheric conditions including the effect of heat treatment. Strength loss was explained by the relaxation of a tempered layer on the glass fibre surface. This tempered layer is present because of the rapid cooling during forming. The surface of the fibre cools first but the inner part of the fibre is still liquid and as it cools it contracts so putting the fibre surface into compression. The compressive stress in the fibre surface has to be overcome before any surface cracks can be opened, hence direct loading of the fibre is delayed until this surface stress is exceeded. Evidence for the removal of the tempered layer by heat treatment was also presented by Das et al [73]. These researchers were investigating the corrosive deterioration of glass fibres. When glass fibres are attacked by 0.5 M sulphuric acid their strengths are degraded because some of the constituents of the glass are leached out through the fibre surface. Heat treatment was used to reduce the subsequent strength loss of fibres in corrosive environments. Again, the fibre strength was temperature dependent. The heat treated fibres were still attacked by the acid but the degree of leaching was reduced. Interestingly, spiral cracks developed on the surfaces of the fibres that had not been heat treated before acid attack but no cracks were seen on the heat treated fibres. The cracks in the unheated samples were due to residual surface stresses which had been removed by heat treatment in the other samples.

Discussion.

Several causes have been reported for the reduction in glass fibre strength during heating,

including dust bonding to the surface, drying of a hydrated layer, ion exchange and annealing of a tempered layer. All these surface phenomena are likely to be responsible to some degree. The effect is both time and temperature dependent but the measured strength losses are very sensitive to the experimental conditions. For example, Cameron [68] reported a residual plateau strength of 40% after heating at 273°C for 3,000 minutes but Thomas [55] found a steady 60% strength retention after only 60 minutes heating at 300°C (Figures 2.4 and 2.5). It will be difficult to predict the strengths of fibres recovered from the fluidised bed process but minimising the bed temperature and bed residence time of the fibres will maximise the recovered fibre strengths.

2.3.2 Fibre modulus.

There is little published work concerned with the effect of heat on the Young's modulus. As discussed in section 2.2.4, the Young's modulus of glass fibres is similar to that of bulk glass and so modulus is not controlled by surface defects in the same way as fibre strength.

2.4 Enhancement of glass fibre reinforcement potential.

It has already been shown that degradation of glass fibres during heating is a surface phenomenon. Therefore it follows that enhancement of the strength of the fibres could be achieved by modification of the degraded fibre surface. Other ways of improving the performance of a composite are to increase the fibre volume fraction or create an interfacial bond.

2.4.1 Reduction of flaw severity.

Ward et al [66] suggested that the recovery of strength on water immersion occurred as a result of chemical attack by the water at the flaw tips which increased the flaw tip radii and reduced their effectiveness as stress concentrators. A faster method of reducing flaw severity, or even removing flaws completely, is etching with hydrofluoric acid [62].

Adams et al [71] investigated the chemical strengthening of glass fibres, finding that covering the fibres with a potassium salt before heat cleaning reduced the degree of strength loss. They postulated that when heated, the salt melted and an ion exchange

occurred. Sodium cations in the glass were replaced by potassium cations from the salt. When the fibres were allowed to cool the glass structure contracted but was prevented from completely so doing at the surface by the presence of the large potassium ions. Hence a surface compressive layer was established which caused the heat induced flaws to close up.

2.4.2 Alignment of fibres.

One method of aligning discontinuous fibres is to disperse them in glycerine and extrude the resultant slurry through a slit, the viscous forces causing the fibres to align in the flow direction [74-77]. Composites made from these aligned sheets were found to have properties similar to those formed from continuous fibre. Electrostatic forces [78], alignment by airflow [79] and directed deposition of a water based slurry [80] have also been investigated.

2.4.3 Sizing.

Sizes are generally chemical emulsions placed onto the surfaces of glass fibres as they are formed which fulfil a number of functions, the most important being protection of the glass fibre surface and chemical linkage of the fibre to the organic polymer when used in a composite [52, 69]. Size formulations contain film formers, such as polyvinyl acetate, to protect the fibres and silane coupling agents to link the fibres to the matrix [52]. Silanes are organofunctional monomers that possess a dual reactivity. Groups at one end of the molecule hydrolyse and form silanols which can then condense with similar groups on the fibre surface [81]. At the other end of the molecule are organic groups which can co-react with organic matrix resins [82]. The structure of the silane can have a large effect on the properties of the composite material [83] and can limit environmental corrosion of the composite [84, 85]. Silanes are also capable of forming networks that can bridge flaws in glass fibres, helping to strengthen them [86].

2.5 Carbon fibre manufacture and properties.

2.5.1 Manufacture.

Rayon, polyacrylonitrile (PAN) or pitch precursors are formed into fibres and then heated to drive off non-carbon atoms and to leave the desired turbostratic graphite crystallites.

With PAN based fibres, alignment of the crystallites can be achieved by stretching the precursor fibre to produce alignment of the molecular chains along the fibre axis. Heating the precursor in air at around 220°C [87] with tension applied leads to a ladder structure being formed. Carbonisation is then achieved by heating in nitrogen at temperatures in excess of 1000°C [88] without tension and then further heat treatment at any temperature up to 3000°C. The Young's modulus and ultimate tensile strength of the carbon fibres is a function of this final heat treatment.

Other methods of producing the desired molecular alignment in the carbon fibres can involve spinning the precursor fibres or application of a tensile stress during the graphitization procedure.

2.5.2 Properties.

Carbon fibres consist of well packed, small crystallites of turbostratic graphite, one of the allotropic forms of carbon [89]. Like graphite, these crystallites are built up of planes of hexagonal arrays of carbon atoms. However, unlike graphite, these planes are not stacked in a regular sequence and their average separation is 0.34 nm, compared to 0.335 nm for graphite [60]. The carbon atoms within a plane are held together by strong covalent bonds but separate planes are only held together by weaker van der Waal bonds. This means that the in plane Young's modulus (910 GPa) is very much higher than the out of plane Young's modulus (30 GPa) [60]. The Young's modulus of a carbon fibre is typically less than 370 GPa due to imperfect alignment of the graphitic planes with the fibre axis.

The strength of the carbon fibre is controlled by imperfections in crystallite alignment which produce irregular shaped voids which act as stress concentrators. Other sources of weakness are macrocrystallites and surface pits which are introduced during manufacture.

It can be seen that the properties of the carbon fibre depend entirely on the size and alignment of the crystallites of turbostratic graphite which are in turn a function of the precise details of the manufacturing process.

2.5.3 Effect of heat.

Carbon fibres share similar chemical properties to bulk carbon. Oxidation in air occurs at temperatures in excess of 400°C [89], and could cause surface pits which would weaken the fibre, but in inert atmospheres carbon fibres can sustain tensile loads at temperatures well over 2000°C [89].

2.6 Conclusions.

The problem of recycling thermoset composite materials has been identified by many other investigators and numerous processes have been proposed. This review has highlighted the effect of reusing thermoset composite recycle in composites. Size reduction is an appropriate way to deal with relatively clean scrap and has achieved some economic success. A process to recycle contaminated scrap is still required and this is where fluidised bed processing can fit in. By focussing on recovering the valuable fibres, the economic viability of the process can be encouraged.

Glass fibres are commonly used to reinforce thermoset resins and so the likely effect of a thermal process on their properties has been established. It has been shown that surface damage is likely to result from heat treatment and that this will cause a weakening of the glass fibres but is unlikely to produce any change in the Young's modulus. It has been established that the degree of weakening is time and temperature dependent although the exact scale of the effect is very sensitive to the precise details of the experimental conditions. The strength loss due to fluidised bed processing will need to be established by experimental investigation.

Finally, several methods of improving the reinforcement potential of thermally recycled glass fibres have been suggested. In a composite material, the bond between the fibre and the matrix is crucial to the composite's properties. Silane treatments may need to be reapplied to the recovered fibres to provide this bond. Improving the strength of the recovered fibres and increasing their packing density will also improve their reinforcement potential and processes and treatments to do this have been reviewed.

Chapter 3.

Heat cleaned glass cloth as composite reinforcement.

3.0 Introduction.

It has already been shown in the literature survey in Chapter 2 that exposing glass fibres to heat can decrease their strength at room temperature by causing a deterioration of the fibre surface [62-68, 72, 90]. The primary objectives of this part of the work were to establish the extent of any degradation, its relationship to process conditions during heat treatment and to investigate the physical properties of thermoset laminates containing heat degraded glass fibres. This work was completed in advance of recycled fibres becoming available from the fluidised bed processing rig and was undertaken as a preliminary study into the reinforcing properties of heat degraded E-glass fibres.

3.1 Experimental details

Samples of woven E-glass cloth (see 3.1.1) were heat treated at 375°C, 500°C and 625°C for periods of up to 60 minutes in an ashing furnace. This range of processing conditions was designed to cover the likely temperatures and residence times that could be encountered by glass fibres during processing in the fluidised bed. A woven cloth was chosen since it was likely to retain its integrity after the heat treatment and so be suitable for lamination. The resulting materials were then laminated with a polyester resin using both hand lay-up (HLU) and resin transfer moulding (RTM) (see 3.1.2). Some of the heated cloths were treated with a silane solution before lamination since the heat treatment was expected to remove the initial size on the glass fibres. The final laminates were tested for tensile strength, tensile modulus, flexural strength and flexural modulus (see 3.1.3).

3.1.1 Preform preparation.

The reinforcement used was manufactured by Courtaulds and was designated Y0736/205/960. This is an 8 end satin cloth with an areal density of 850 gm⁻² containing continuous E-glass fibres with a diameter of 9 μm. This fabric contains nominally 0.15% by weight of a size based on methacrylate chromic chloride which is compatible with polyester resin systems. The exact size formulation is proprietary but was identified by the

designation '205'. During the manufacture of this cloth, the glass fibres are subjected to a heat cleaning process at 375°C which removes the weaving size in preparation for the application of the polyester compatible size. Five layers of fabric 150 mm long and 280 mm wide were cut from the cloth with the shortest dimension orientated in the warp direction of the fabric. The layers were then stacked to form a preform. The preforms were placed in a preheated furnace for the required period of time. On removal, the preforms were allowed to cool to room temperature within fifteen minutes. One sample was cooled slowly to room temperature by leaving it in the furnace and switching off the heating elements.

Some samples of heat treated cloth were resized with a polyester compatible silane treatment. The silane used was OSI Specialities silane treatment A174 which is a gamma methacryloxypropyltrimethoxy silane. A 1% silane solution was prepared by adding A174 to distilled water which had been buffered to pH 4 with acetic acid. After steady mixing the silane hydrolysed over time and was ready to use after standing for one hour. The appropriate preforms were immersed in the silane solution for five minutes and then removed, drained and dried in air overnight. Weighing the samples before and after silane treatment enabled the dosing level to be calculated and this was found to be approximately 0.25% by weight in each case. One of the heated samples was returned to the manufacturers for reapplication of the original size (identification 205).

3.1.2 Moulding details.

Hand lay-up samples were prepared in a 170 mm by 300 mm by 4 mm deep picture frame mould at room temperature using a Cray Valley orthophthalic unsaturated polyester resin 6345.001 with a cobalt/MEKP accelerator/initiator system.

The RTM laminates used Akzo Perkadox 16 (bis-(4-tertiary butyl cyclohexyl) peroxy dicarbonate) as an initiator and were moulded at 65°C. A 540 mm by 520 mm by 4 mm deep mould containing the preform was closed with a Fox and Offord upstroking press. The preform was centrally positioned within the mould cavity and was surrounded by continuous filament random mat (CFRM) which acted as an absorbent for excess resin. Resin was injected into the centre of the top surface of the preform.

Both HLU and RTM samples had a nominal thickness of 4 mm, a nominal fibre volume fraction of 41 % and were post cured at 70°C for one hour before testing.

3.1.3 Testing.

All test procedures were based on BS 2782. Eight tensile specimens 150 mm by 25 mm were prepared and tested using an Instron Universal testing machine, model 1195, at a cross head speed of 5 mm min⁻¹. Sample extension was measured by crosshead displacement. Ultimate tensile strength and tangent modulus at 0.2% strain were calculated from the force against extension curves. Use of the cross head displacement as a measure of sample extension will not give an absolute value for the laminate modulus since some of the measured displacement will be due to compliance in the testing machine. However, this method should give figures for laminate modulus that are comparable for these experiments since the testing machine settings were identical in each case. Flexural specimens 15 mm by 70 mm were tested on the same testing machine over a span of 56 mm. The crosshead speed was 1 mm min⁻¹ and for the flexural tests, the sample displacement was measured by a linear variable differential transformer (LVDT) which measured the position of the striking plate. This displacement was equated to sample deflection. Flexural strength and flexural modulus (calculated between strains of 0.05 % and 0.25 %) were recorded.

Void contents were measured by immersion and fibre volume fractions were determined by ashing (BS 2782, part 10, method 1002). A JEOL scanning electron microscope was used to study the fracture surfaces of the tensile specimens.

3.2 Results and discussion.

Laminate fibre volume fractions and void contents are shown in Table 3.1. The increase in the fibre volume fraction of the experimental plaques from the nominal level of 41 % is due to resin shrinkage during curing leading to a reduction in laminate thickness. The glass fibres with sizing in good condition, i.e. those heated at 375°C and those with reapplied commercial sizing, wet out easily and consequently formed laminates with low void contents.

Table 3.1 Laminate fibre volume fractions and void contents.

Sample description	Fibre volume fraction range	Void content range
All HLU samples	40% - 44%	2.7% - 4.2%
RTM samples (500°C and 625°C)	44% - 49%	3.0% - 5.1%
RTM sample (205 sizing)	53%	0.3%
RTM samples (375°C)	47% - 51%	0.5% - 1.1%

3.2.1 Laminate tensile strength.

625°C Series.

At a furnace temperature of 625°C it can be seen that after only twenty minutes heating of the reinforcing cloth, the strength of the HLU laminates generally fell to a plateau where the strength was approximately one quarter of the value for a laminate containing virgin glass cloth (Figure 3.1). Similar strength losses were also seen for the RTM samples (Figure 3.2).

Figure 3.1 Effect of heat cleaning on tensile strength.

Furnace temperature: 625°C.
 Resin: unsaturated polyester.
 Reinforcement: woven glass cloth.
 Process: HLU.

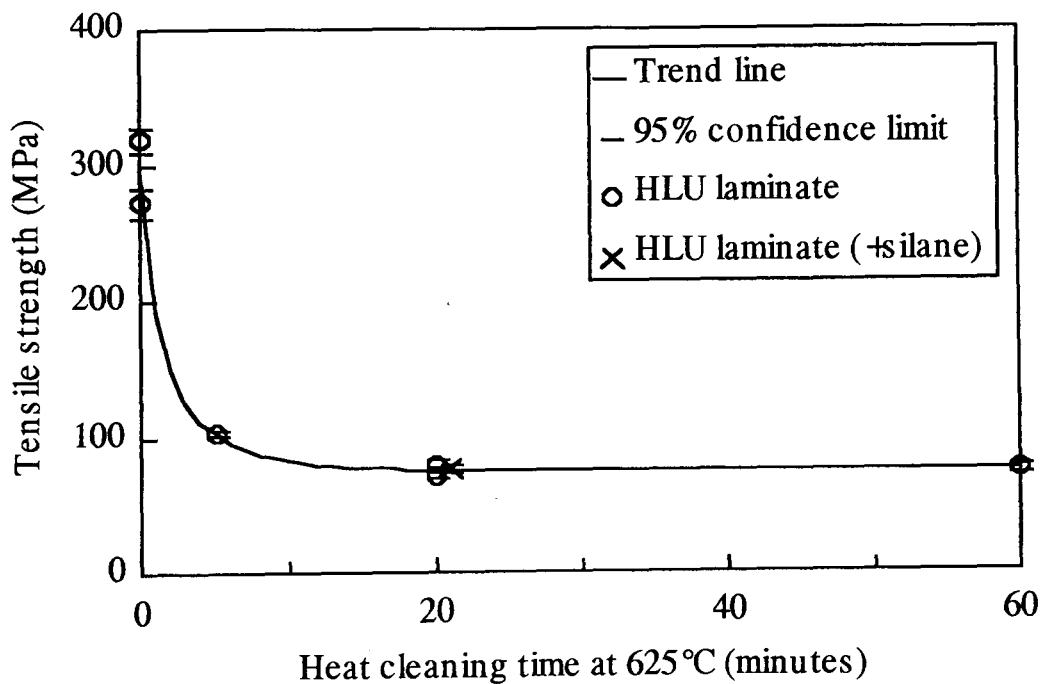


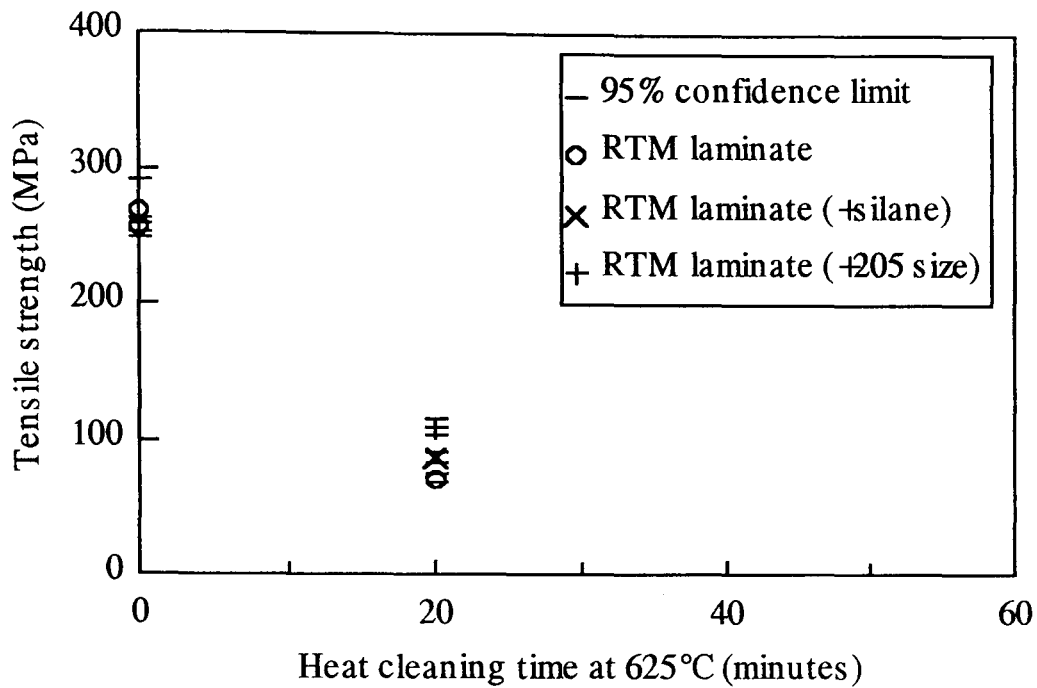
Figure 3.2 Effects of heat cleaning on tensile strength.

Furnace temperature: 625°C.

Resin: unsaturated polyester.

Reinforcement: woven glass cloth.

Process: RTM.



There was no further reduction in strength for fabrics treated for beyond twenty minutes. Silane coating the heated fabric made no significant difference to the laminate strength. Study of the failure surfaces for these specimens shows that the silane treatment improved the bonding of the resin to the fibres. Figure 3.3 shows that the heat cleaned fibres had almost no affinity for the surrounding polymer. This contrasts sharply with Figure 3.4 where polymer is clearly seen bonded to the fibre surfaces. The fact that this improved bond did not give an improvement in tensile strength suggests that the fibres were severely weakened which was responsible for the lower tensile strength. The RTM samples showed similar properties to the HLU samples. Given the difference between the measured strengths of the two control samples it cannot be said that the silane treatment has produced a significantly stronger laminate. The laminate containing cloth heated and then treated with the original size has a slightly higher strength, 110 MPa against 80 MPa, but this could be accounted for by its higher than average fibre volume fraction, 53% against 47% (Table 3.1) and the scatter in the results.

Figure 3.3

SEM micrograph of the fracture surface of a laminate containing glass cloth heated at 625°C for twenty minutes.

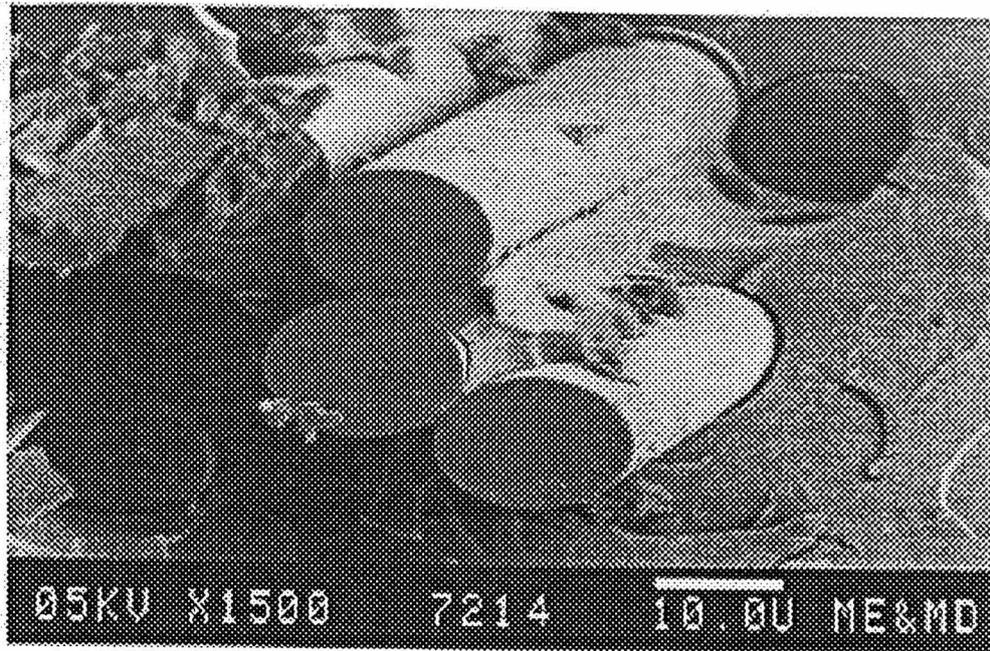
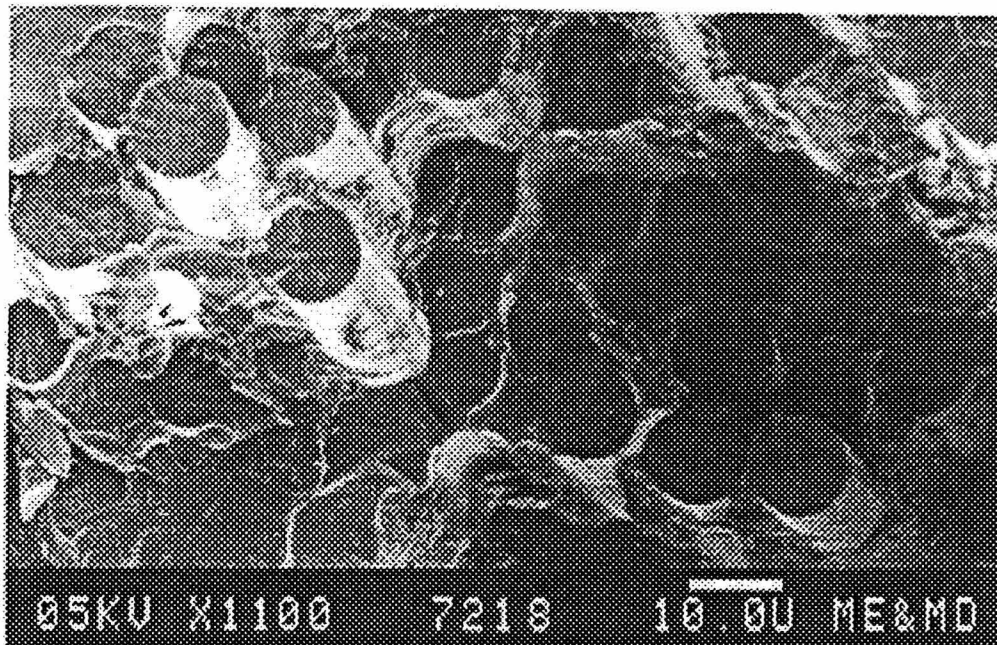


Figure 3.4

SEM micrograph of the fracture surface of a laminate containing glass cloth heated at 625°C for twenty minutes and then silane coated.



500°C Series.

For fibres treated at 500°C, the tensile strengths of the mouldings were between 30% (60 minutes heating) and 80% (20 minutes heating) higher than the corresponding results at 625°C. However, the strength decreased with heat cleaning time (Figure 3.5) and for

periods greater than 60 minutes it appeared that the strength had reduced to approximately that for fibres heat treated at 625°C. Silane coating produced a significant increase in tensile strength (approximately 25%) which suggested that the interfacial effect was significant in this case and that the original sizing on the fibres had been destroyed by the heat treatment. The moulding that contained the preform which was allowed to cool slowly performed no differently to the faster cooling samples. This suggests that no further degradation occurred beyond the initial heating period and that the cooling rate is not significant.

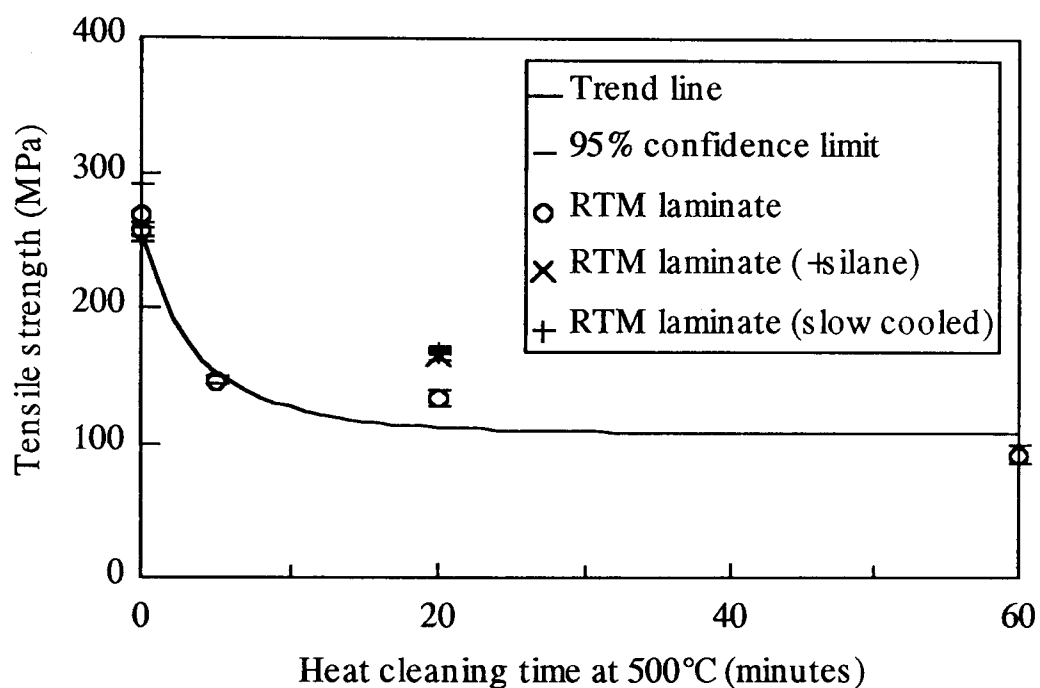
Figure 3.5 Effects of heat cleaning on tensile strength.

Furnace temperature: 500°C.

Resin: unsaturated polyester.

Reinforcement: woven glass cloth.

Process: RTM.



375°C Series.

Heating at 375°C also produced a reduction in tensile strength for up to 20 minutes heating followed by a plateau of constant strength for beyond 20 minutes heating (Figure 3.6). In this case a reduction in strength of 25% was measured for heating in excess of 20 minutes. This was less than that measured for the samples prepared with cloth that had been heated at 500°C and 625°C, for which strength reductions of 60% and 70% respectively were measured. Silane treating the cloth that had been heated for 20 minutes

did not lead to any improvement in laminate tensile strength. This implies that the original size on the cloth had not been destroyed by the heat treatment and was still functional.

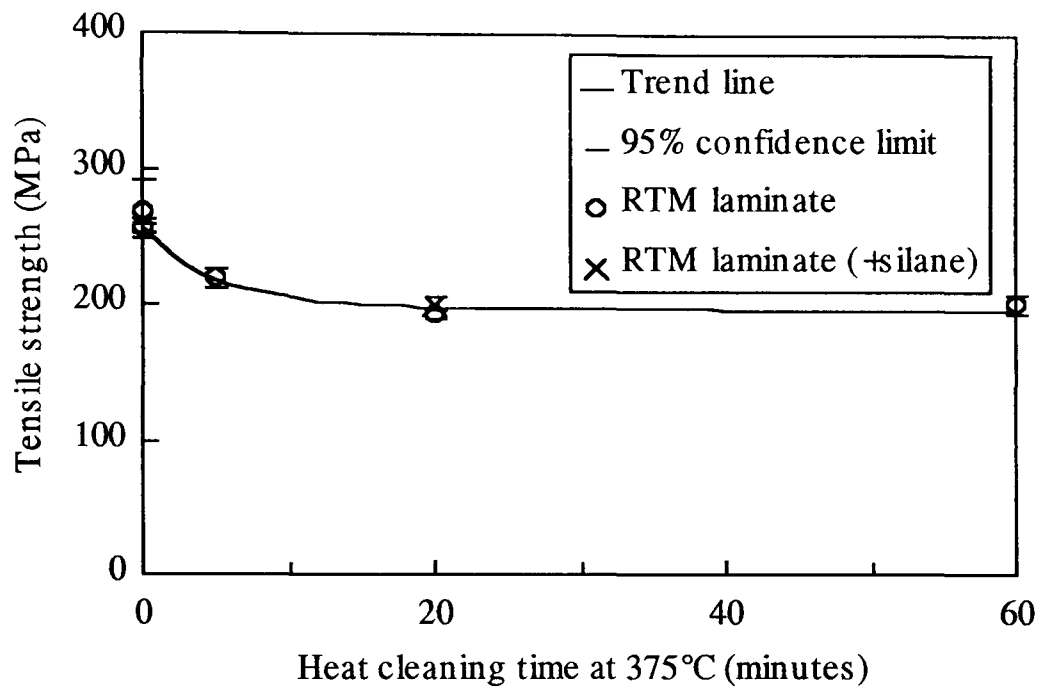
Figure 3.6 Effects of heat cleaning on tensile strength.

Furnace temperature: 375°C.

Resin: unsaturated polyester.

Reinforcement: woven glass cloth.

Process: RTM.



Discussion.

These results agree with those measured by Thomas [55] who found a similar variation of tensile strength with period of heat treatment for single E-glass filaments, reporting residual strengths of approximately 35% after 5 minutes heating at 600°C. No further reduction in strength was noticed for heating periods of up to 4 hours. The strength reduction was found to decrease with the furnace temperature while the time for the strength to fall to a steady value increased (Figure 2.5).

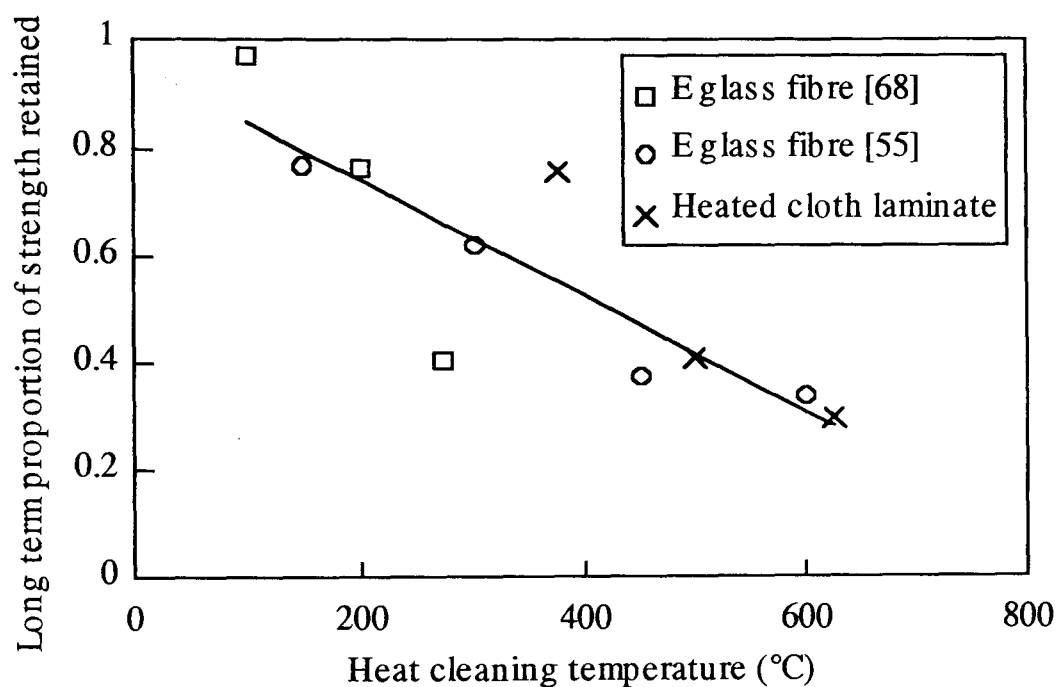
The reduction in laminate tensile strength with increasing reinforcement time at temperature can be represented by an equation of the form:

$$\epsilon = \frac{a}{1 + be^{-ct}} \quad 3.1$$

where ϵ is the ratio of the tensile strength of a laminate containing cloth heated for time

t to one containing untreated cloth and a, b and c are constants for a given temperature. It can be seen that a is the asymptotic value of the residual strength as the duration of the heat cleaning process tends to infinity. Values of a were calculated for the three series of laminates and for the E-glass fibres investigated by Cameron [68] and Thomas [55]. The calculated values for a are plotted against heat cleaning temperature in Figure 3.7. It can be seen that there is an approximately linear decrease in the long term retention of strength over the range 100°C to 625°C and that the published data for single fibres are comparable with that for the laminates.

Figure 3.7 Proportion of virgin strength retained after long term heat treatment as a function of treatment temperature.

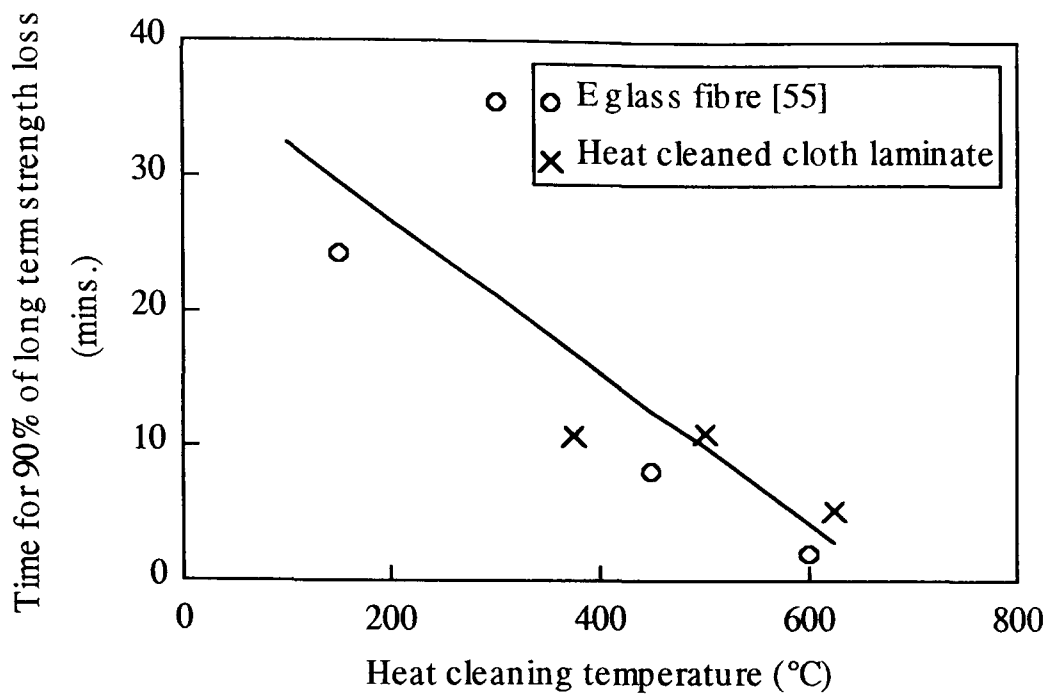


Rearrangement of Equation 3.1 gives

$$t = \frac{-1}{c} \ln \left[\frac{1}{b} \left(\frac{a}{\epsilon} - 1 \right) \right] \quad 3.2$$

which allows calculation of the heat cleaning time to produce a given proportion of the long term strength reduction. The time to achieve 90% of the long term strength loss as a function of temperature for the heated cloth laminates and the E-glass fibres studied by Thomas is shown in Figure 3.8. There is an approximately linear decrease in the time required to produce this degree of strength loss as the heat cleaning temperature increases.

Figure 3.8 Time to achieve 90% of long term strength reduction as a function of processing temperature for E-glass fibres and laminates containing heat cleaned cloth.



3.2.2 Laminate flexural strength.

Only the RTM samples made from cloths heated at 625°C and 500°C were tested for flexural strength.

625°C Series.

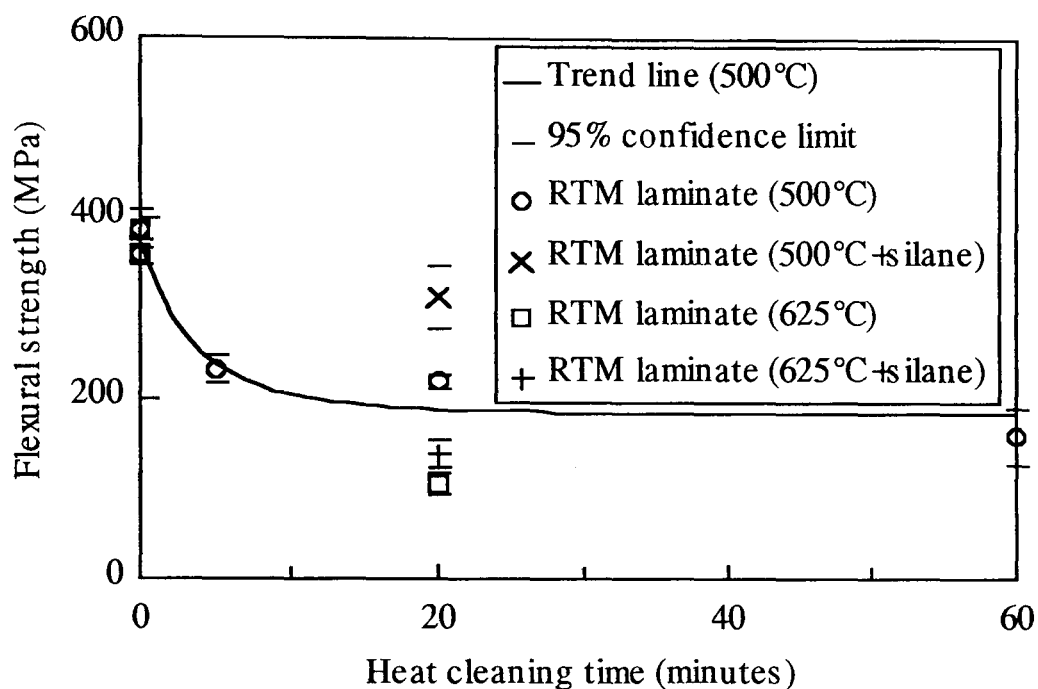
The results are presented in Figure 3.9. The degree of flexural strength loss measured was similar to that measured for tensile strength (approximately 75% reduction from control values after 20 minutes heating). Silane coating did not produce any significant increase in flexural strength for the samples heated for 20 minutes.

500°C Series.

These results are also shown in Figure 3.9. A similar trend to the tensile strength measurements can be seen. After twenty minutes heating of the cloth the resultant laminate flexural strength fell to approximately 50% of the control value. On resizing, a strength increase of almost 50% was observed which was similar to that measured for the tensile strengths, given the scatter in the results. It is unlikely that any effect of the water in the size solution on fibre strength would have occurred. As discussed in Section 2.3.1, immersion in water for one month was needed to restore the strength of fibres heated at

350°C for one hour [66] and so the improved laminate strength is due to the improved fibre-matrix bond.

Figure 3.9 Effects of heat cleaning on flexural strength.
 Furnace temperatures: 500°C and 625°C.
 Resin: unsaturated polyester.
 Reinforcement: woven glass cloth.
 Process: RTM.



3.2.3 Laminate tensile modulus.

For both the RTM and the HLU laminates, a wide spread of results was measured for the control samples containing unheated cloth (Figures 3.10, 3.11, 3.12 and 3.13). Given this spread it appears that heat treatment of the reinforcing cloth has not produced any significant reduction in laminate tangent modulus at 0.2% strain and, likewise, that silane coating the fibres has little effect on this property. Thomason [91] also found little effect of interfacial bond strength on composite modulus with a glass reinforced polypropylene. Since the initial modulus of a composite is largely insensitive to the level of fibre-matrix adhesion (assuming perfect wetting) these results suggest that there is no effect of heating on the modulus of the glass fibres.

3.2.4 Laminate flexural modulus.

No significant effect of reinforcement preheating on the flexural moduli of the laminates was found (Figures 3.14 and 3.15).

Figure 3.12 Effects of heat cleaning on tangent modulus.

Furnace temperature: 500°C.

Resin: unsaturated polyester.

Reinforcement: woven glass cloth.

Process: RTM.

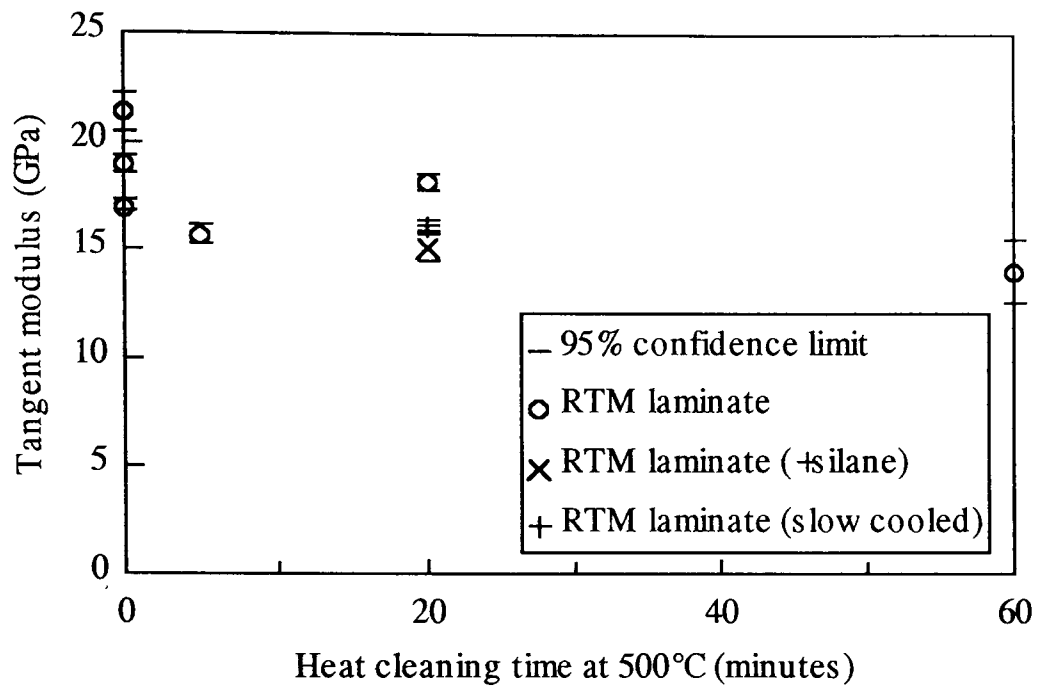


Figure 3.13 Effects of heat cleaning on tangent modulus.

Furnace temperature: 375°C.

Resin: unsaturated polyester.

Reinforcement: woven glass cloth.

Process: RTM.

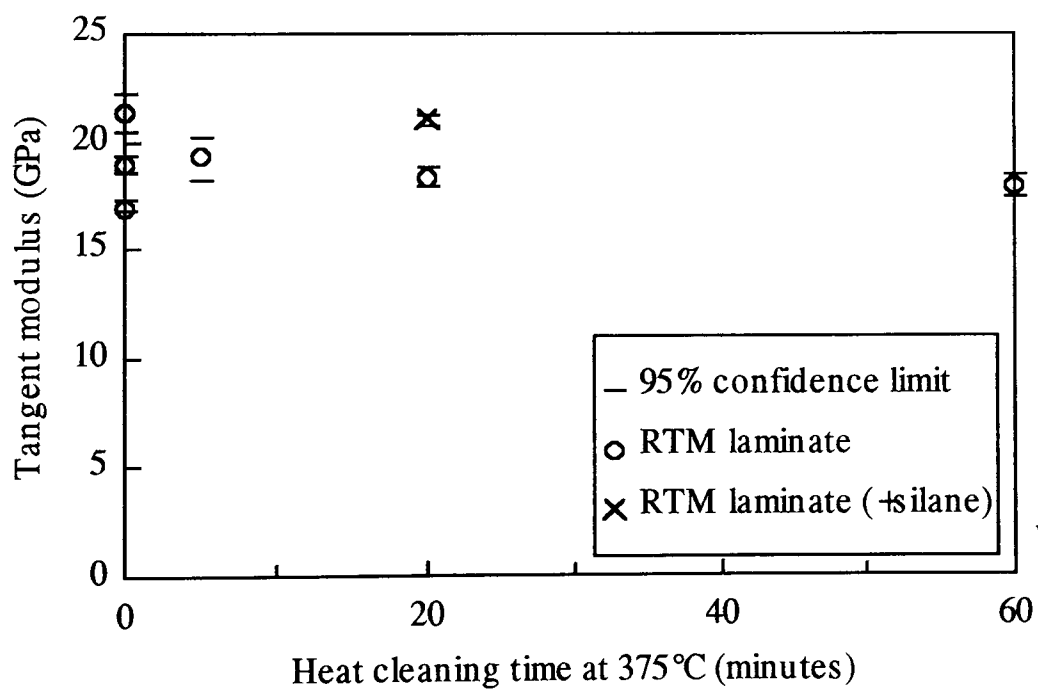


Figure 3.14 Effects of heat cleaning on flexural modulus.

Furnace temperature: 625°C.

Resin: unsaturated polyester.

Reinforcement: woven glass cloth.

Process: RTM.

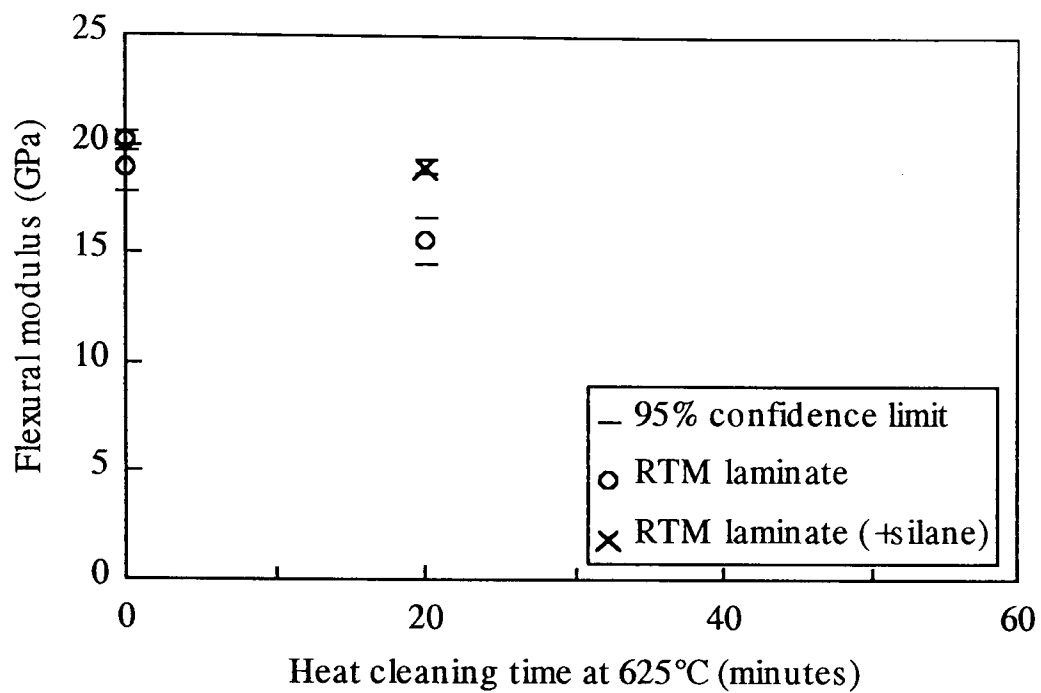


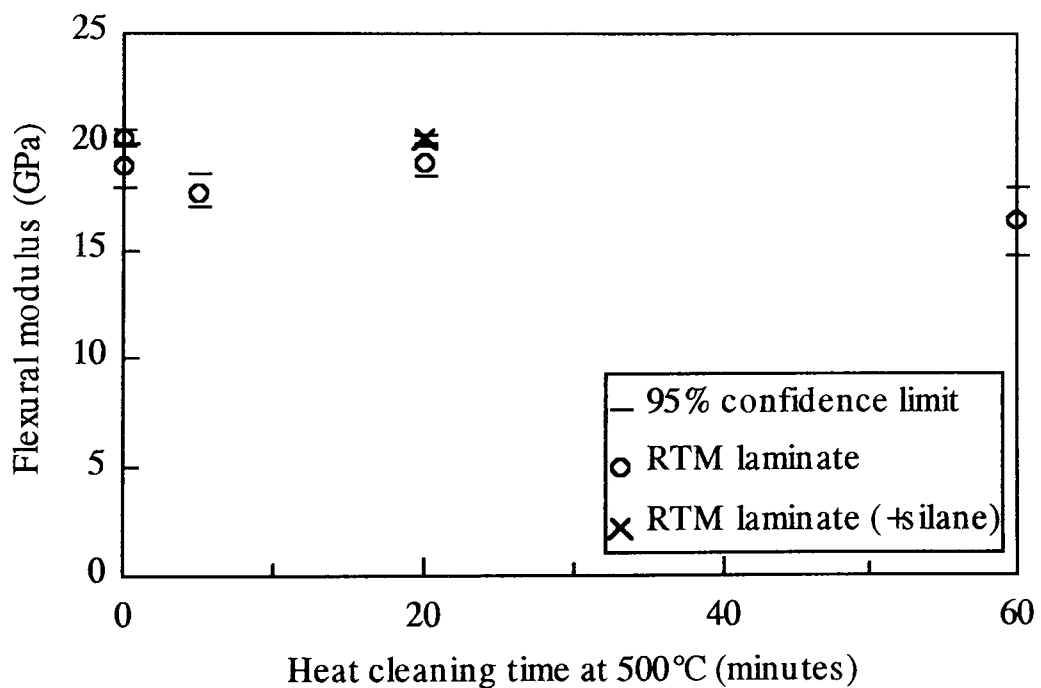
Figure 3.15 Effects of heat cleaning on flexural modulus.

Furnace temperature: 500°C.

Resin: unsaturated polyester.

Reinforcement: woven glass cloth.

Process: RTM.



3.2.5 Laminate strain at failure.

The strain at failure of the control laminates was approximately 2.2%. After heating the glass reinforcement for times in excess of 20 minutes at 375°C, 500°C and 625°C the strain at failure of the laminates was reduced to steady values of 1.5%, 1.0% and 0.5% respectively. A 40% improvement in strain at failure was measured if the reinforcement heated at 500°C for twenty minutes was silane coated before lamination. These trends closely follow those measured for tensile and flexural strength.

3.3 Conclusions.

Laminates were made with heat cleaned glass cloth as reinforcement. Their mechanical properties were measured to investigate the effect of the heat treatment.

The strength of the laminates decreased with increasing treatment time up to 20 minutes. Beyond 20 minutes heating no further effect was seen. As the treatment temperature was increased, the strength of the laminates after 20 minutes heating decreased from 80% of the control strength at 375°C to 40% at 500°C and 25% at 625°C. Resizing the cloth only improved the laminate strength in cases where the heat treatment was sufficient to destroy the original size but not so great that the glass strength was reduced to approximately that of the resin alone. These results imply that the glass reinforcement has been weakened and similar trends have been reported in the literature for single glass filaments.

No significant effect of heat treatment or resizing was found on the tensile and flexural moduli at low strains. This implies that the Young's modulus of the glass reinforcement is not affected by the heat cleaning. This conclusion is supported by evidence presented in the literature survey.

Conclusions to be drawn on the processing conditions in the fluidised bed most likely to lead to the recovery of useful fibres are:

- the bed residence time should be minimised.
- the bed temperature should be minimised whilst still allowing adequate removal of any polymer.
- the recovered fibres may need to be resized if used in a composite.

- the degree of weakening will need to be established by experiment.

The next chapter will describe the experimental determination of the recovered fibre strengths and also the results of investigations into their lengths and moduli. Full characterisation will allow an appropriate end use to be identified.

Chapter 4

Recovered fibre characterisation.

4.0 Introduction.

A fluidised bed system was chosen to process scrap thermoset composites because it is particularly suited to separating fibres from polymer and contaminating materials. However, the uses to which fibres recovered from thermoset composites can be put will depend on many factors including: the physical form and properties of the fibres and contamination on the fibre surface. This chapter will start with a brief description of the pilot scale fluidised bed processing rig and will then describe the results of experiments undertaken to determine the effect of processing conditions on the physical and mechanical properties of recovered glass fibres. One of the attractive properties of glass fibres is their relatively high specific strength. This strength is exploited in many composite applications and would be an attractive property for any recovered fibres. It has already been shown in Chapter 3 that heat treated glass fibres have reduced strengths compared to virgin glass fibres. The strengths of recovered fibres will be investigated. The lengths of fibres also determine their reinforcement efficiency and so measurements of their length distributions will be presented. In semi-structural applications, ultimate composite strength is a secondary consideration to structural stiffness. The fibres provide this stiffness and so the modulus of the reinforcement is critical. For this reason, the effect of fluidised bed recycling on the elastic moduli of glass fibres will be described.

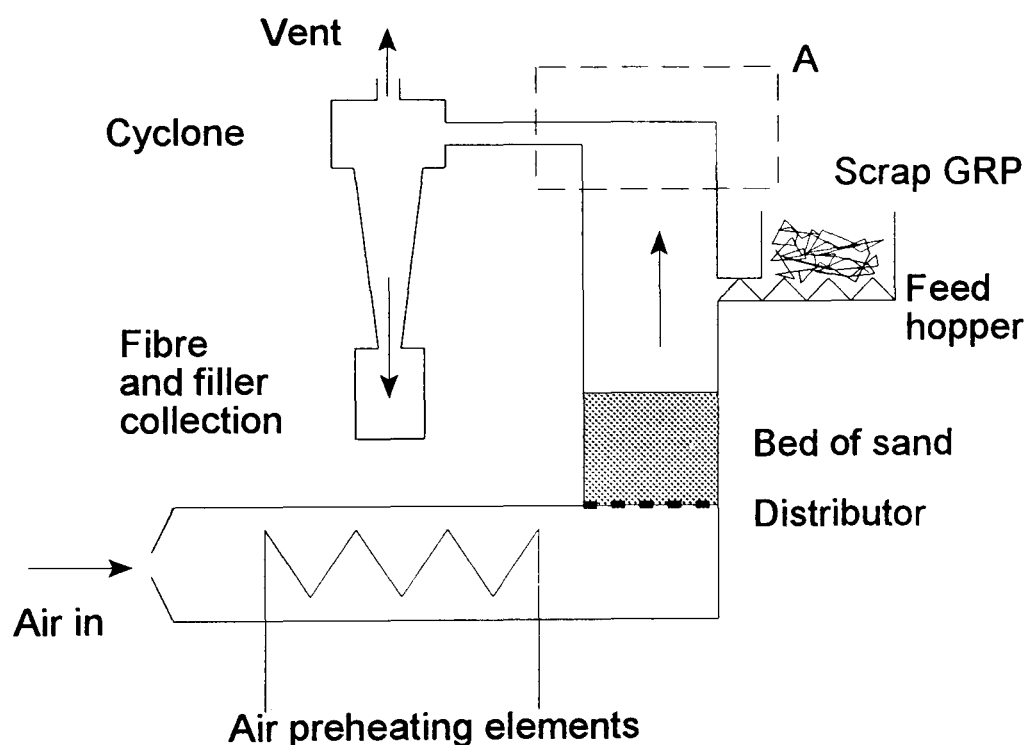
4.1 Fluidised bed processing rig.

Fenwick and Kelly were responsible for the design and operation of the FBPR which was in a continual state of development for the duration of the research work presented in this thesis [92]. The heating elements and the fluidised bed remained unchanged but there were two distinct phases of FBPR development defined by two different collection systems for the recovered fibres: collection by cyclone (dry) and collection by rotating screen (wet).

Air is preheated by a bank of electric heaters, with a maximum rating of 43 kW, and passes to a chamber underneath the fluidised bed where the air flow turns through 90° and

passes through a distribution plate. The plate supports a bed of sand of 150 mm static depth and 312 mm diameter which is fluidised by this flow. Crushed, scrap composite is fed from a hopper by a centreless pig tail screw on to the top of the fluidised bed where the polymer decomposes due to the heat and the churning action of the sand. As the polymer degrades, the fibres and any fillers are released from the composite and are carried with the airstream to the freeboard. With the dry collection system the airborne fibres and fillers are separated from the air stream by a cyclone and are collected, together, in a collection vessel (Figure 4.1). The disadvantages of this system are that the fibres are contaminated by the loose filler particles and are subjected to abrasion by other fibres and process equipment.

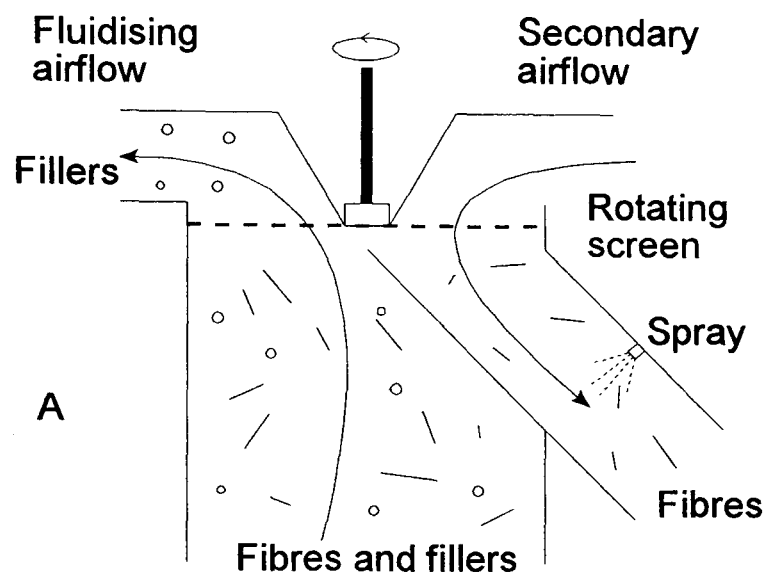
Figure 4.1 Schematic diagram of the FBPR with the cyclone collection system in place.



The wet system uses a rotating screen (Figure 4.2) at the top of the freeboard, situated at position A in Figure 4.1, to remove the fibres from the airstream preferentially. The freeboard is divided in two and the airflow is forced up one side where it then passes through a rotating screen. Long fibres are trapped on the screen while other particles are carried through the mesh by the air stream to a cyclone which is used to collect the filler particles and short fibres. The mesh carrying the trapped fibres rotates to the other side of the divide at the top of the freeboard where a counter current of cold air blows the

fibres from the mesh and into a water spray which washes them into a water filled collection vessel. Not only does the rotating screen system improve the separation of fibre and filler streams but the fibres are quickly removed from the hot air and lubricated with water to decrease the risk of fibre damage.

Figure 4.2
Schematic diagram of the rotating screen separation device.



The main operating parameters for the FBPR are bed temperature (up to 750°C) and fluidizing velocity (up to 1.7 m/s).

4.2 Feed materials.

Fibres were successfully recovered from many thermoset composite systems using the FBPR [93]. Three glass fibre and one carbon fibre based thermoset composites, representing a wide range of composite styles, were used as feedstock for optimization of the rig processing conditions and characterization of the recovered fibres. The details of the formulations of these composites are given in Table 4.1.

Samples of SMC feed were produced by processing in a knife type shredding mill (used by the Bird Group for shredding cable) and collecting particles that passed through a 20 mm screen. Samples of both glass and carbon FW components and the sandwich panel were cut into pieces of approximate size 50 mm by 50 mm with a band saw and then

processed at Brunel University through an Alpine 25MZ hammer mill with a 10 mm outlet screen. In all cases, the resultant materials were collected and stored in sealed containers prior to fluidised bed processing.

Table 4.1 Composite feed materials processed with the FBPR from which fibres were recovered for characterization.

Composite	SMC	Filament Wound	Foam cored sandwich panel	Filament Wound Carbon
Source	Autopress Composites	Dow Deutschland	Aston Martin	GKN
Component	Gas meter box	Effluent pipe	Boot lid	Propshaft
Fibre type	E-glass	E-glass	E-glass	PAN based carbon*
Fibre diameter	13 μm	13 μm	13 μm	7.5 μm
Fibre content	22% w/w 25 mm chopped roving †	65% w/w Continuous roving	15% w/w CFRM	56% w/w Continuous roving
Matrix content	25% w/w Polyester	35% w/w Epoxy	35% w/w Polyester	44% w/w Epoxy
Calcium carbonate content	35% w/w	-	20% w/w	-
Aluminium hydroxide content	15% w/w	-	-	-
Polyurethane foam core	-	-	30% w/w	-
Process aids	3% w/w	-	-	-

† Owens Corning Fiberglas SMC roving RO7EX1.

*Toray T300 B-12K-5 O B, having standard modulus and high strength.

4.3 The strength of recovered fibres.

The strength of the recovered fibres was measured with the aim of defining the optimum processing conditions in the fluidised bed for recovering valuable fibres.

4.3.1 The Weibull distribution.

The strength of a brittle fibre is governed by the stress threshold of the most severe flaw present on the surface and can be likened to the strength of a chain which is controlled by its weakest link. The strength of such materials is best described by a statistical distribution function proposed by Weibull [58] in 1951.

An expression for the two parameter Weibull probability density function, $P(\sigma)$, is given in Equation 4.1:

$$P(\sigma) = \frac{w\sigma^{(w-1)}}{\sigma_0^w} e^{-\left(\frac{\sigma}{\sigma_0}\right)^w} \quad 4.1$$

Where σ_0 and w are distribution parameters and σ is the fibre strength. σ_0 , known as the scale parameter, is the 63.2 percentile of the fibre strength population. The shape parameter, w , is inversely proportional to the spread of fibre strengths.

A term can be introduced into the Weibull distribution to account for the volume of material under test. Griffith [53] found that the strength of a brittle solid depends on the volume of the sample. The longer or thicker a glass fibre, the more likely it is to contain a very severe flaw and so the weaker it will be (Section 2.2.3). For the tests described in the following sections a constant gauge length of 10 mm was chosen for comparison between different samples of recovered fibre. Fibres of this length were common among the recovered fibres and allowed accurate alignment of the fibres during the tensile testing. All the fibres tested had the same nominal diameter and so the volume term could be omitted for comparison purposes.

4.3.2 Experimental method.

The single fibre tensile strength test method is outlined below. This method is based on ASTM method D3379-75 “Tensile strength and Young’s modulus for high modulus single filament materials”.

A sample of at least 20 individual filaments was taken from the reclaimed fibres which had

been collected from the exhaust gas flow of the FBC rig. Each fibre was attached with Delta Adhesives Extra Superglue cyanoacrylate adhesive to a 25 mm by 50 mm paper frame by which the fibre could be easily handled for diameter measurement and strength testing. The test gauge length was defined by the distance between the two anchoring points and was nominally 10 ± 1 mm. Fibre diameters were determined using a Panasonic F10 video camera attached to a Reichert microscope with an objective lens giving a sixty-threefold magnification. The enlarged ($\times 1250$) image of an individual fibre was viewed on a monitor. The screen was calibrated with a stage micrometer so that the fibre diameters could be measured directly. Surface contamination of recovered fibres and the size on fibres taken from virgin rovings made accurate determination of the fibre diameter difficult and the estimated accuracy of these measurements was $\pm 5\%$.

The fibres were tested for tensile strength using an Instron Universal testing machine fitted with a 1 N load cell and at a crosshead speed of 1 mm min^{-1} . Test room conditions were held at 23°C and 50% RH by an air-conditioning unit. The paper frames were gripped between the jaws of the testing machine and then the sides of the frame were burnt through by a hot wire to leave the unsupported fibre suspended between the two sets of jaws. Any pre-tension in the fibre was removed by careful adjustment of the crosshead position before testing.

A Weibull distribution function was fitted to the measured fibre strengths using a statistical analysis software package, Genstat [94]. This produced values for the Weibull parameters σ_0 and w , values for their associated standard errors and a measure of the deviance of the distribution from the measured strengths.

4.3.3 Reproducibility.

The reproducibility of the test method was established by conducting tests on repeat samples of virgin glass fibres and fibres recovered from the SMC feed at a bed temperature of 450°C (fluidising velocity 1.7 ms^{-1}) using the FBPR with the cyclone collection system in place. The virgin fibres tested were from an Owens Corning roving grade RO7EX1, as used in the original SMC. The two samples of fibre recovered from the SMC were taken from the top and bottom of the collection bin.

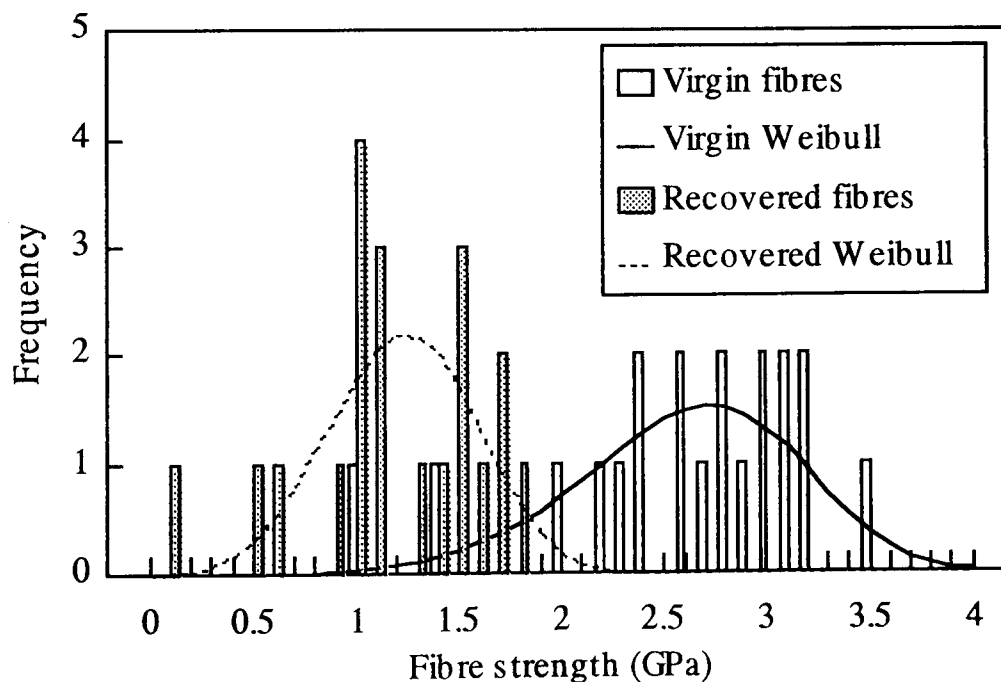
Results.

Statistics for the measured fibre strengths are shown in Table 4.2. Frequency histograms and fitted distributions are shown for one of the virgin fibre samples and one of the recovered fibre samples to give an illustration of the goodness of fit of the calculated distributions to the observed values (Figure 4.3).

Table 4.2 Weibull parameters for fibre strength distributions. Calculated using Genstat [94] for fibres taken from virgin roving and fibres recovered from SMC at 450°C. All χ^2 values were calculated on one degree of freedom.

Fibre source	virgin roving	virgin roving	SMC	SMC
σ_0 (GPa)	2.77	2.85	1.29	1.63
σ_0 error (GPa)	0.11	0.10	0.08	0.09
w	5.6	6.4	3.7	4.4
w error	1.1	1.2	0.7	0.8
N	20	20	19	19
χ^2	0.30	1.52	3.22	1.84

Figure 4.3 Single fibre strength distributions.
 Fibre description: E-glass, 13 μm diameter.
 Virgin fibre: Owens Corning roving RO7EX1.
 Recovered fibre source: SMC feed
 Fluidised bed conditions: 450°C, 1.7 ms^{-1} .
 Gauge length: 10 mm.



Discussion.

The χ^2 values for each sample of fibres show that the calculated Weibull distributions fit the measured strengths at a significance level of 5%. It can be seen that the fibre strength distribution parameters for the two virgin samples are not significantly different (Table 4.2). This is to be expected for fibres manufactured by a well controlled process and shows that the strength test can be considered to be consistent. Scale parameters (σ_0) for the two samples of fibre recovered from the SMC feed at 450°C show a greater difference. This could be explained by their two different thermal histories within the fluidised bed. The average residence time of the fibres in the fluidised bed is not known. During operation of the FBPR it was noted [92] that some fibres were released as soon as the feed was introduced but that some fibres were trapped in the bed for the duration of the trial (normally less than 60 minutes). Fenwick [92] has shown that volatilisation of the composite polymer is an endothermic process which can maintain the fibres below the bed temperature until they are exposed to the hot gas. It has already been shown that the strength of heat treated fibres depends on the time spent at elevated temperature and although samples of fibres taken from the same area of the collection bin might be expected to have similar thermal histories, this is unlikely to have been the case for samples taken from different parts of the collection bin and this could explain the measured discrepancy.

4.3.4 Effect of processing conditions on recovered fibre strength.

Samples of recovered fibres were tested for tensile strength to investigate the strength loss and to indicate optimum conditions for the recovery of strong fibres. Fibres were recovered from the SMC at fluidised bed temperatures of 450°C, 550°C and 650°C and at fluidising velocities of 1.3 ms⁻¹ and 1.7 ms⁻¹ using the cyclone recovery system. These conditions represent the full range over which the SMC could be successfully processed. Below 450°C the polyester resin does not break down whilst temperatures over 650°C severely weaken the glass fibres (Chapter 2). At fluidising velocities of less than 1.3 ms⁻¹ glass fibres were not swept from the fluidised bed and at fluidising velocities higher than 1.7 ms⁻¹ substantial amounts of bed sand were ejected.

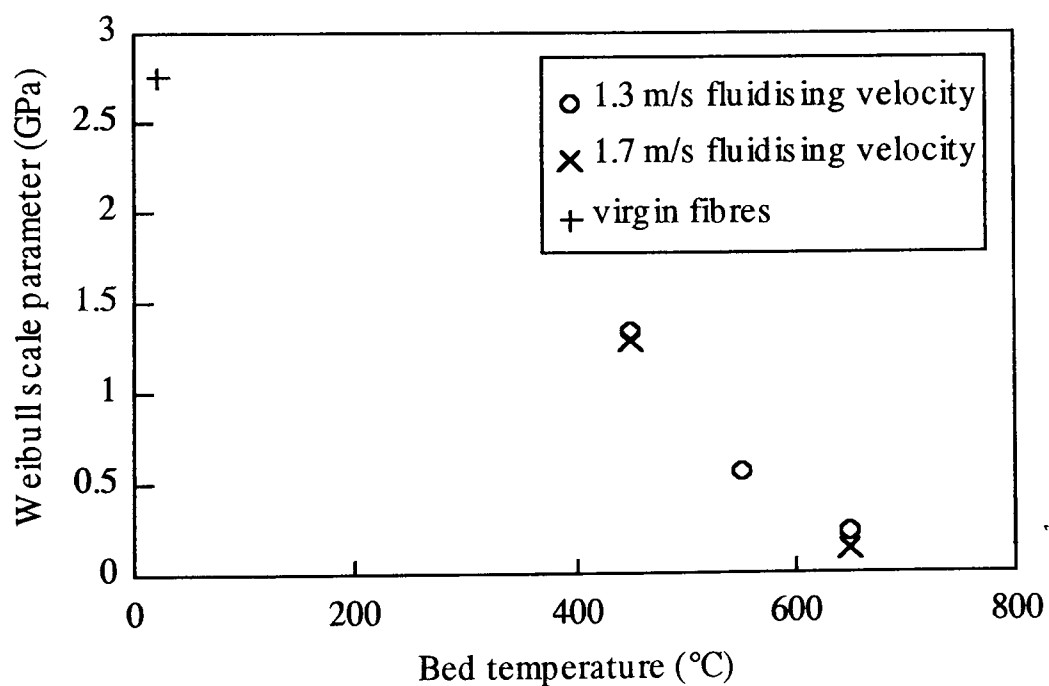
Results.

Statistics for the recovered fibres are shown in Table 4.3. A graph of Weibull scale parameter σ_o against fluidised bed temperature is shown in Figure 4.4.

Table 4.3 Weibull parameters for fibre strength distributions. Calculated by Genstat [94] for fibres recovered under different FBPR conditions from the SMC feed. All χ^2 values calculated on one degree of freedom.

Bed temperature (°C)	450	450	550	650	650	virgin
Fluidising velocity (ms ⁻¹)	1.3	1.7	1.3	1.3	1.7	
σ_o (GPa)	1.34	1.29	0.56	0.23	0.14	2.77
σ_o error (GPa)	0.05	0.08	0.10	0.06	0.03	0.11
w	6.0	3.7	1.4	1.2	1.3	5.6
w error	1.1	0.7	0.3	0.3	0.2	1.1
N	20	19	18	13	19	20
χ^2	1.99	3.22	9.89	0.45	1.52	0.30

Figure 4.4 Effect of bed temperature on Weibull scale parameter.
 Virgin fibre: Owens Corning roving RO7EX1.
 Recovered fibre source: SMC
 Gauge length: 10 mm.



Discussion.

It can be seen from Figure 4.4 that as the fluidised bed temperature increases the strength of the recovered fibres, as represented by σ_0 , decreases. This strength decrease is approximately linear over the range of bed temperatures investigated. The bed residence times are not known. Fibres are elutriated from the bed almost as soon as the feed material is introduced and, in most cases, operation of the rig was ended after one hour of processing. Thus the maximum bed residence time was one hour. These results compare favourably with those presented in Figure 3.7 for the proportion of virgin strength retained for heat treatment of long duration (the asymptotic value). It appears, therefore, that bed residence times are longer than the minimum needed for 90% of the long term strength loss, as given in Figure 3.8.

It would appear that fluidising velocity has little effect on recovered fibre strength over the range investigated. Bed residence time is expected to be inversely related to air fluidising velocity and it has already been shown that fibre strength depends on time at temperature. This suggests that the single fibre strength test is insensitive to fluidising velocity. Any such effect is dwarfed by the effect of processing temperature and can probably be disregarded.

4.3.5 Comparison of rotating screen and cyclone collection systems.

Initial development of the FBPR was carried out with the cyclone collection system described in Section 4.1.1. This system collected the fillers and fibres from the feedstock in a single collection vessel. One obvious improvement to the FBPR was to alter it to recover fibres and fillers separately. The rotating screen separator was designed by Fenwick [92] to achieve this. A cold water spray system was also added so that recovered fibres were cooled quickly and lubricated to prevent fibre deterioration by abrasion against other fibres or process plant. The spray also offered the opportunity to resize the fibres if required. To test whether glass fibres collected with the rotating screen system were recovered with higher strengths than those collected with the cyclone system, fibres were recovered from SMC feed using both recovery systems and identical fluidised bed processing conditions.

Results.

Weibull distribution parameters for the strengths of the recovered fibres are shown in Table 4.4. A graph showing the calculated Weibull strength distributions for the two samples of fibres is shown in Figure 4.5.

Table 4.4 Weibull parameters for fibre strength distributions. Calculated by Genstat [94] for fibres recovered from SMC using rotating screen and cyclone collection systems. Fluidising velocity 1.3 ms^{-1} in each case. Degrees of freedom for χ^2 given in brackets.

Collection system	Cyclone	Rotating screen	Cyclone	Rotating screen
Fluidised bed temperature ($^{\circ}\text{C}$)	450	450	550	550
σ_0 (GPa)	1.34	1.56	0.56	0.70
σ_0 error (GPa)	0.05	0.10	0.10	0.06
w	6.0	3.6	1.4	2.2
w error	1.1	0.6	0.3	0.3
N	20	27	18	27
χ^2	1.99 (1)	0.42 (2)	9.89 (1)	1.54 (2)

Discussion.

χ^2 values show that Weibull distributions give a good fit to the measured fibre strengths (except for the sample collected at 550°C with the cyclone system). At both processing temperatures investigated there has been a slight increase in the strengths of the fibres recovered using the rotating screen system over the cyclone system. The sizes of the uncertainties in the scale parameters make it difficult to draw any firm conclusions. It appears that use of the rotating screen system for recovering glass fibres may lessen the reduction in strength of the glass fibres during collection by reducing the time spent at temperature but this is insignificant compared to the degree of fibre weakening that occurs within the fluidised bed.

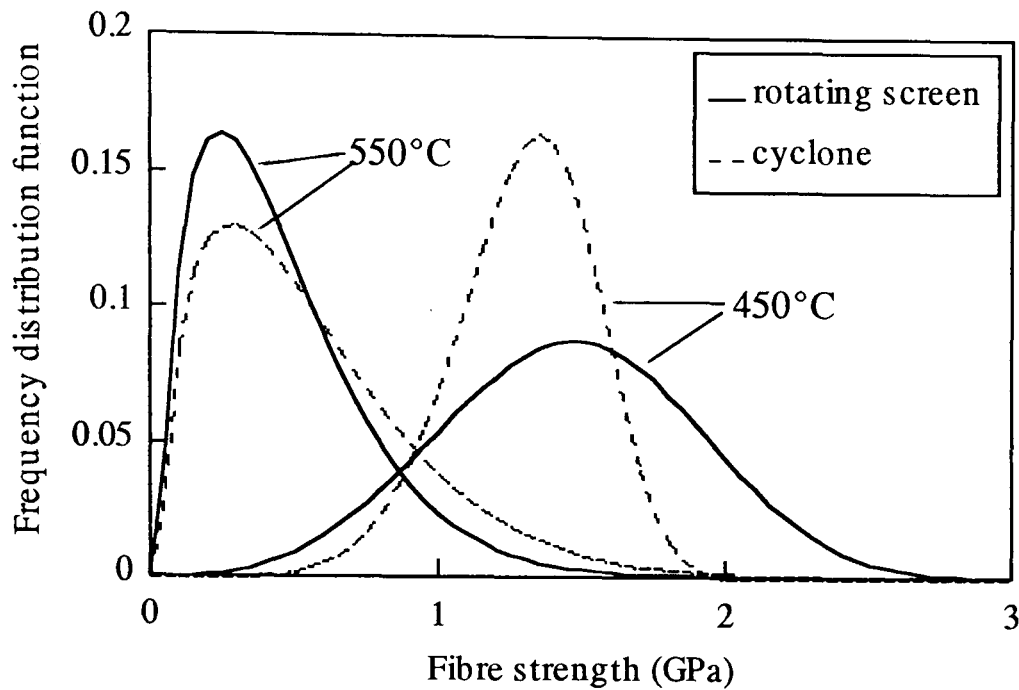
Figure 4.5 Effect of recovery system on Weibull strength distributions for single fibres.

Fibre type: E-glass.

Source: SMC.

Fluidised bed conditions: 450°C and 550°C.

Gauge length: 10 mm.



4.3.6 The strength of fibres recovered from FW pipe.

Fibres were recovered from the FW pipe using the rotating screen collection system and fluidised bed temperatures of 450°C and 500°C. The strengths of these fibres were measured using the technique already described. Scale and shape parameters for the fitted Weibull distributions are shown in Table 4.5.

Fibre recovered from the FW pipe at 450°C have strengths comparable to those recovered from the SMC feed at the same temperature, which is as expected. The two samples of fibres recovered from the FW pipe show little difference in strength distribution. The fibres recovered at 500°C have similar Weibull strength distribution parameters to those recovered at 450°C. This supports the view that under any given fluidised bed conditions some fibres will be released very quickly, and avoid complete degradation, whilst others will be trapped in the bed and suffer the full loss of strength attributable to that bed temperature. If this is true, then the fibres recovered from the FW pipe at 500°C must have been released from the fluidised bed relatively quickly and those recovered at 450°C, relatively slowly.

Table 4.5 Weibull distribution parameters for fibre strength distributions. Calculated by Genstat [94] for fibres recovered from FW pipe at 450°C and 500°C. All χ^2 values calculated on one degree of freedom.

Fluidised bed temperature (°C)	450	500
Fluidising velocity (ms ⁻¹)	1.3	1.3
σ_o (GPa)	1.22	1.15
σ_o error (GPa)	0.08	0.08
w	3.9	3.6
w error	0.7	0.6
N	18	20
χ^2	0.28	1.63

4.3.7 The strength of recovered carbon fibres.

Due to their different chemical and physical properties, the carbon fibre reinforced composites were processed under slightly different conditions to those used for the glass fibre reinforced composites. Oxidation of carbon fibres in air occurs at temperatures over 400°C but temperatures in excess of this value are required for the breakdown of the epoxy matrix. Experience indicated that a temperature of 450°C was the lowest that could be successfully used and that 500°C would produce fibres with less organic contamination. Fibres were recovered with the FBPR operating at 450°C and 500°C respectively. The rotating screen collection system was used to recover the recycled carbon fibres from the fluidising air stream.

A fluidising velocity of 1.0 ms⁻¹ was used. This is lower than the velocities used for the recovery of glass fibres. The fluidising velocity was reduced to a minimum value to prevent partially processed fibre bundles from being elutriated from the bed. The smaller carbon fibre diameter and reduced density compared to glass fibres ensured that single carbon fibres released from the decomposing matrix were successfully removed from the bed by the reduced fluidising stream.

The method used for measuring the strength of recovered glass fibres was used (section

4.3.2). The recovered fibres were tested against fibres taken from the same grade of virgin roving used to manufacture the FW propshaft, Toray T300-12K-50B. Twenty five samples of each fibre type were prepared but due to their high stiffness the fibres were easily broken during handling and so fewer than 25 measurements were made in some cases.

Results.

Weibull parameters for the measured fibre strength distributions are given in Table 4.6 and fitted and measured strength distributions for the virgin and recovered at 450°C fibres are shown in Figure 4.6.

Table 4.6 Weibull distribution parameters for virgin and recovered carbon fibre strength distributions. Calculated by Genstat for fibres recovered from the FW propshaft at 450°C and 500°C and virgin Toray T300 fibres.

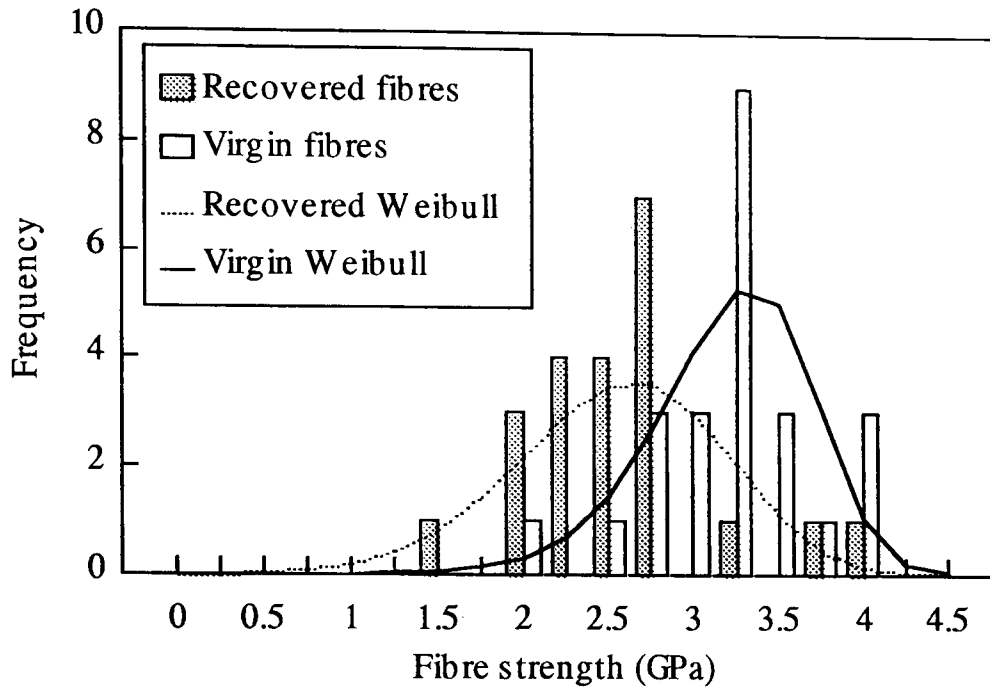
Fluidised bed temperature (°C)	450	500	Virgin
σ_0 (GPa)	2.65	2.29	3.27
σ_0 standard error (GPa)	0.13	0.22	0.09
w	4.7	2.9	8.1
w standard error	0.7	0.7	1.3
N	22	14	24
χ^2	3.75 (2)	0.36 (1)	2.56 (2)

Figures in brackets are degrees of freedom.

Discussion.

All the Weibull distributions presented in Table 4.6 fit the measured strengths at a 5% significance level. The Weibull scale parameter describing the distribution of strengths of the carbon fibres recovered at 450°C was 81% of that of virgin fibres of the same grade. Carbon fibres recovered at 500°C were weaker than those recovered at the lower bed temperature and retained only 70% of their initial strength. The carbon fibres were less severely weakened than glass fibres recovered under similar conditions (50% strength retention for E-glass fibres recovered at 450°C, section 4.3).

Figure 4.6 Single fibre strength distributions.
 Fibre description: PAN based carbon, 8 μm diameter.
 Virgin fibre: Toray roving.
 Recovered fibre source: FW propshaft.
 Fluidised bed conditions: 450°C, 1.0 ms^{-1} .
 Gauge length: 10 mm.



Carbon fibres are brittle materials, like glass fibres, and their strengths are therefore controlled by cracks, acting as stress concentrators. It is possible that scratches are introduced on to the carbon fibre surfaces during FBPR processing or that some sites on the surface are more prone to oxidation leading to the formation of cracks. It is unlikely that there is any change in the basic structure of the carbon fibres which is fixed during the final high temperature treatment stage of their manufacture and is very stable. Carbon fibres are less prone to surface damage than glass fibres and, in some cases, do not need a protective size to be applied during manufacture [89] and this may account for part of their improved ability to resist weakening during fluidised bed processing.

The recovered carbon fibres and the virgin fibres had the same fibre diameter (8 μm), within experimental uncertainty. Yin et al [95] measured a reduction in the diameter of carbon fibres after heating at temperatures over 550°C in air. If the fibres were well separated and air was allowed access to all sides of the fibre, the diameter was found to decrease linearly with time at temperature. At a temperature of 550°C a 10% diameter decrease was measured after nearly six hours heating. In contrast heating at 700°C for one

hour produced a diameter decrease of approximately 50%. These results imply that carbon fibres would need to be resident in a fluidised bed at 500°C for times greater than six hours to produce a measurable decrease in diameter. In both the cases described, processing of the CFRP feed materials was completed within two hours and so no significant diameter reduction should be expected, assuming the fibres were only subjected to the bed temperature.

4.4 Recovered fibre lengths.

The reinforcement provided by a fibre to a polymer matrix depends on the fibre strength, fibre modulus, fibre-matrix bond and the length of the fibre. According to the shear lag theory developed by Cox [96] there are regions at the ends of a fibre which do not carry the full load in a stressed composite. The total length of this ineffective region depends on the bond between the fibre and the matrix. For short fibres, the ineffective length is a large proportion of the total fibre length and so their reinforcement potential is reduced. The degree of reinforcement which can be provided by reclaimed fibres can be predicted if the fibre length distribution is known.

Glass fibres recovered from SMC, FW pipe and sandwich panel feeds (Table 4.1) were analysed for length. The variation in fibre lengths within a batch of recovered fibres, the effect of temperature on recovered fibre lengths and the lengths of fibres recovered from various feed materials were investigated.

4.4.1 Method.

An image analysis system set up in the Mechanical Engineering Department at the University of Nottingham was used to measure the lengths of the recovered fibres. The system comprises two distinct parts: image capture and image analysis.

A sample of recovered fibres was manually dispersed in a 100 mm diameter petri dish using tweezers and Perspex rods sharpened to a point at one end. The petri dish was then placed on a piece of black card with a 50 mm diameter aperture. This in turn was supported approximately 200 mm above a 180 mm diameter Phillips 25 W circular fluorescent tube by a Perspex cylinder. This arrangement caused that part of the petri dish

above the hole in the supporting card to be illuminated evenly. A vertically adjustable mounting supported a Panasonic WV BL200/B CCTV video camera approximately 50 mm above the sample. The camera was fitted with a 1 mm spacing ring and a 16 mm Cosmicar television lens and was connected to a PC running DT-Open Layers software [97] which displayed an image of the fibres on a monitor. The image was focused by adjusting the position of the camera and the focal length of the lens. The intensity of the image could be adjusted via the lens aperture. A setting of f 11 produced an image of acceptable quality. A 37 mm by 28 mm frame containing the fibres was captured by the imaging software as a 768 pixel by 576 pixel digital image.

The captured image was then processed by Aphelion Image Understanding software [98]. This software was used to run a macro (Appendix A) which identified the fibres in the image and measured their lengths. This system could not measure fibres of length less than 400 μm (Appendix A).

The Nottingham system was calibrated using a sample of fibres of known length (Appendix A). Also, samples of recovered fibres were measured with both the Nottingham system and a commercially available system developed at the Interdisciplinary Research Centre (IRC) in Polymer Science and Technology at the University of Leeds [99] which demonstrated that the Nottingham system gave an accurate assessment of the fibre lengths (Appendix A).

4.4.2 Length distribution variation within a batch of recovered fibres.

The fluidised bed processing rig with the rotating screen collection system was used to recover fibres from the FW pipe feed at a bed temperature of 500°C. Five samples of fibres were taken from different positions in the collection bin and their length distributions were measured.

Results.

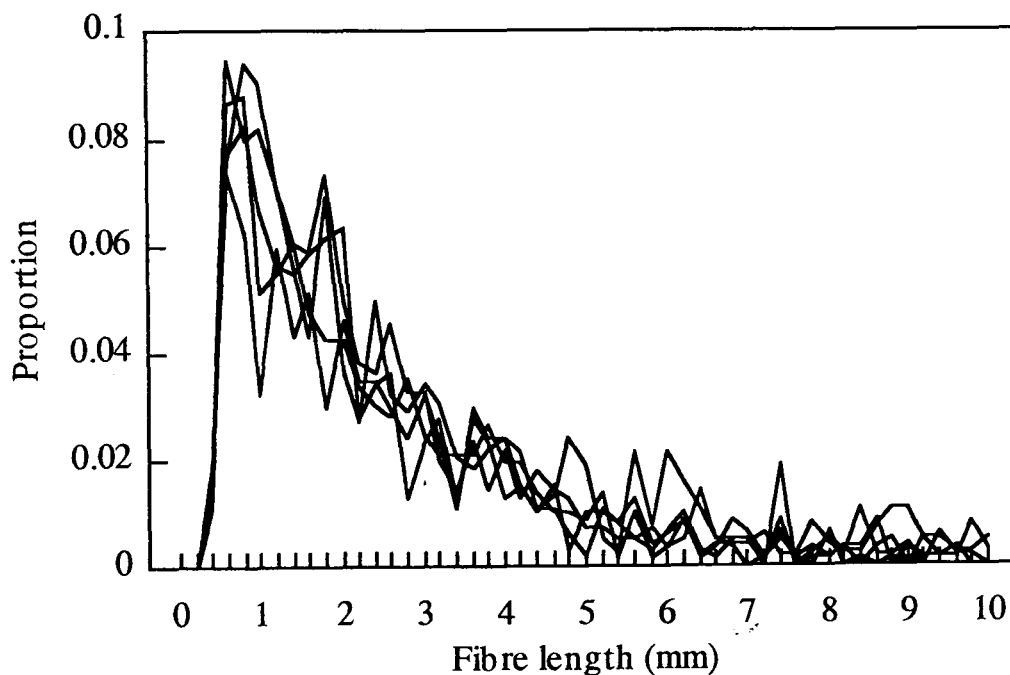
Weight and number average lengths (Appendix A, Equations A.1 and A.2) are presented in Table 4.7 and length distribution histograms for the five samples are shown in Figure 4.7.

Table 4.7 Weight and number average fibre lengths for five samples of recovered fibres taken from one FBPR trial. The fibres were recovered from FW pipe with a fluidised bed temperature of 500°C.

Sample	1	2	3	4	5
L_n (mm)	2.77	2.66	2.63	2.89	3.49
L_w (mm)	5.85	4.82	4.71	5.79	5.98
N	554	575	539	456	363

Figure 4.7 Length distribution of recovered fibres (5 samples).

Source: FW pipe.
 Fluidised bed temperature: 500°C.
 Collection system: rotating screen.
 Measurement system: Nottingham, 200 μm bins.



Discussion.

Table 4.7 and Figure 4.7 show that the five samples of recovered fibres had similar length distributions. The five samples were taken from different positions within the bulk of the recovered fibres and so represent the output from the fluidised bed at different times during the trial. Therefore, these results suggest that the length distribution of recovered fibres does not vary over time, unlike the recovered fibre strengths (Section 4.3.3).

4.4.3 The effect of fluidised bed temperature on recovered fibre lengths.

The fluidised bed processing rig with the rotating screen collection system was used to recover fibres from the FW pipe feed at a bed temperature of 450°C. A sample of fibres was prepared and analysed with the Nottingham fibre length measurement system. The results of this analysis are compared with the results of length measurements performed on fibres recovered from the same material but with a fluidised bed temperature of 500°C presented in the previous section.

Results.

Mean fibre lengths for the fibres recovered at 450°C and 500°C are compared in Table 4.8. The fibre length distributions are shown in Figures 4.8 and 4.9.

Table 4.8 Weight and number average fibre lengths for fibres recovered from FW pipe feed with a fluidised bed temperatures of 450°C and 500°C.

Process temperature	450°C	500°C
L_n (mm)	2.07	2.84
L_w (mm)	3.47	5.41
N	500	2487

Discussion.

Comparison of the mean fibre lengths presented in Table 4.8 show that the fibres recovered at the higher temperature have greater mean lengths. One explanation is that fibres are liberated from the fluidised bed more quickly at higher temperatures and so suffer less mechanical damage from the bed sand. However, this difference is probably not significant and may just be an indication of the batch to batch variation. Fluidised bed temperature had little effect on recovered fibre length over this range.

Figure 4.8 Length distribution of recovered fibres.

Source: FW pipe.

Fluidised bed temperature: 450°C.

Collection system: rotating screen.

Measurement system: Nottingham, 200 μm bins.

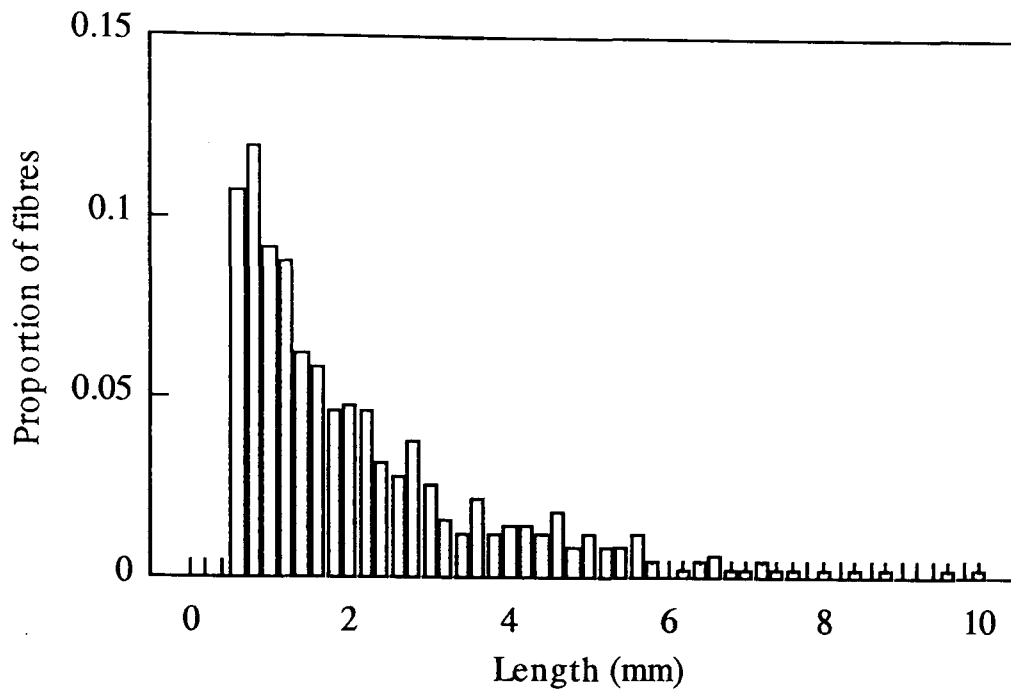


Figure 4.9 Length distribution of recovered fibres.

Source: FW pipe.

Fluidised bed temperature: 500°C.

Collection system: rotating screen.

Measurement system: Nottingham, 200 μm bins.

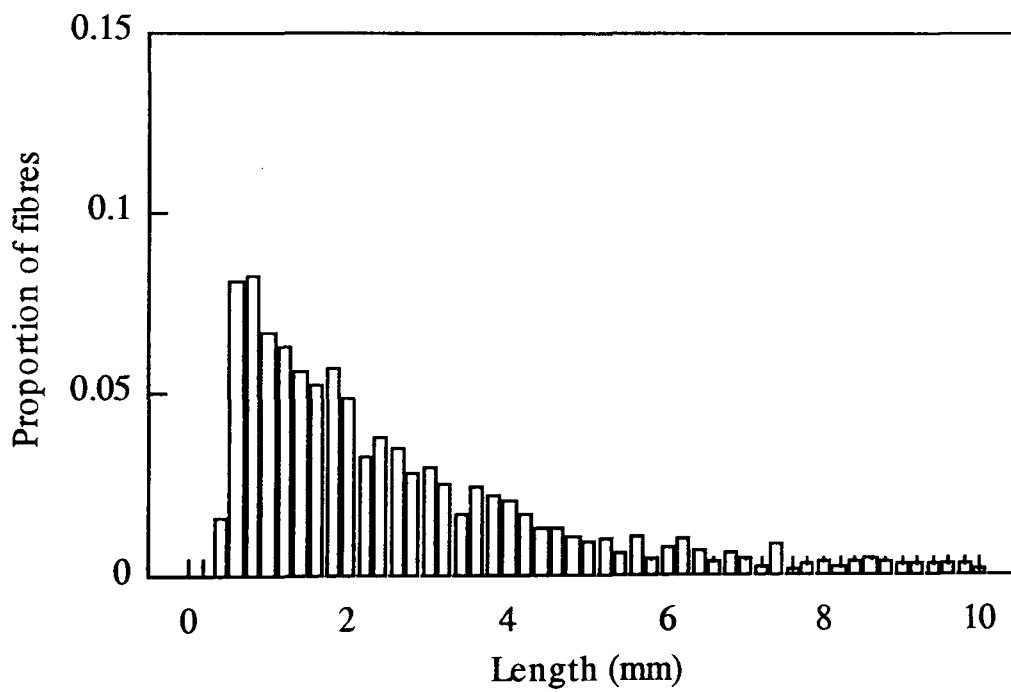


Figure 4.10 Length distribution of recovered fibres.

Source: SMC.

Fluidised bed temperature: 450°C.

Collection system: cyclone.

Measurement system: Nottingham, 200 μm bins.

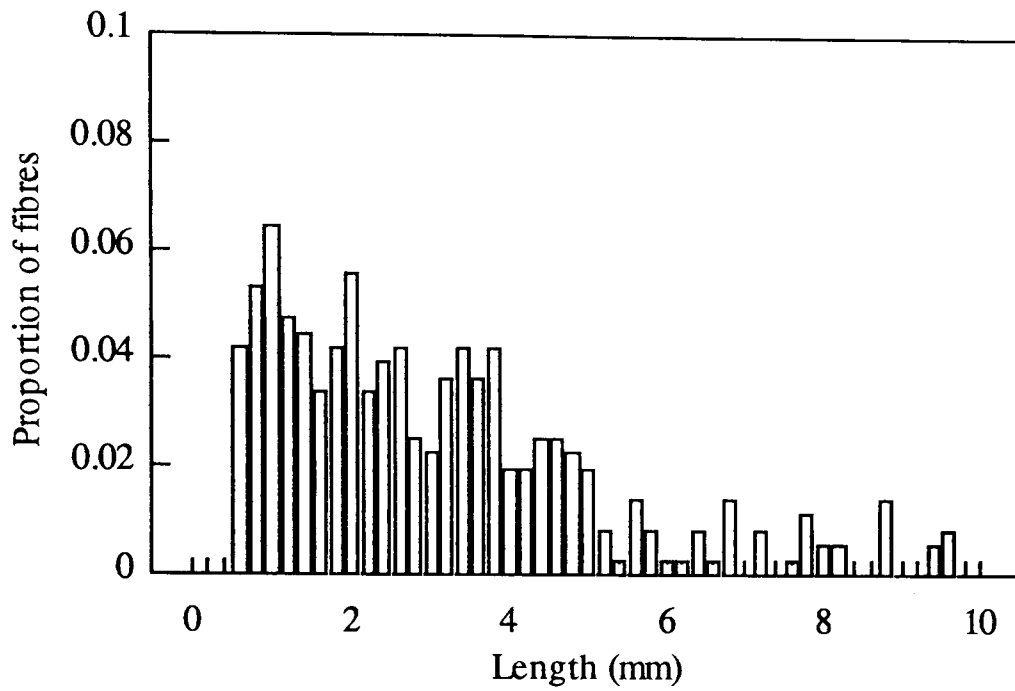


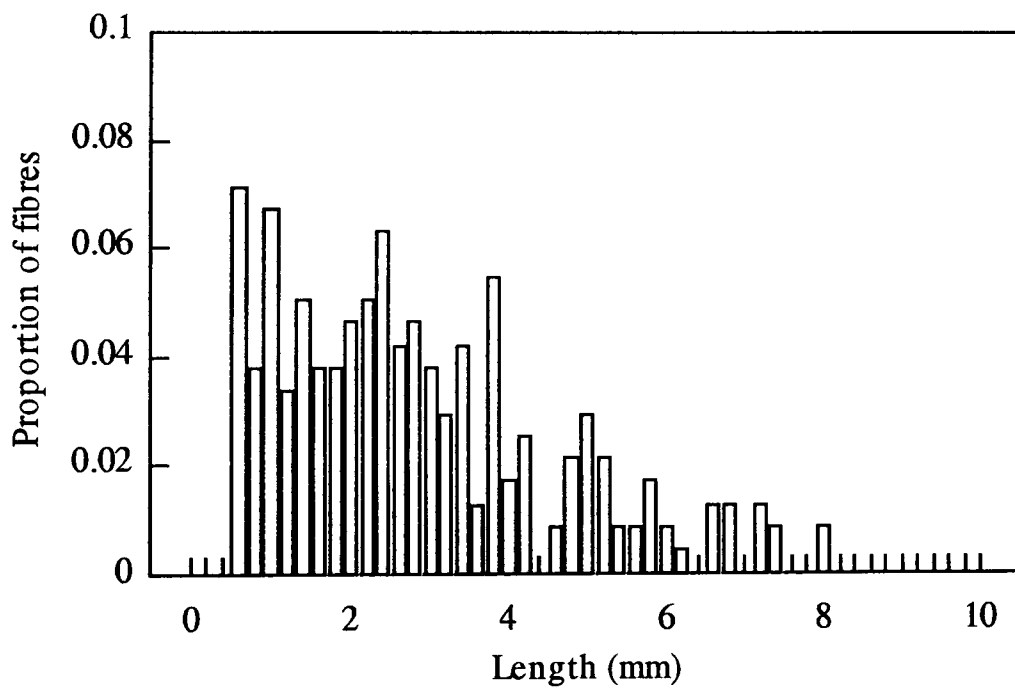
Figure 4.11 Length distribution of recovered fibres.

Source: Sandwich panel.

Fluidised bed temperature: 450°C.

Collection system: rotating screen.

Measurement system: Nottingham, 200 μm bins.



4.4.4 Fibre length distributions of fibres recovered from various feed materials.

Fibres were also recovered from the polyurethane foam cored glass/polyester sandwich panel (Table 4.1) at 450°C with the rotating screen filter and SMC at 450°C with the cyclone collection system and these results are presented here and compared to the fibre length distributions already measured.

Results.

The results already presented (Table 4.8) for the FW pipe samples recovered at 450°C and 500°C are compared with the mean lengths of fibres recovered from the SMC and the sandwich panel in Table 4.9. The measured length distributions for the SMC and sandwich panel fibres are shown in Figures 4.10 and 4.11 respectively.

Table 4.9 Number and weight average lengths of recovered fibre samples.

	Composite feed material			
	SMC	FW pipe		Panel
FB temperature (°C)	450	450	500	450
L_n (mm)	3.31	2.07	2.84	2.88
L_w (mm)	5.55	3.47	5.41	4.26
N	355	500	2487	238

Discussion.

Fibres recovered from the SMC feed at 450°C had an average fibre length of 3.31 mm, 60% greater than those fibres recovered from the FW pipe (average length 2.07 mm) at the same temperature. The weight average length of the fibres recovered from the SMC was also 60% greater than that measured for the fibres recovered from the FW pipe. The longer fibres arising from the SMC feed were attributed to the fact that the SMC feed was prepared by shredding and screening to 20 mm but the FW pipe and sandwich panel feeds were prepared by hammer milling and screening to 10 mm. Particle size distributions for two types of SMC shredded to pass through a 20 mm screen and hammer milled through a 10 mm screen [100] show that the fraction of fine material is much greater in the hammer milled sample and so there are likely to be more short fibres. The rotating screen

(with a 1 mm mesh) might have been expected to result in few short fibres being recovered but this effect does not seem to be significant. Use of a 400 μm cut off for the length measurements may have removed any effect of the rotating screen collection system.

The fibres recovered from the SMC and sandwich panel feeds have similar shaped length distributions which are significantly different from those from the FW pipe. There are more short fibres in the sample recovered from the FW pipe. This requires further investigation but could be due to the behaviour of the composite during initial size reduction. Both the SMC and the sandwich panel had fibre fractions below 25% w/w with lower thicknesses and stiffnesses than the FW pipe material and so may be less prone to damage during the size reduction operation.

4.5 The stiffness of recovered fibres.

The modulus of a fibre is critical to its performance in a composite. The effect of processing on fibre Young's modulus was investigated.

4.5.1 Method.

Fibre modulus can be measured by tensile [101] or ultrasonic [102] techniques. These both require specialised apparatus and so a vibrating cantilever method was employed. Relevant cantilever theory and a description of this test method are given in Appendix D.

4.5.2 Effect of processing conditions on the modulus of glass fibres.

The Young's moduli of fibres taken from virgin E-glass roving (Owens Corning grade RO7EX1) were measured using the vibrational technique described in Appendix D. Fibres recovered from the FW pipe at bed temperatures of 450°C and 500°C using the rotating screen collection system were also tested. The results are given in Tables 4.10, 4.11 and 4.12.

Discussion.

An accepted value for the Young's modulus of an E-glass fibre is 69 - 72 GPa [103] which is within the range measured for the single virgin E-glass using this vibrational method

(Table 4.10). The Young's moduli of the recovered fibres are not significantly different to that measured for the virgin fibres, given the experimental uncertainty in the measurements. The variation in the Young's modulus values for the recovered fibres is greater than that measured in the virgin fibres. This increase can probably be accounted for by surface contamination, which has two effects. The first is to make accurate determination of the fibre diameter difficult and the second is to alter the dynamics of the vibrating fibre which changes the frequency at which the system resonates.

Table 4.10 Young's moduli of glass fibres taken from Owens Corning Fiberglas virgin roving grade RO7EX1. Standard deviation given in brackets.

Fibre	E(f ₂) (GPa)	E(f ₃) (GPa)	E(f ₄) (GPa)	E(f ₅) (GPa)	E(f ₆) (GPa)	E mean (GPa)
1	*	67	69	67	71	69
2	*	77	74	76	*	76
3	70	70	69	*	*	70
4	67	72	74	*	*	71
combined						71 (3)

* resonance could not be determined.

Table 4.11 Young's modulus figures for glass fibres recovered from FW pipe at 450°C. Standard deviation given in brackets.

Fibre	E(f ₂) (GPa)	E(f ₃) (GPa)	E(f ₄) (GPa)	E mean (GPa)
1	103	93	95	97
2	78	80	80	79
3	66	65	66	66
4	71	69	72	71
5	*	98	*	98
6	84	*	*	84
combined				80 (13)

* resonance could not be determined.

Table 4.12 Young's modulus figures for glass fibres recovered from FW pipe at 500°C. Standard deviation for combined figures given in brackets.

Fibre	E(f ₂) (GPa)	E(f ₃) (GPa)	E(f ₄) (GPa)	E mean (GPa)
1	54	54	57	55
2	76	64	64	68
3	58	57	59	58
4	86	71	74	77
5	83	86	91	87
combined				69 (13)

Both the recovered and virgin glass fibres have a circular cross section which is not expected to vary significantly over the test length and so the assumption of a constant circular cross section for the fibres is valid. It has already been stated that surface contamination can hinder accurate diameter measurement and it is the uncertainty in the fibre diameter measurement which is the main source of uncertainty in the calculation of Young's modulus. The effect of surface contamination on the dynamics of the vibrating fibre are negligible in comparison. A 50 μm cube of a typical filler material attached to the end of the fibre (worst case) would only produce a 3% change in the calculated modulus compared to a coefficient of variance of 19% for the fibres recovered at 500°C.

Damping of the fibre oscillations can probably be ignored. Other researchers [104] using shifts in the resonant frequency of a vibrating fibre to measure a small mass attached to the fibre's end, measured the damping coefficient and found it to be negligible.

Loewenstein [52] states that the density of glass fibres is approximately 2% less than that for bulk glass of the same composition due to the rapid quenching of the fibres during manufacture. The fibre density used in the calculation of Young's modulus is that for an virgin E-glass fibre. However, heating the fibre during recovery may allow some relaxation of the structure with the result that fibre density may increase. Since Young's modulus is linearly related to beam density (Equation D.5) this should not produce a large

error in the calculated value for the Young's modulus of the recovered fibres.

These results show that there is little difference between the Young's modulus of virgin and recovered glass fibres, which is in agreement with results presented in Chapter 3.

4.5.3 Effect of processing conditions on the modulus of carbon fibres.

The vibrating cantilever beam method was used to measure the Young's modulus of carbon fibres recovered from the FW propshaft at 500°C and carbon fibres taken from virgin roving of the same grade (Toray T300 B-12K-5 O B).

Fibres with lengths of approximately 15 mm were tested for Young's modulus. Five fibres from each sample were tested and the frequencies of the second, third and fourth resonant modes of vibration were used to calculate the fibre modulus.

Results.

The diameters of the recovered and virgin samples of carbon fibre were measured as part of the Young's modulus analysis. The fibre diameters and Young's modulus figures are shown in Table 4.13.

Table 4.13 Virgin and recovered carbon fibre diameters and Young's moduli. The figures in brackets are standard deviations.

	Virgin	Recovered at 500°C
Fibre diameter (μm)	8.2 (0.5)	6.8 (0.7)
Fibre modulus (GPa)	146 (22)	169 (62)

Discussion.

The reduced diameter of the recovered fibres is probably not statistically significant but may be an indication that oxidation of the fibre surface is starting to happen. Oxidation of the carbon fibres is expected at 500°C but only at a very slow rate. It is possible that pieces of crushed CFRP feed material could attain temperatures higher than the bed due to heat liberated by the combustion of the polymer.

Huxley [89] reports that the coefficient of variation of Young's modulus for carbon fibre filaments is typically 11%. The coefficient of variation for the virgin fibres is 15.1% whilst for the recovered fibres it is 36.7%. Any difference in Young's modulus between the virgin and recovered fibres is masked by the large amount of scatter.

Values for resonant frequency, fibre length, fibre diameter and fibre density are combined to calculate the Young's modulus of the fibre. Their associated uncertainties must also be combined to calculate the uncertainty in the value for Young's modulus. The greatest contribution to the uncertainty in the measurement of the Young's modulus of an individual fibre comes from the determination of the fibre diameter. Error theory predicts an uncertainty in the value for Young's modulus of the single fibres of approximately 8%.

Other sources of uncertainty are the assumptions that the fibres are clean and cylindrical. Particulate matter on the fibre surface will affect the frequencies at which the fibres start to resonate by altering the dynamics of the system. If the fibre is not cylindrical the assumptions made in deriving the expression for the Young's modulus would be incorrect. For the carbon fibres tested, optical and scanning electron microscopy indicated that the fibres did have a circular cross section.

Heat treatment in an oxidising atmosphere during fibre recovery might be expected to cause some limited oxidation of the fibre surface. Researchers [105-109] have found that the outer sheath of a carbon fibre can contain more highly aligned graphitic planes than the interior and so removal of this layer could lead to a reduction in fibre stiffness. However, the basic alignment and structure of the carbon crystallites within the core of the fibre, which are developed and fixed during the high temperature treatment phase of the fibre manufacture process, should not be affected by the relatively low temperatures encountered in the fluidised bed. Therefore, the Young's modulus of a carbon fibre, which is a function of the crystallite structure, should not be severely affected by the recovery process provided oxidation is limited. The results of this work are in agreement with this hypothesis.

4.6 Enhancement of recovered glass fibres.

Four factors affecting the level of reinforcement given by fibres to a matrix material are fibre strength, fibre modulus, fibre length and the fibre to matrix bond. Fibre strength was chosen as a potential area for enhancement.

4.6.1 Ion stuffing.

Ion stuffing or chemical strengthening is a technique used to improve the strength and abrasion resistance of bulk glass (Section 2.4.1). Similar techniques were investigated for application to recovered glass fibres.

Method.

A sample of fibres recovered from the SMC feed at a bed temperature of 450°C and using the cyclone recovery system was washed vigorously in tap water to remove any filler contamination. Approximately half of the fibres were soaked in a 3% solution of potassium nitrate and then removed and dried at room temperature in air. The fibres were found to be coated with approximately 30% by weight of potassium nitrate. These fibres were then placed in a preheated furnace at 500°C for one minute, removed, allowed to cool and then washed with a 3% solution of acetic acid to remove traces of the salt. The other half of the sample was washed in a 3% solution of acetic acid as a control.

Fibres taken from both samples were tested for tensile strength using the method described in Section 4.1.1.

Results.

Weibull distribution parameters are shown in Table 4.14 and the fitted probability density functions are shown in Figure 4.12.

Table 4.14 Weibull parameters for fibres recovered from SMC feed at 450°C with and without ion stuffing. All χ^2 values calculated on two degrees of freedom.

Treatment	Control	KNO ₃ , 500°C, 1 minute
σ_o (GPa)	1.76	2.04
σ_o error (GPa)	0.10	0.08
w	3.4	4.9
w error	0.5	0.7
N	29	29
χ^2	6.69	0.81

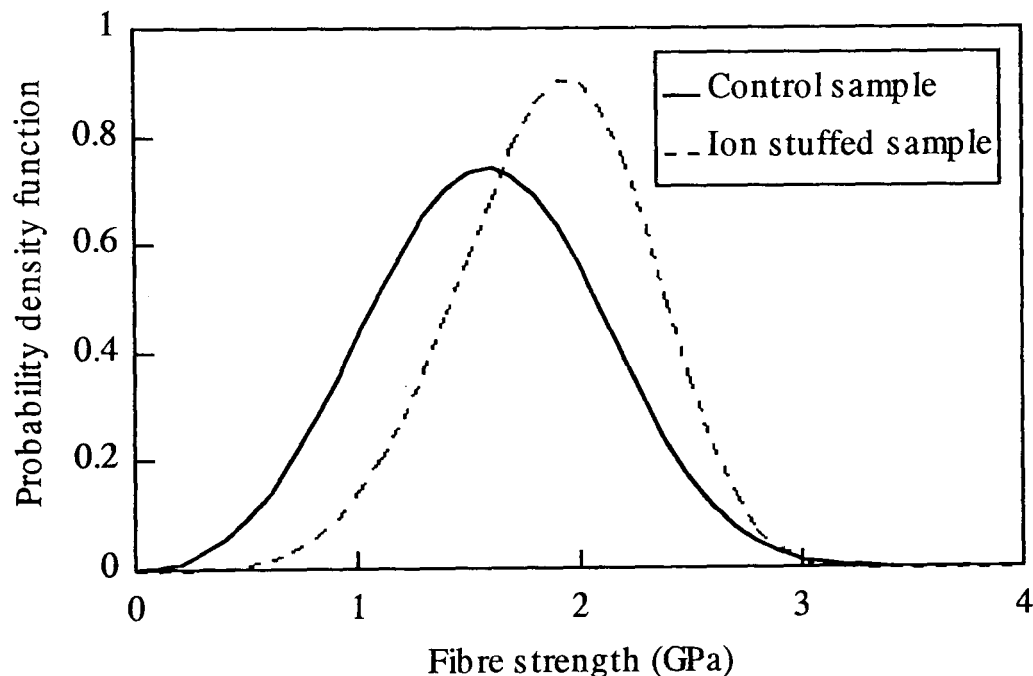
Figure 4.12 The effects of ion stuffing using potassium nitrate on recovered glass fibre strength.

Feed material: SMC.

Fluidised bed temperature: 450°C.

Ion stuffing conditions: 500°C, 1 minute.

Gauge length: 10 mm.



Discussion.

As predicted, ion stuffing the glass fibres significantly improved the strength of the recovered glass fibres. The Weibull scale parameter was increased by 16%. Although Table 4.2 suggests that there is some variation in strength between samples recovered under the same FBPR conditions, in this case both samples were taken from the same cluster of recovered fibres and were likely to have experienced similar thermal histories.

Fibres held in a curved state during the ion stuffing procedure were found to have been set in position after the treatment and this is further evidence that ion exchange had taken place.

No attempt was made to optimise the ion stuffing process and greater increases in strength might be achieved under different treatment conditions.

4.7 Conclusions.

Fibres have been recovered from a variety of thermoset composites. The properties of these fibres have been measured in order to characterise them and the effect of the recovery process fully.

It was found that the strengths of the recovered glass fibres decreased with increasing processing temperature. Fibres recovered at 450°C had approximately 50% of the strength of virgin fibres and those recovered at 550°C and 650°C retained only 20% and 7% of the virgin fibre strength respectively. Similar strength losses have been measured by other researchers (Chapter 2) and were attributed to the generation of flaws on the glass surface by numerous processes. Process temperature had the greatest effect on recovered fibre strength whilst bed residence time had a much smaller effect.

Carbon fibres were not as severely weakened as glass fibres. Carbon fibres recovered at 450°C and 500°C retained 80% and 70% of their virgin strength respectively. Degradation could be caused by abrasion and oxidation. Carbon fibres have good resistance to abrasion and are only slowly oxidised at these temperatures and so they retain their strength rather better than glass fibres.

For all the composites investigated, the number average length of the recovered fibres varied between 2 mm and 3 mm and the weight average length between 3.5 mm and 5.5 mm. As expected, fibres recovered from SMC shredded through a 20 mm screen generally had greater average lengths than those recovered from FW pipe and sandwich panel composites which were hammer milled through a 10 mm screen. The shape of the length distribution curves varied between samples. There was a high proportion of short fibres

amongst those recovered from the FW pipe and this was thought to be a result of hammer milling such a high fibre fraction composite.

The lengths of the recovered carbon fibres were not measured.

It was found by a vibrational method that the moduli of recovered glass and carbon fibres did not differ significantly from those of virgin fibres of the same grade. The modulus of a material is a function of its molecular structure which is not affected by processing in the fluidised bed over the range of temperatures investigated.

The recovered glass fibres can be strengthened by an ion exchange reaction on the fibre surface in which small metal cations are replaced by larger metal cations which create a compressive load in the fibre surface. This load limits the severity of any cracks present.

Given these fibre properties it is possible to predict their reinforcement potential in a new composite and this will be the theme of the next chapter.

Chapter 5.

The reinforcement potential of recovered fibres.

5.0 Introduction.

The ideal application, from both an environmental and economic perspective, for the reuse of fibres recycled from thermoset composites is as reinforcement in new thermoset composites. An investigation was undertaken into the efficiency of reinforcement provided by recovered fibres in a simple fibre and resin laminate. To maximise the reinforcing effect it is necessary to maximise the fibre volume fraction and this is normally achieved by aligning the fibres to some degree. Fibres are recovered by the fluidised bed rig in a random three dimensional orientation and so require further processing before use in a composite. Wet formed webs, in which the fibres have a random two dimensional orientation, give improved fibre packing and so the potential for an increase in fibre volume fraction when used as reinforcement in a composite material. For this reason, wet formed webs of virgin and recovered glass fibres and recovered carbon fibres were made and then impregnated with an epoxy resin. The resultant prepreg sheets were stacked and hot pressed to form laminates. These laminates were then tested and their measured properties were compared with predicted properties calculated from well known theories using the recovered fibre properties measured in Chapter 4.

5.1 Sample preparation.

Laminates were produced for mechanical testing using the methods described in the following sections.

5.1.1 Web preparation.

One sample of virgin glass fibres, three samples of recovered glass fibres and one sample of recovered carbon fibres were used to form the fibre webs. A summary of the processing conditions and feed materials used in the recovery of these fibres is given in Table 5.1. These fibres were randomly aligned in 2 dimensions by using the apparatus and method described in Section 6.2.1 for making glass fibre veils.

The fibres described in Table 5.1 were used in this investigation because their strengths, lengths (not the carbon fibres) and moduli had already been well characterised (Chapter 4). Contamination was washed away from the recovered fibres during the web formation process and binder was not applied. Instead, excess dispersion medium was removed by a vacuum box and the samples were allowed to dry at room temperature. The dry glass fibre webs were then placed on a nylon mesh which carried them through a trough containing a 1% epoxy resin compatible silane solution (OSi Specialities grade A-187) and then over a vacuum box (Figure 6.2). Excess silane solution was removed by the vacuum box and the resulting webs were allowed to dry at room temperature. The webs prepared with 18 mm long, 13 μm diameter wet chopped strands supplied by Owens Corning Veil Ltd. were prepared in an identical way. The final level of silane on the glass webs was calculated to be approximately 1%. The carbon fibre webs were not silane coated. The nominal areal densities of the glass fibre and carbon fibre webs were 65 gm^{-2} and 45 gm^{-2} respectively.

Table 5.1 Description of fibres used in laminate construction.

Label	WCS	SMC450	FW450	FW500	CF500
Fibre source	18 mm WCS	SMC	FW pipe	FW pipe	Shaft
Collection system	na	cyclone	rotating screen	rotating screen	rotating screen
FB temp. ($^{\circ}\text{C}$)	na	450	450	500	500

5.1.2 Laminate preparation.

The webs were converted into prepreg at GKN Technology Limited with a proprietary GKN resin system. The resin system was described as a toughened epoxy with aromatic amine curing agent and a T_g above 180 $^{\circ}\text{C}$. No further information can be given for commercial reasons. Between 20 and 22 plies of each prepreg grade were compression moulded at 164 $^{\circ}\text{C}$ for 18 minutes to form a plaque approximately 2 mm thick. The exact number of plies used was varied to produce a final fibre volume fraction in the laminate of approximately 25%. Finally, the plates were removed from the mould and post cured at 185 $^{\circ}\text{C}$ for 200 minutes.

5.2 Laminate testing.

Rectangular test pieces 180 mm by 10 mm were cut from the moulded plates. Five pieces from each laminate were tested in tension at a cross head speed of 1 mm min⁻¹ using an Instron Universal testing machine, model 1195. The specimen gauge length was 80 mm and sample extension was measured over a 50 mm gauge length using an Instron extensometer. Ultimate tensile strength and Young's modulus were recorded.

For measuring the flexural properties of the experimental laminates, rectangular test pieces 45 mm by 15 mm were cut from the moulded plates. Five pieces from each laminate were tested at a cross head speed of 1 mm min⁻¹ over a test span of 32 mm using the same testing machine. Indentor displacement was measured by a LVDT and was equated to sample deflection. Flexural strength and flexural modulus were recorded.

Both sets of test were based on BS 2782.

5.3 Results.

Void contents were measured by immersion and fibre volume fractions were determined by ashing. Procedures for making these measurements are given in Appendix B. When ashing composite materials containing glass fibres, temperatures of over 500°C can be used for extended periods to remove the matrix material without any effect on the mass of the remaining fibres. This is not true of carbon fibre reinforced composites. Procedures involving acid digestion of the matrix material exist for determining the fibre volume fraction of CFRP [110] but in this case, careful heat treatment was used. Samples of the recovered carbon fibre reinforced laminate were weighed before and after heating at 450°C for one hour. Ash remaining after this treatment had the appearance of clean carbon fibres. Similar heat treatment of a section of virgin carbon fibre tow caused a 20% weight loss but it was expected that the presence of the matrix material in the composite sample would protect the fibres from oxidation for the majority of the period of heating and so the fibre volume fraction measured in this way would be a close approximation to the true value. Laminate densities, void contents and fibre volume fractions are shown in Table 5.2.

Table 5.2 Fibre volume fractions and void contents for experimental laminates.

Label	WCS	SMC450	FW450	FW500	CF500
Density (gcm ⁻³)	1.57	1.54	1.52	1.46	1.24
Fibre volume fraction	0.26	0.25	0.26	0.23	0.22
Void content	0.00	0.00	0.04	0.05	0.07

Tensile strengths of the experimental laminates are compared in Figure 5.1 and flexural strengths in Figure 5.2. Tensile moduli of the experimental laminates are compared in Figure 5.3 and flexural moduli in Figure 5.4.

Figure 5.1 Ultimate tensile strength of experimental laminates.

Prepreg: random fibre / epoxy, 20 - 22 plies.

Fibre volume fraction: 25% nominally.

Fibres: virgin glass (WCS), recovered glass (SMC450, FW450, FW500), recovered carbon (CF500).

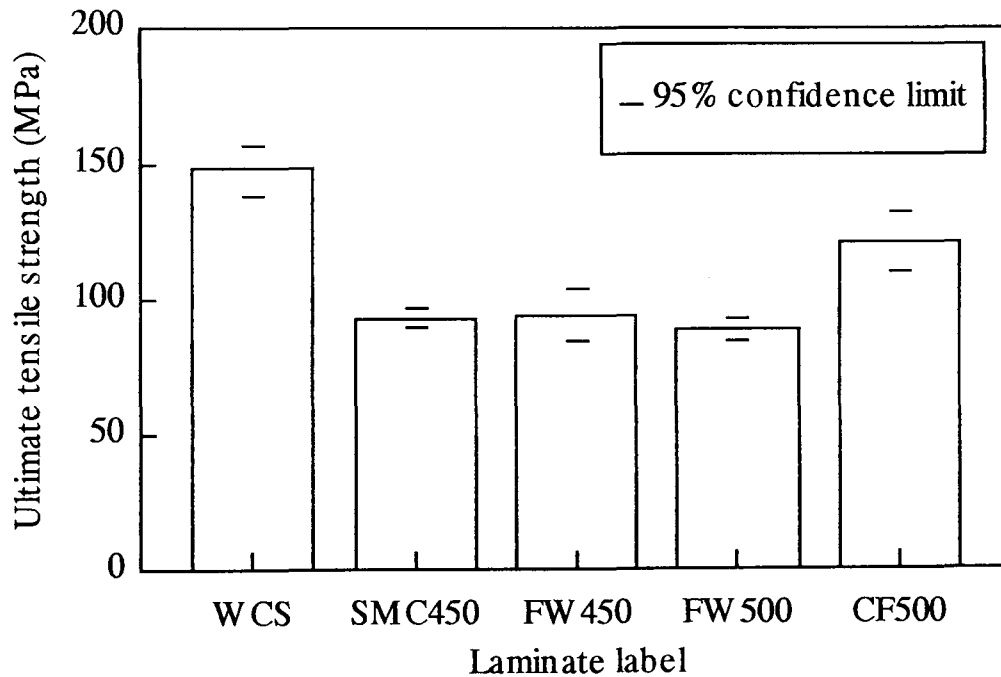


Figure 5.2 Flexural strength of experimental laminates.

Prepreg: random fibre / epoxy, 20 - 22 plies.

Fibre volume fraction: 25 % nominally.

Fibres: virgin glass (WCS), recovered glass (SMC450, FW450, FW500), recovered carbon (CF500).

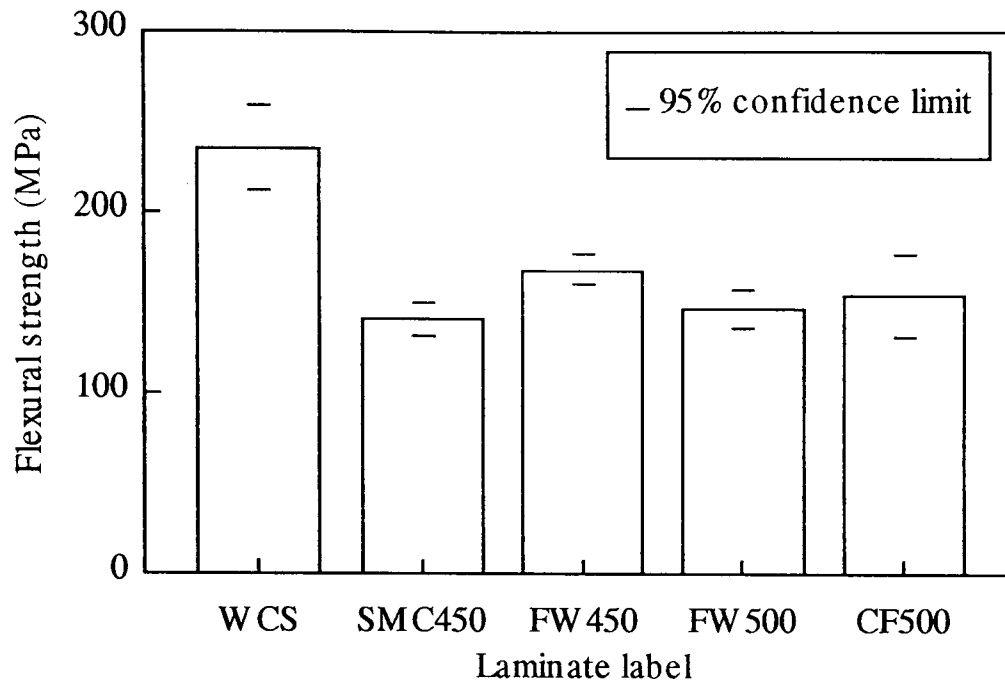


Figure 5.3 Young's modulus of experimental laminates.

Prepreg: random fibre / epoxy, 20 - 22 plies.

Fibre volume fraction: 25 % nominally.

Fibres: virgin glass (WCS), recovered glass (SMC450, FW450, FW500), recovered carbon (CF500).

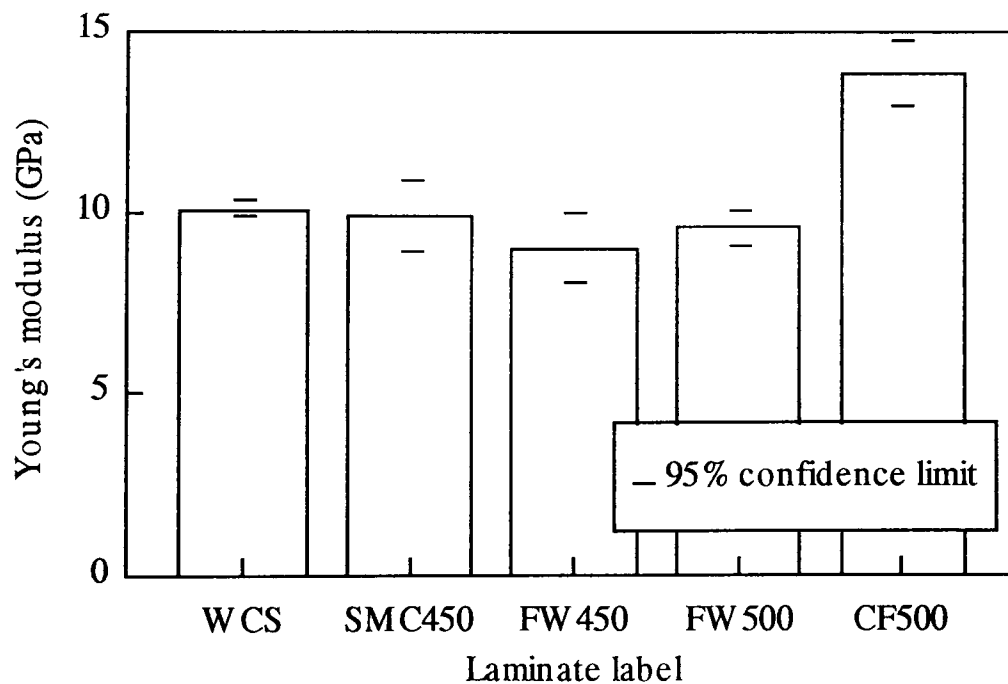
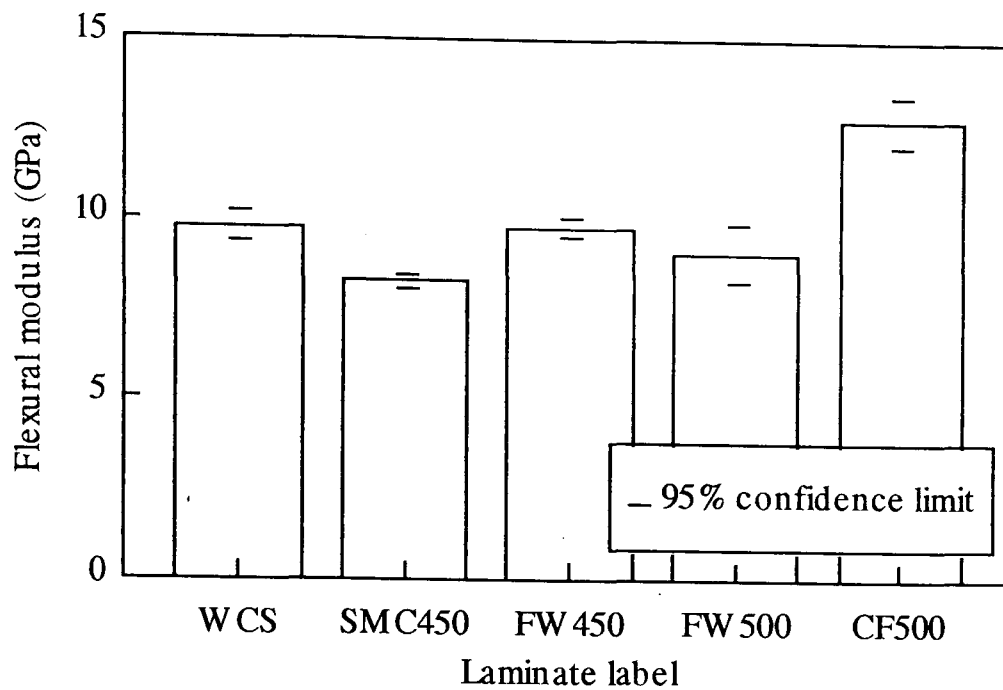


Figure 5.4 Flexural modulus of experimental laminates.

Prepreg: random fibre / epoxy, 20 - 22 plies.

Fibre volume fraction: 25 % nominally.

Fibres: virgin glass (WCS), recovered glass (SMC450, FW450, FW500), recovered carbon (CF500).



5.4 Discussion.

For two dimensionally aligned, random in plane, 13 μm diameter fibres of lengths up to 18 mm, the maximum volume fraction obtainable is approximately 20% to 30% [111]. It can be seen in Table 5.2 that the experimental laminates had close to their maximum volume fraction of reinforcing fibres present. Any attempt to increase the volume fraction of fibres would have led to the creation of voids or a reduction in the aspect ratio of the reinforcing fibres [91].

The tensile strengths of the laminates containing reclaimed glass fibres are equivalent, given the degree of scatter. The average tensile strength of these laminates is approximately 60% of the virgin fibre laminate tensile strength. The tensile strength of the recovered carbon fibre laminate is approximately 30% greater than for the recovered glass fibre laminates. Both these observations are broadly in agreement with the measured single fibre tensile strengths. The tensile strengths of the WCS filaments have not been measured and so an accurate comparison cannot be made.

There is some variation between the flexural strengths of the laminates containing recovered glass fibres but the average flexural strength is also approximately 60% that of the flexural strength of the virgin fibre laminate. The flexural strength of the recovered carbon fibre laminate is approximately equivalent to those of the recovered glass fibre laminates. Increased void content and surface imperfections, to which flexural properties are sensitive [112], may account for these findings.

The Young's moduli of the laminates containing glass fibres are equivalent, given the degree of scatter. Similar trends are seen with the flexural moduli, although there is more scatter in the results. The laminate containing recovered carbon fibres is approximately 50% stiffer than the glass fibre laminates. These observations are in agreement with the single fibre properties presented in Chapter 4.

5.5 Theoretical laminate properties.

Intuitively, the results presented in Section 5.4 seem in agreement with the conclusions drawn from measuring the properties of recovered fibres in Chapter 4. Further analysis was done to see how the measured mechanical properties of the experimental laminates compared to the predicted behaviour given the properties of the recovered fibres presented in Chapter 4.

5.5.1 Theoretical moduli of the experimental laminates.

The well known rule of mixtures for predicting the Young's modulus of a composite containing continuous unidirectional fibres is:

$$E_c = E_f V_f + (1 - V_f) E_m \quad 5.1$$

Cox [96] introduced a fibre length efficiency factor, η_l , to account for the fact that, when discontinuous fibres are present, a significant part of the length of a fibre provides ineffective reinforcement. Tensile forces acting on a composite material are transferred to the reinforcing fibres through shear stresses at the fibre-matrix interface. These tensile stresses vary from zero at the fibre ends to a maximum value in the middle of the fibre. That part of the fibre where the tensile stresses are less than 90% of the applied stress are defined as being ineffective. Krenchel [113] introduced another factor, a fibre orientation

factor, η_θ , to account for the fact that fibres that are randomly aligned in 2 dimensions are less efficient at providing reinforcement than those aligned in the direction of the applied stress. The modified equation is then:

$$E_c = \eta_\theta \eta_l E_f V_f + (1 - V_f) E_m \quad 5.2$$

Where η_θ was calculated by Krenchel and has the value 0.375 and η_l has the value:

$$\eta_l = \left[1 - \frac{\tanh\left(\beta \frac{L}{2}\right)}{\left(\beta \frac{L}{2}\right)} \right] \quad 5.3$$

where:

$$\beta = \left[\frac{2G_m}{E_f r^2 \ln\left(\frac{R}{r}\right)} \right]^{\frac{1}{2}} \quad 5.4$$

and L is the fibre length, r is the fibre radius, G_m is the shear modulus of the matrix and 2R is the interfibre spacing given by:

$$R = r \left[\frac{\pi}{4V_f} \right]^{\frac{1}{2}} \quad 5.5$$

for fibres packed in a square array.

Assumptions.

The fibre volume fraction was measured for each laminate. The WCS fibres had nominal diameters of 13 μm . The diameters of the recovered fibres were measured during tensile strength testing (Chapter 4). The value for the shear modulus of the matrix material was not measured but was provided by GKN Technology Ltd. [114]. Glass fibre Young's modulus was given a nominal value of 72 GPa [103] for both virgin and recovered fibres, as suggested by the results presented in Chapter 4. A value of 169 GPa (Chapter 4) was used for the Young's modulus of the recovered carbon fibres. This information is

summarised in Table 5.3.

It was assumed that no fibre breakage had occurred during manufacture of the laminates. Virgin glass fibres were assumed to be 18 mm long and the reclaimed glass fibres were assumed to have the length distributions described in Chapter 4. No account was taken of the possibility that short fibres had been lost during the web formation stage. The fibre length distribution of the recovered carbon fibres was not measured. Due to the small diameter and the opacity of the carbon fibres, the Nottingham system could not be used and the high magnification Leeds University IRC system was not available. Instead, the length distribution of the fibres recovered from the FW pipe at 450°C was used as an approximation. Both feed materials were of similar construction and were prepared for processing in a similar way and so similar fibre length distributions were expected. A reinforcement efficiency factor was calculated for each 100 μm fibre length band in the distribution, using Equation 5.3, and multiplied by the volume fraction of fibres within that group. These results were then summed over the full fibre length range to find the total efficiency factor, η_l . Values of η_l are given in Table 5.3 along with the predicted laminate tensile moduli calculated using Equation 5.2.

Table 5.3 Predicted and measured laminate moduli.

Laminate	WCS	SMC450	FW450	FW500	CF500
Fibre volume fraction, V_f	0.26	0.25	0.26	0.23	0.22
Fibre diameter, $2r$ (μm)	13	13	13	13	7.5
η_l	0.997	0.957	0.935	0.959	0.942
Fibre modulus, E_f (GPa)	72 †	72 †	72 †	72 †	169
Matrix modulus, E_m (GPa) ‡	3.0	3.0	3.0	3.0	3.0
Matrix shear modulus, G_m (GPa) ‡	1.2	1.2	1.2	1.2	1.2
Predicted modulus, E_c (GPa)	9.2	8.7	8.8	8.3	15.5
Measured modulus (GPa)	10.1	9.9	9.0	9.6	13.9

† reference [103]

‡ reference [114]

Discussion.

The measured modulus for each laminate is close to the predicted value. For the carbon fibre reinforced laminate the measured modulus is less than that predicted. It is not surprising that there is some discrepancy given the simplifications inherent in the rule of mixtures.

Theory predicts a lower value of Young's modulus for the laminates containing recovered glass fibres compared to that reinforced with virgin fibres. The degree of this reduction is masked by the variation in the measured values which is of the same order. For laminates with identical fibre volume fractions, the reduction in Young's modulus is due to the reduced reinforcement efficiency of the short fibre fraction of the reclaimed fibres.

5.5.2 Theoretical strength of the experimental laminates.

The Kelly-Tyson [115] model can be used to predict the tensile strength, σ_c , of a discontinuous, aligned fibre composite:

$$\sigma_c = \frac{\tau}{D} \sum_i L_i V_i + \sigma_f \sum_j [V_j (1 - \frac{L_c}{2L_j})] + (1 - V_f) \sigma_{um} \quad 5.6$$

where τ is the interfacial strength, $V_{i,j}$ are the volume fractions of fibres of length $L_{i,j}$, σ_f is the fibre strength, σ_{um} is the matrix stress at the fibre failure strain, D is the fibre diameter and L_c is a critical length defined by:

$$L_c = \frac{\sigma_f D}{2\tau}. \quad 5.7$$

The matrix stress at the fibre failure strain can be calculated using the relation:

$$\sigma_{um} = \frac{E_m \sigma_f}{E_f} \quad 5.8$$

Equation 5.6 is based on the rule of mixtures but with the fibre strength contribution split into two terms. Load is transferred to the fibres by shear forces acting at the fibre / matrix interface. The stress in the fibre builds up from zero at the fibre ends to a maximum value at the centre of the fibre. If the fibre is shorter than the critical length, insufficient stress

is built up to fracture the fibre. In this case the mean stress carried by the fibre is proportional to its length. The first summation term in Equation 5.6 is the contribution to the laminate strength from the fibres of sub-critical length. For fibres longer than the critical length, the shear stresses build up sufficient tensile stress to fracture the fibre. In this case the mean stress in the fibre is a function of both fibre strength and fibre length. The second summation term in Equation 5.6 is the contribution from fibres of length greater than the critical length. In this term it can be seen that as the fibre length increases the correction due to the ineffective length at either end of the fibre tends to zero and the mean stress in the fibre tends towards the fibre breaking stress. The final part of the equation is the contribution to the laminate strength due to the matrix material.

Equation 5.6 must be modified to take into account the fact that the experimental laminates have a random fibre arrangement. It is possible to introduce an orientation factor for the fibre contribution terms in Equation 5.6. The size of this factor can be determined by comparing the results of tensile testing with the predictions of the model for a unidirectional composite. Hull [60] gives a typical value of 60 MPa for the interfacial shear strength of a glass fibre well bonded to a polyester matrix. If this figure is assumed to apply to the epoxy / glass, epoxy / carbon systems under investigation, then fibre critical lengths can be calculated using equation 5.7 and the Weibull scale parameters measured for the recovered and virgin fibre strengths and presented in Chapter 4. A summary of the relevant physical properties required to calculate the theoretical strength of the experimental laminates is presented in Table 5.4.

All WCS fibres were assumed to have super-critical lengths. For the recovered fibres, measurements presented in Chapter 4 were used and contributions from sub and super-critical fibres were summed. As with the estimated modulus, no fibres were assumed to be lost or broken during sample preparation. The contribution to the laminate strength of the sub-critical fibres was negligible. The estimated tensile strengths for aligned fibre composites and the measured tensile strengths for the two dimensional random reclaimed fibre laminates are compared in Table 5.4.

Table 5.4 Predicted and measured laminate strengths.

Laminate	WCS	SMC450	FW450	FW500	CF500
Fibre volume fraction, V_f	0.26	0.25	0.26	0.23	0.22
Fibre diameter, D (μm)	13	13	13	13	7.5
Fibre strength, σ_f (GPa)	2.80	1.45	1.22	1.15	2.29
Fibre modulus, E_f (GPa)	72 †	72 †	72 †	72 †	169
Matrix modulus, E_m (GPa) ‡	3	3	3	3	3
Interfacial strength, τ (MPa)	60	60	60	60	60
Critical fibre length, L_c (μm)	303	157	132	125	143
Predicted strength for a unidirectional composite, σ_c (MPa)	808	402	350	297	527
Measured strength of the random fibre composites (MPa)	148	93	94	88	121
Orientation factor	0.09	0.13	0.18	0.20	0.18

† reference [103]

‡ reference [114]

Discussion.

As expected, the measured strengths of the laminates containing randomly oriented fibre reinforcement are substantially lower than the predicted unidirectional strengths for laminates containing the same volume fraction of fibre. The measured strengths of the laminates containing recovered glass fibres are equal given the scatter but there is a wide variation between the predicted strengths of the same laminates. Thomason [112] measured an empirical fibre orientation factor of approximately 0.2 with a polypropylene / glass composite made using a wet laid process and this ratio was found to be independent of fibre length and fibre volume fraction. It was suggested that this ratio was a fundamental constant describing the reduction in laminate strength due to the random orientation of the fibres. The calculated orientation factors for the laminates containing recovered fibres are in good agreement with this observation, given the assumptions made. The smaller orientation factor measured for the laminate containing 18 mm long WCS fibres could be caused by preferential alignment of the fibres perpendicular to the test direction within this sample but this effect was not investigated further.

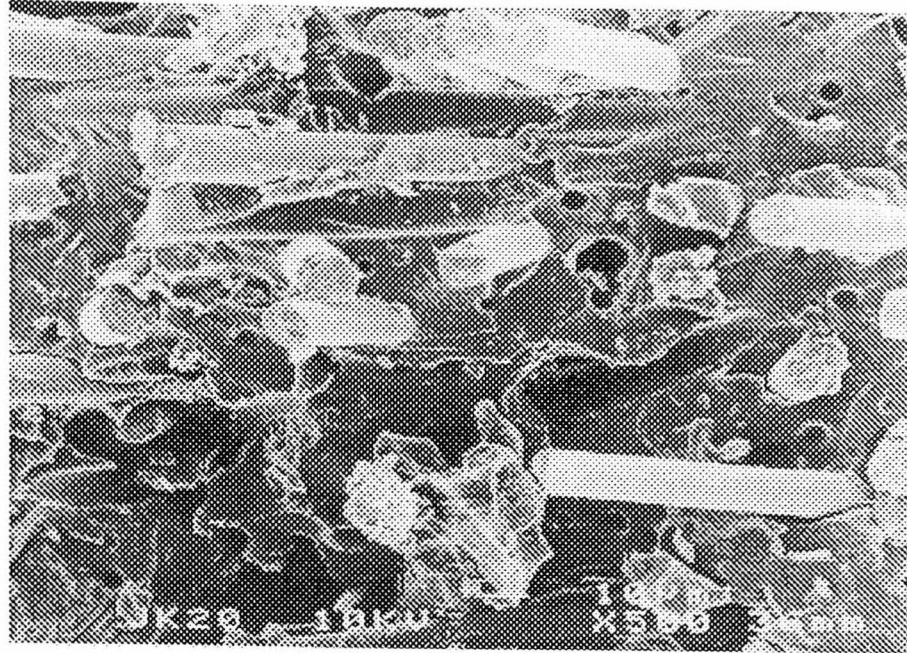
Figure 5.5 Fracture surface of glass / epoxy Laminate WCS (containing 26% v/v virgin glass fibres) showing a poor matrix to fibre bond.



Scanning electron micrographs of the fracture surfaces of two specimens, one containing virgin glass fibres and the other reclaimed glass fibres, are shown in Figures 5.5 and 5.6. In both cases it can be seen that there is little evidence of bonding between the fibre surface and the matrix material. This was probably due to a film of hydroxy ethyl cellulose from the dispersion medium which coated the fibres and hindered proper functioning of the silane treatment. This may mean that the value used for the interfacial shear strength was an over estimate and this implies that the fibre critical lengths may have been under estimated. If a reduced figure of 30 MPa [60] is assumed for the interfacial shear strength there would be no difference to the predicted strength of the virgin fibre laminate, since all the fibres would still be over the critical length (which would double), but the theoretical strength of Laminate SMC would be reduced by 1.5% to 396 MPa. It can be seen that the theoretical laminate strength is quite insensitive to the interfacial shear strength over the range 30 MPa to 60 MPa for this system.

In practice laminate strength is improved by increasing the length of the reinforcing fibres even when the critical length is already exceeded [112]. This can be due to a reduction in the number of fibre ends which can act as sites of stress concentration and the increased proportion of fibre length carrying the applied stress.

Figure 5.6 Fracture surface of epoxy / glass Laminate SMC450 (containing 25% v/v glass fibres recovered from SMC feed at 450°C) showing a poor matrix to fibre bond.



A slurry process for preform manufacture has been developed by other researchers [80, 116, 117]. Glass fibres recovered from scrap thermoset composites by the fluidised bed are particularly suitable for further processing by this method and opportunities for their reuse might be extended by this preform preparation technique. Reuse in thermoplastic matrices could also be achieved by a wet slurry process [118, 119].

5.6 Conclusions.

Laminates containing virgin and recovered glass fibres and recovered carbon fibres were prepared and their mechanical properties measured.

The measured moduli of the glass reinforced laminates was equivalent for the virgin and recovered fibres. A predicted reduction can be accounted for by the presence of fibres shorter than the critical length within the reclaimed fibres but the effect was of the same order as the variation in the measured values and so was not observed. The laminate reinforced with recovered carbon fibres was approximately 50% stiffer than those containing glass fibres which is due to the greater Young's modulus of the carbon fibres.

The measured tensile strengths of the experimental laminates were in the same ratio as the

strengths of their reinforcing fibres. These trends were not so clear in the flexural strengths, possibly due to imperfections in the samples. Using the Kelly-Tyson model all of the virgin fibres and the vast majority of the reclaimed fibres exceeded the critical length figures. Therefore, fibre length is not important in determining the theoretical laminate strength and laminate strength is mainly controlled by the strength of the reinforcing fibres. However, it is known that increasing the length of super-critical fibres can lead to an increase in composite strength [112].

The mechanical properties of the laminates containing recovered fibres confirm the recovered fibre properties presented in Chapter 4 and show that the recovered fibres are ideal for reuse in applications where strength is not critical but adequate stiffness is still required. Two such applications are a veil and a dough moulding compound and investigations into the use of recovered glass fibres in these products are presented in Chapters 6 and 7.

Chapter 6.

Use of recovered glass fibres in glass veils.

6.0 Introduction.

To provide an economic incentive for recovering glass fibres from scrap thermoset composites a high value end use for the fibres must be found. Glass fibres are recovered from the fluidised bed as weakened monofilaments and a glass veil is one example of a high value product where fibre strength is not critical and monofilaments are required. Veil is often used on the surface of a GRP moulding to improve its surface appearance and corrosion resistance. This chapter will start with a description of commercial veil manufacturing processes and will then investigate the processing of recovered fibres. The effect of the presence of reclaimed fibres on the wet strength, tensile strength and permeability of a standard veil material will be described. A set of conclusions will be presented.

6.1 The commercial manufacture of glass veils.

Two methods of manufacturing glass veil are commonly used in industry.

6.1.1 Dry process.

Glass rods are drawn into a furnace at approximately 1300°C. Here, the rods melt and are drawn into fibres by a drum rotating at a fixed speed. The fibres are then chopped and laid onto a moving carrier wire by a series of reciprocating carriages that ensure an even fibre distribution. Individual fibres can have lengths of several metres. A binder mix is impregnated into the veil which then passes through a drying oven to produce the finished, cured product. Before wind up the edges are trimmed. No size is applied to the glass but a vegetable oil mist is used to help the fibres adhere to the drawing drum.

6.1.2 Wet process.

This process is similar to a paper making process. Wet chopped strands (WCS) of up to 25 mm in length are fed from a hopper into a mixing chest where they are dispersed in a water based dispersion medium at a consistency of approximately 0.2%. The dispersion

medium (also called white water) is a suspension of dispersion aids, viscosity modifiers and foam suppression agents. The dispersion aids help to separate the fibre bundles into mono-filaments and the viscosity modifiers prevent dispersed fibres from entangling. Both the dispersion aids and the viscosity modifiers form solutions that are prone to foaming during mixing and so the foam suppression agents are added to prevent this undesirable phenomenon. From the mixing chest the slurry is transferred to a holding chest and then into a dilution tank where the slurry consistency is reduced by a factor of ten to 0.02% by the addition of more dispersion medium. The slurry is pumped from this tank to the forming wire through which the white water is removed by a vacuum box as the sheet forms. The dispersion medium is recirculated to the dilution chest.

The glass fibre web is lifted from the forming wire, impregnated with an appropriate binder and dried and cured in a long oven. At the wind up, edges are trimmed and the sheet can be slit to the required width.

This process should be suitable for converting recovered fibres into veil.

6.2 Veil processing with recovered glass fibres.

Samples of fibres recovered from both the SMC and FW pipe feed were used as partial and full replacement for virgin fibres in a veil product to assess their effect on processing.

6.2.1 Method.

The veil product chosen as a benchmark for the investigation into the effect of using recovered fibres was nominally a 70 gm⁻² veil containing 20% by weight of Rohm and Haas Primal HA-16 acrylic binder and 18 mm long, 13 μm diameter E-glass fibres supplied by Owens Corning Veil (UK) Ltd. in a wet chopped strand (WCS) form. Both the binder and the fibres are used to manufacture veil product at the Owens Corning Veil (UK) Ltd. plant. Samples of this veil were manufactured on a laboratory scale using fibres recovered from the SMC feed by the fluidised bed at 450°C and with a fluidising velocity of 1.3 ms⁻¹ and the cyclone collection system in place. The recovered fibres were used as a partial (50%) and full replacement for the virgin fibres.

Veil samples were also prepared containing glass fibres recovered from the FW pipe at 450°C and 550°C using the cyclone separation system and at 450°C using the rotating screen separator.

Slurrying procedure and dispersion medium.

Both recovered and virgin fibres were dispersed separately at a concentration of 0.2% in a 5 l beaker containing 3.5 l of dispersion medium. A Heidolph RZR2021 laboratory mixer was used with a mixer speed of 1100 rpm for 20 minutes. This standard procedure was found to produce a well dispersed slurry of virgin fibres. The dispersion medium consisted of 3 gl⁻¹ of a viscosity modifier, Cellosize grade HEC WP 52000HP supplied by Croxton and Garry Ltd., 0.6 gl⁻¹ of an anionic surfactant, Lankropol KO2 manufactured by Akcros Chemicals, and 0.3 gl⁻¹ of an antifoaming agent, Bevaloid 6686W manufactured by Rhône Poulenc, dispersed in distilled water. Virgin and reclaimed fibres were dispersed separately and combined just before the forming stage because it was noted that the recovered fibres interfered with the proper dispersion of the virgin fibres. Many factors affect the performance of the dispersion medium [120] , including age, and so fresh batches of dispersion medium were prepared every two weeks. During use it was noted that filler contamination washed from the recovered fibres accumulated in the forming tank. No effect of the contamination on the performance of the dispersion medium was observed since it was replaced regularly. In a commercial plant, particulate material would have to be removed from the dispersion medium to prevent excessive accumulation.

Web formation.

A schematic diagram of the apparatus used to make the veil samples is shown in Figure 6.1. A 470 mm diameter cylinder houses a close fitting PVC frame which in turn carries a 1 mm stainless steel mesh. The frame and mesh were pushed to the bottom of the cylinder and the dilute slurry was poured into the cylinder together with more dispersion medium to bring the final slurry consistency to 0.02%. The slurry was briefly agitated to stop any swirling motion and the mesh was lifted up through the fibre slurry to form a circular web of glass fibres of 360 mm diameter. The web was allowed to drain for 10 minutes before being carefully transferred to the binder applicator.

Figure 6.1
Schematic diagram of the laboratory scale web former.

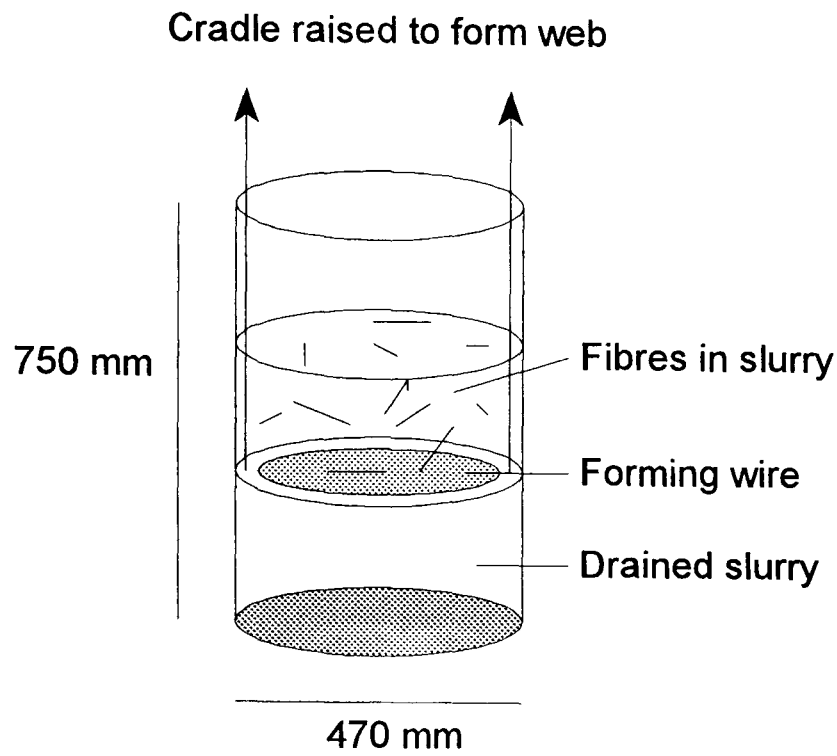
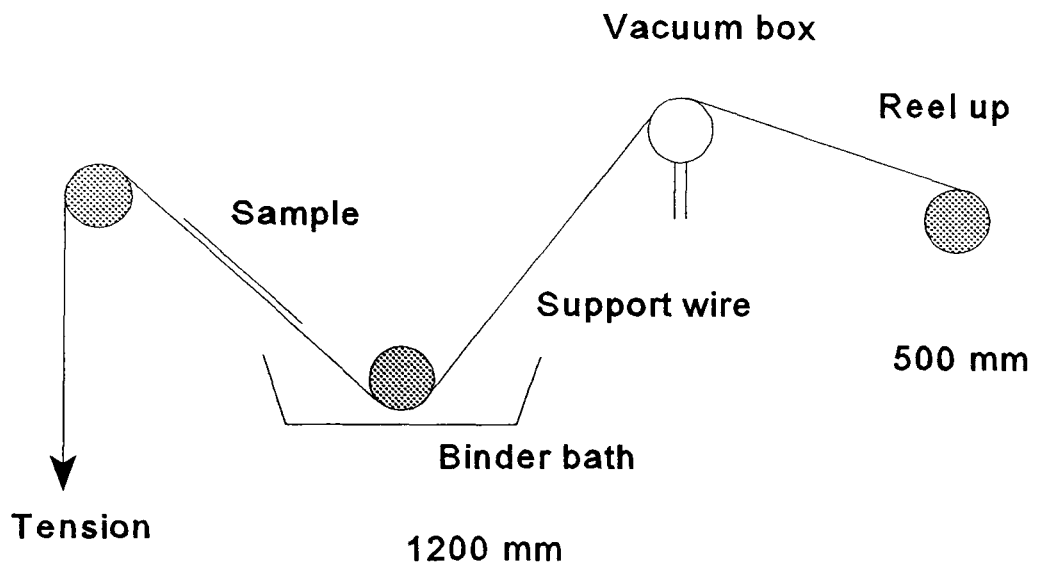


Figure 6.2
Schematic diagram of the laboratory scale binder applicator.



Binder application.

The binder applicator is shown in Figure 6.2. The drained web of fibres was placed on a 1 mm nylon mesh which carried the sample through a resin bath, where the binder fully

wetted the fibres, and then over a vacuum box where excess binder was removed to achieve the desired pick up. Binder addition was controlled by adjusting the solids content of the binder emulsion with dilution water. Once the excess resin had been removed the samples were dried at 100°C for twenty minutes before being cured at 180°C for one minute.

6.2.2 Discussion.

On their own, all the samples of reclaimed fibres were successfully dispersed using the standard slurring procedure although some bundles of parallel fibres were visible in the veil samples (Figure 6.3). These are thought to be remnants of the fibre bundles in the original feed that are held together by partially combusted matrix material. In the case where fibres recovered from the SMC were used, filler contamination gave the reclaimed fibre web a brown tone compared to the virgin fibre web which was white. Some partially combusted matrix material is visible in Figures 6.3 and 6.4 which are scanning electron micrographs of a veil containing only reclaimed fibres. It can also be seen in Figure 6.4 that the dispersion of the glass fibres is good when they are not held together by matrix and that there do not appear to be any short fibres. This is an unexpected observation, despite the restricted field of view, given the fibre length distributions measured for the recovered fibres. This is evidence that short fibres are lost through the forming wire during processing.

It was found that reclaimed and virgin fibres could not be successfully dispersed in the presence of each other. The reclaimed fibres stopped the WCS bundles from breaking apart. Veil manufacturers have noticed this problem when dispersing sized and unsized fibres together in the same vessel [102]. Due to differences in the surface chemistry of the two types of fibre, the unsized fibres tend to wrap around the sized fibre bundles and stop them from separating. Virgin and reclaimed fibres had to be dispersed separately and the two slurries combined immediately before formation, without any detrimental effect on the final web.

Figure 6.3 SEM of veil containing only recovered fibres.
Fibre source: FW pipe.
Fluidised bed temperature: 450°C.
Binder content: 20% nominal.
Note: parallel fibres held by partially burnt matrix material.

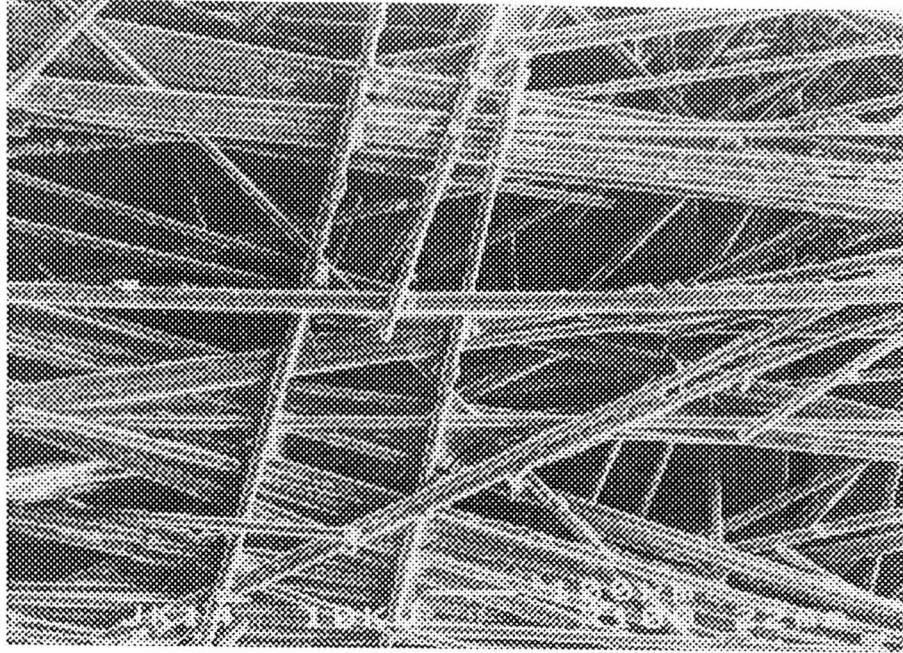
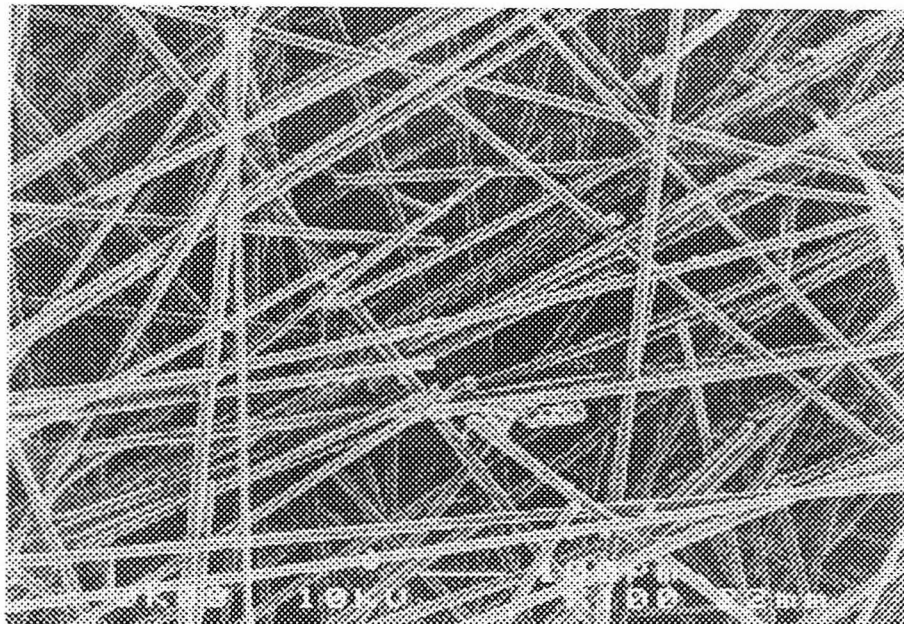


Figure 6.4 SEM of veil containing only recovered fibres.
Fibre source: FW pipe.
Fluidised bed temperature: 450°C.
Binder content: 20% nominal.



6.3 Veil wet strength.

The strength of the glass web as it forms on the forming wire is critical to the successful manufacture of the glass veil material. The web must have sufficient strength to allow it

to be lifted from the wire and passed through the binder application plant. After binder application, the veil is supported as it dries and has developed its full strength by the time it reaches the wind up stage.

It was apparent during manufacture of the experimental veil materials that the wet strength of the web was reduced by the presence of reclaimed fibres, although no attempt to quantify this effect was made. Rupture of a wet web occurs by failure of the fibre to fibre interactions and not by fibre breakage. Wet web strength is therefore controlled by the number of fibre to fibre interactions in the web. The significant proportion of short fibres in the reclaimed fibre samples reduces the number of fibre to fibre interactions in the web and hence the wet web strength. This phenomena has implications for the manufacture of veil materials containing reclaimed fibres where a degree of wet strength is required.

To investigate the likely effect of using short fibres on the wet strength of veil materials, samples of bound veil were made with glass fibres of different lengths and diameters and with low to medium binder contents. Low binder contents approximated the wet strength case where there are only weak bonds between the fibres but allowed samples to be investigated that were easier to handle.

6.3.1 Method.

Veil samples were produced on a laboratory scale, using the method described in section 6.2.1. The fibres used in this study were WCS of the following dimensions:

18 mm long, 13 μm diameter, 13 mm long, 13 μm diameter,
13 mm long, 11 μm diameter, 6 mm long, 11 μm diameter.

Samples were tested for strength using the procedure described in Section 6.4.1.

6.3.2 Results.

Veil breaking lengths were calculated from the measured breaking loads using Equation 6.2. Breaking length is the maximum length of material that can be suspended vertically without breaking under its own weight. It can be calculated without measuring the thickness of the veil, which can be difficult to determine reliably, and used to compare veil strengths. Details of the experimental veil areal densities and breaking lengths are

given in Table 6.1. Graphs of veil breaking length against fibre length are given in Figures 6.5 and 6.6.

Table 6.1 Areal density and breaking lengths for experimental veil samples.

Fibre length (mm)	Fibre diameter (μm)	8% binder content			13.5% binder content		
		Areal density (gm^{-2})	Breaking load (N)	Breaking length (m)	Areal density (gm^{-2})	Breaking load (N)	Breaking length (m)
6	11	57.6	28.5	2017	62.9	81.6	5291
13	11	60.5	52.3	3525	65.9	87.0	5382
13	13	59.7	18.0	1229	67.7	54.9	3309
18	13	55.5	44.7	3284	62.4	52.0	3398

Figure 6.5 Effect of fibre dimensions on veil breaking length.

Veil substance: 60 gm^{-2} nominally.

Binder level: 8.5% w/w.

Binder type: acrylic.

Fibre type: Owens Corning Fiberglas WCS.

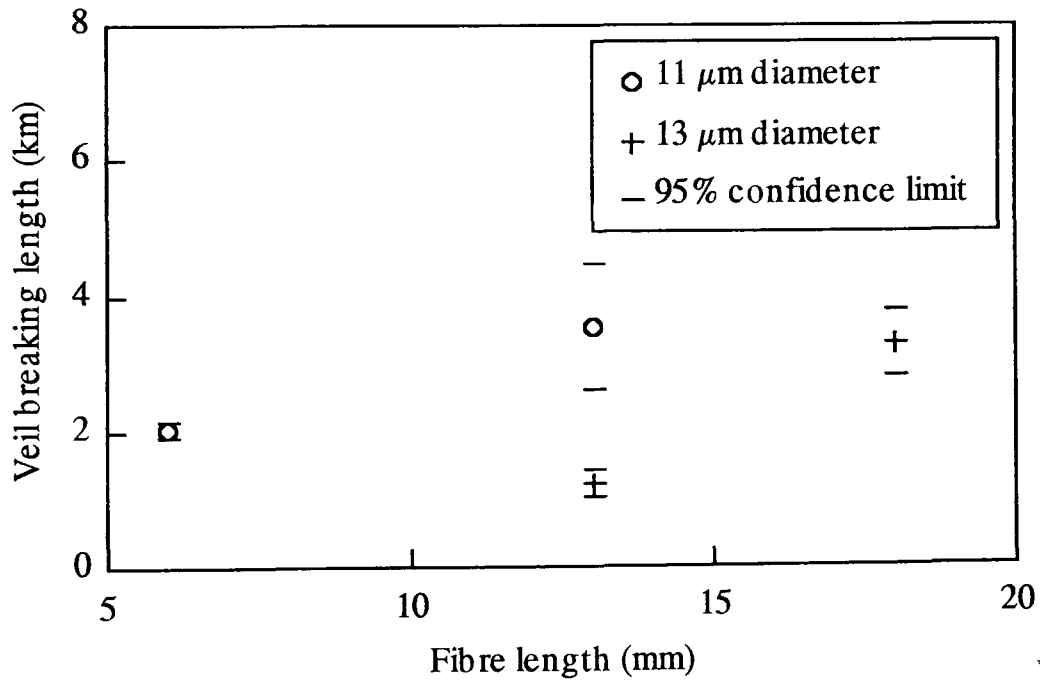


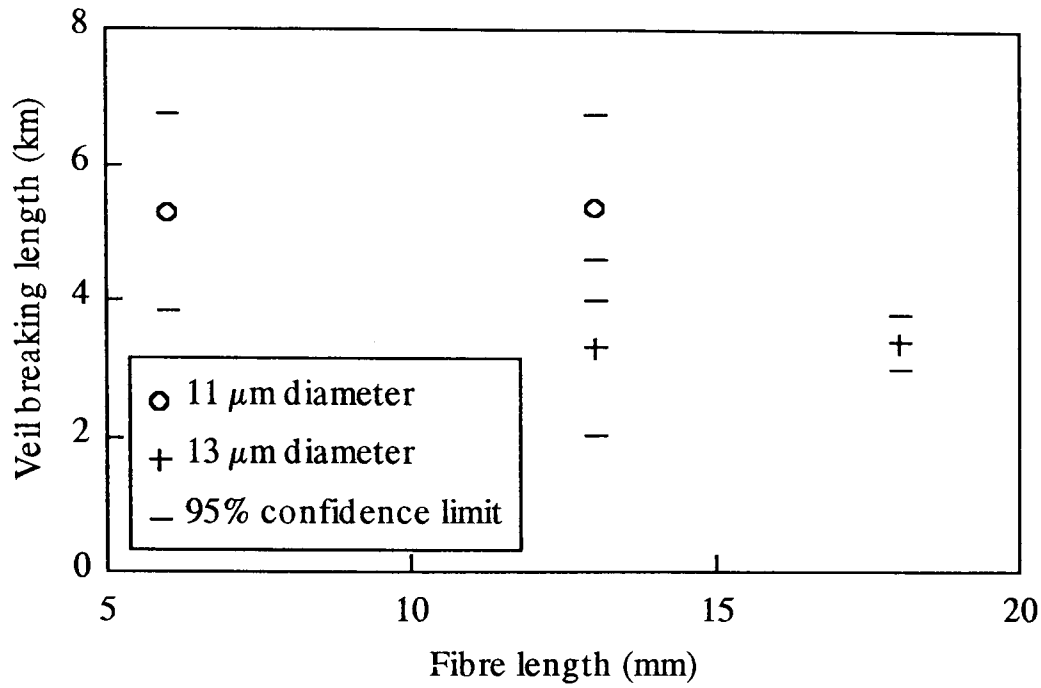
Figure 6.6 Effect of fibre dimensions on veil breaking length.

Veil substance: 65 gm⁻² nominally.

Binder level: 13.5% w/w.

Binder type: acrylic.

Fibre type: Owens Corning Fiberglas WCS.



6.3.3 Discussion.

The wet strength of a web of fibres depends on the areal density of the web, the diameter and length of the fibres and the strength of the fibre to fibre interactions [121]. Fibre strength has no effect on the magnitude of the wet strength because no fibres are broken in the rupture of a wet web, only fibre to fibre bonds. The strength of the fibre to fibre bond depends on the moisture content of the web since this bond is created by the action of the surface tension of the water present where two fibres meet.

Kallmes et al [121] used probability theory to describe the properties of a web of fibres. They derived an expression for the web strength by calculating the number of fibres in a random, two dimensional arrangement crossing an imaginary line of rupture. They then proceeded to calculate the number of fibres anchoring these fibres in the network. Seth et al [122] used these results to predict the wet strengths of webs made from cellulose pulp. They derived an expression for the force per unit width (F) required to rupture a network:

$$F = \frac{S^2 L}{\pi^2 C^2} f_s \quad 6.1$$

where S is the areal density of a network of fibres of length L and mass per unit length C and where f_s is the frictional resistance to sliding of each fibre to fibre contact. The frictional resistance depends on the fibre surface and the moisture content of the web. Assuming that f_s is constant for networks of glass fibres of known moisture content then the wet strength of the network is directly proportional to the fibre length and indirectly proportional to the square of the linear density of the fibres.

Figure 6.5 shows that in the case of a veil with a low binder content, veil strength increases with fibre length and decreases with fibre diameter. These are the trends predicted by Equation 6.1 for a wet web of fibres. At higher binder levels, veil strength is independent of fibre length and diameter, given the confidence limits of the measurements (Figure 6.6). This indicates that veil strength is now controlled by the fibre strength and not the fibre to fibre interactions since the fibres are now securely held by the binder.

The reclaimed fibres used in the manufacture of the veil samples analysed during these investigations were of the same diameter and density, and therefore linear density, as the virgin fibres used. Assuming similar moisture contents for the wet webs, Equation 6.1 implies that the wet strengths of the experimental veils are directly proportional to the lengths of their constituent fibres. Dispersion of the fibres prior to forming the fibrous network is not thought to shorten the fibres and so little change in the fibre length distribution should be expected. However, it is possible that the shortest fibres present may be lost through the forming wire which is a 1 mm square mesh. Fibres of length less than 1 mm account for only 3.5% of the total mass of fibres in a sample recovered from the SMC feed (Chapter 4). There would be a correspondingly small increase in the weighted fibre length of such a sample if those fibres were lost and so little effect on veil wet strength. The distribution of fibre lengths in a recovered fibre veil material was not measured and so no further conclusions can be drawn.

6.4 Veil strength.

The strength of a veil material is generally not critical, the only requirement being that the veil be handleable and able to withstand any subsequent processing. It seems likely that

weakened fibres could be used in a veil product although an increased areal density might be required to match the strength of a virgin veil, which could affect the economics of this application. Investigations into the effect of the presence of recovered fibres on veil strength were carried out.

6.4.1 Method.

Veil samples were produced on a laboratory scale, using the method described in section 6.2.1. The fibres used in this study were glass fibres reclaimed from SMC feed at bed temperatures of 450°C and 550°C using the cyclone recovery system and virgin WCS of 18 mm length and 13 µm filament diameter. The veil samples contained 0%, 50% and 100% by weight of the recovered fibres and were bound with the acrylic emulsion already described. For one series of samples a silane, VS-142 amino alkyl silicone, supplied by OSi Specialities was added to the binder [82] at a 2% loading to investigate the effect of improving the binder to fibre bond on the strength of the veil. Veil areal density and binder content were nominally 75 gm⁻² and 20% by weight respectively. Eight samples of size 150 mm by 25 mm were cut from each veil sample and were cured at 180°C for one minute before testing. Sample breaking load was measured with an Instron Universal testing machine, model 1195, with a gauge length of 100 mm and a crosshead speed of 50 mm min⁻¹. The metal jaws were lined with masking tape to protect the veil material from crushing during tightening.

The veil breaking lengths (L_b) were calculated from their breaking loads (B), areal density (S) and width (W) using the relationship:

$$L_b = \frac{B}{SWg} \quad 6.2$$

where g is the acceleration due to gravity.

Repeat samples of veil containing 100% virgin fibres were made and tested to investigate the effect of variability in the laboratory sample preparation on veil strength.

The binder content of each sample of veil was determined by heating the broken tensile

samples at 625°C for five minutes to remove the binder and recording the weight loss.

6.4.2 Results.

Veil formulations and breaking lengths are shown in Tables 6.2 and 6.3 and Figures 6.7 and 6.8.

Table 6.2 Experimental veil formulations containing fibres recovered at 450°C and their breaking lengths.

Fibre level (%)		Silane	Areal density (gm ⁻²)	Binder level (%)	Breaking load (N)	Breaking length (m)
virgin	450°C reclaim					
100	0	no	74.7	20.5	112.5	6135
100	0	no	70.7	17.4	100.6	5802
100	0	yes	73.3	19.9	137.1	7626
50	50	no	82.0	23.5	128.1	6370
50	50	yes	81.3	19.4	99.0	4965
0	100	no	69.3	23.4	60.3	3530
0	100	yes	80.0	20.3	49.5	2497

Table 6.3 Experimental veil formulations containing fibres recovered at 550°C and their breaking lengths.

Fibre level (%)		Silane	Areal density (gm ⁻²)	Binder level (%)	Breaking load (N)	Breaking length (m)
virgin	550°C reclaim					
100	0	no	74.7	20.5	112.5	6135
100	0	no	70.7	17.4	100.6	5802
100	0	yes	73.3	19.9	137.1	7626
50	50	no	75.3	19.9	94.5	5090
50	50	yes	72.7	18.9	84.5	4711
0	100	no	70.7	20.1	41.0	2365
0	100	yes	64.0	20.4	30.3	1911

Figure 6.7 Effect of reclaimed fibre content on veil breaking length.
 Virgin fibres: OCF WCS, 18 mm length, 13 μm diameter.
 Recovered fibres: SMC feed, 450°C recovery temperature.
 Areal density: 75 gm^{-2} .
 Binder content: 20%.

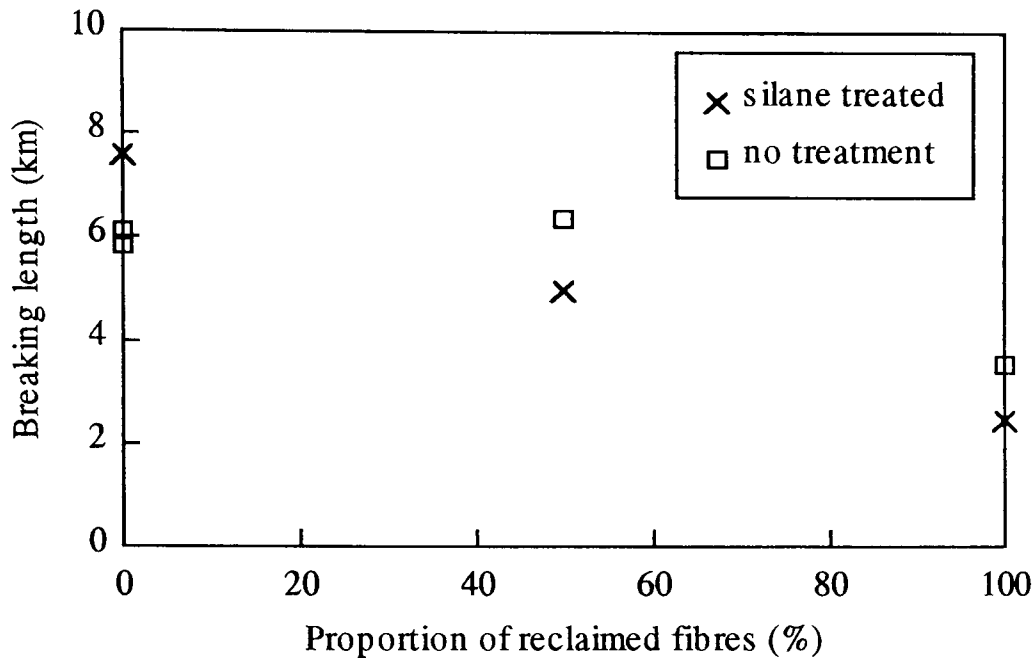
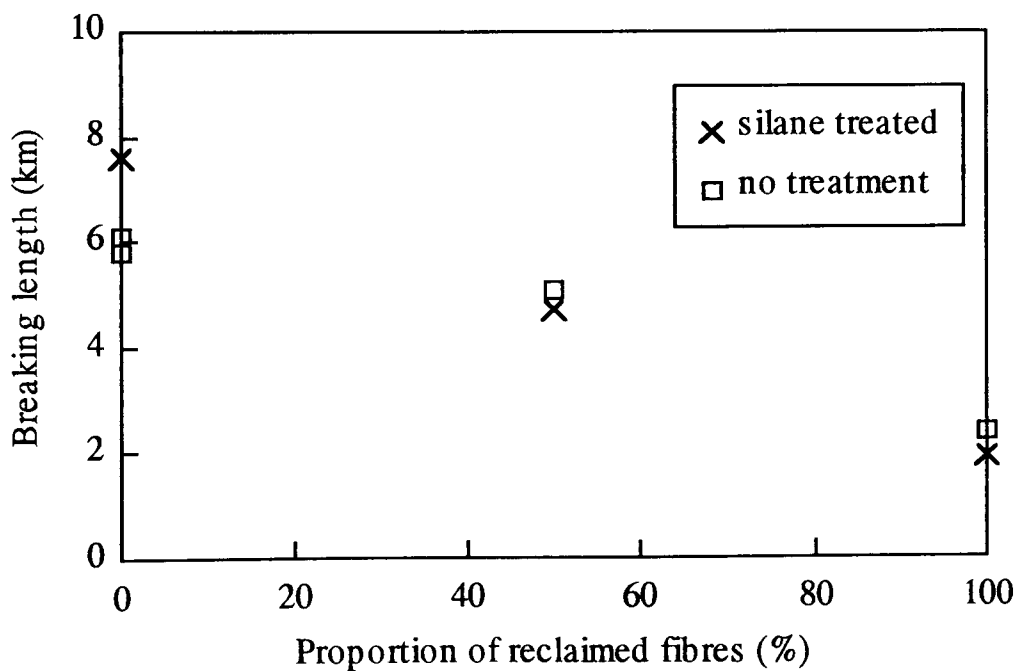


Figure 6.8 Effect of reclaimed fibre content on veil breaking length.
 Virgin fibres: OCF WCS, 18 mm length, 13 μm diameter.
 Recovered fibres: SMC feed, 550°C recovery temperature.
 Areal density: 75 gm^{-2} .
 Binder content: 20%.



6.4.3 Discussion.

Results presented in Section 6.3.3 suggest that, at high binder levels, veil strength is dominated by the strength of the glass fibres. It should be expected that with binder levels of nominally 20% the strength of these veil samples should be related to fibre strength. This hypothesis is supported by the results of these investigations where increasing the level of recovered fibres in a veil material decreases the veil strength. Veil with a complete replacement of the virgin fibres by fibres recovered at 450°C has a breaking length that is approximately 50% of that for the virgin fibre veil. This agrees well with the results, presented in Chapter 4 of this thesis, that the fibres recovered at 450°C have retained 49% of the strength of virgin fibres (the strength of the WCS fibres was not measured but is expected to be comparable to that of virgin roving fibres). For the sample of veil made with fibres recovered at 550°C the veil strength is 40% of that of virgin fibre veil although the fibres recovered at 550°C only retain 20% of the strength of virgin fibres. It can be concluded therefore that veil strength does not depend on fibre strength alone, it will also be a function of fibre length and binder content.

Use of a silane treatment did not improve the strength of the veil which is as expected, because veil failure is thought to be due to fibre breakage and not rupture of fibre to binder bonds.

6.5 Veil permeability.

When a glass veil is used on the surface of a GRP moulding it must be readily impregnated by the resin or a poor surface finish will result. In almost all moulding techniques the surface veil layer will be filled by resin flowing through the thickness of the veil. The through thickness permeabilities of some experimental veil samples containing reclaimed fibres were measured to investigate the effect of the recovered fibres.

6.5.1 Method.

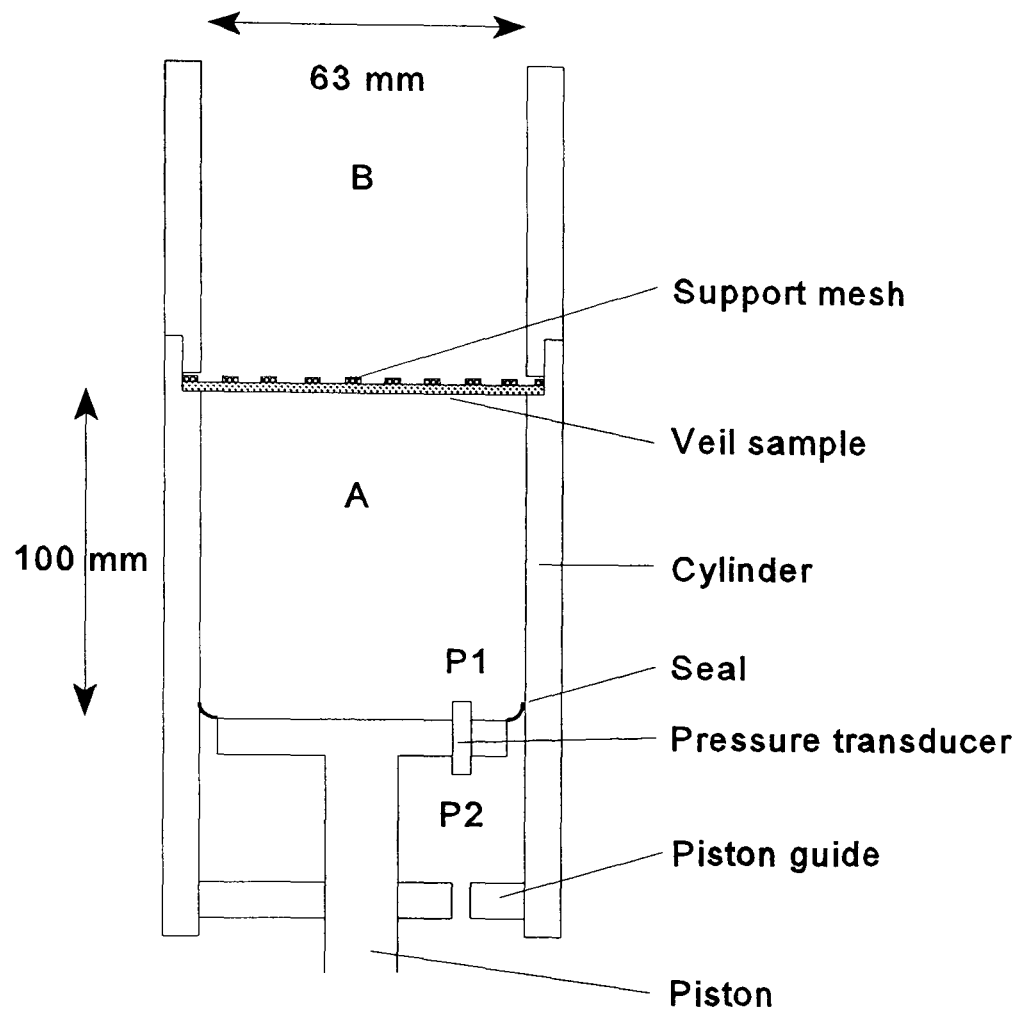
Darcy's law can be used to derive a value for the hydrodynamic permeability (k) of a sample and can be expressed in the form [123]:

$$\frac{Q}{A} = \frac{k}{\mu} \frac{\Delta p}{\Lambda} \quad 6.3$$

where volumetric flow rate (Q), sample area (A), fluid dynamic viscosity (μ), pressure drop (Δp) and sample length (Λ) are known.

Figure 6.9

Schematic diagram of the rig used to measure the dynamic permeabilities of the experimental veil samples.



The crosshead of an Instron Universal testing machine was used to drive a piston through a cylinder containing a standard SAE 30 motor oil with a viscosity typical of that of a common thermosetting resin at moulding temperatures (measured at room temperature with a Brookfield viscometer and found to be 280 cP). A sample of veil material was clamped against the end of the cylinder and the piston forced the oil through the sample at a fixed flow rate (see Figure 6.9). A differential pressure gauge was used to monitor the difference in pressure between the oil behind the veil sample and atmospheric pressure. For each sample, Δp was measured at 5 flow rates between 1 mls⁻¹ and 25 mls⁻¹ and the gradient of the plot of Δp against Q was used to calculate the veil permeability. To generate a significant pressure difference, 4 plies of veil with a total areal density of

nominally 240 gm^{-2} were used per test. The binder content of the veil samples was nominally 12.5% by weight and was determined by ashing.

Typical pressure traces over time for one of the veil samples are shown in Figure 6.10. The steady state pressure drops taken from Figure 6.10 are plotted against flow rate in Figure 6.11.

Figure 6.10 Pressure drop across a veil sample as a function of time at a series of flow rates.

Veil formulation: 30% reclaimed fibres.

Areal density: $4 \times 60 \text{ gm}^{-2}$.

Binder content: 15%.

Oil viscosity: 280 cP.

Recovered fibres: from SMC feed at 450°C .

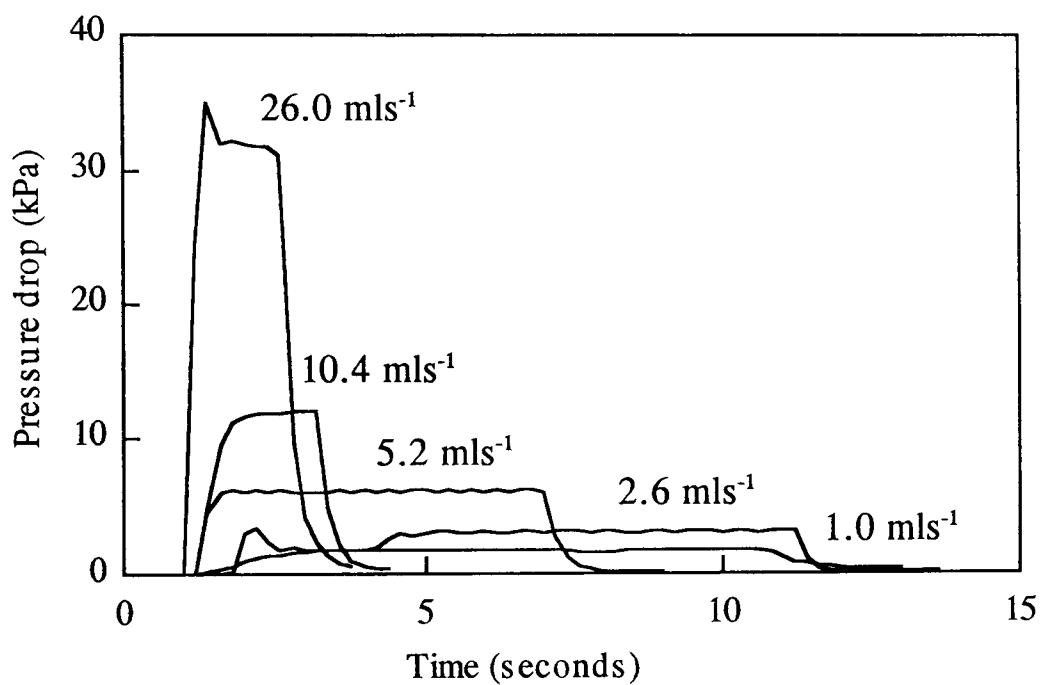


Figure 6.11 Steady state pressure drop across a veil sample as a function of flow rate.

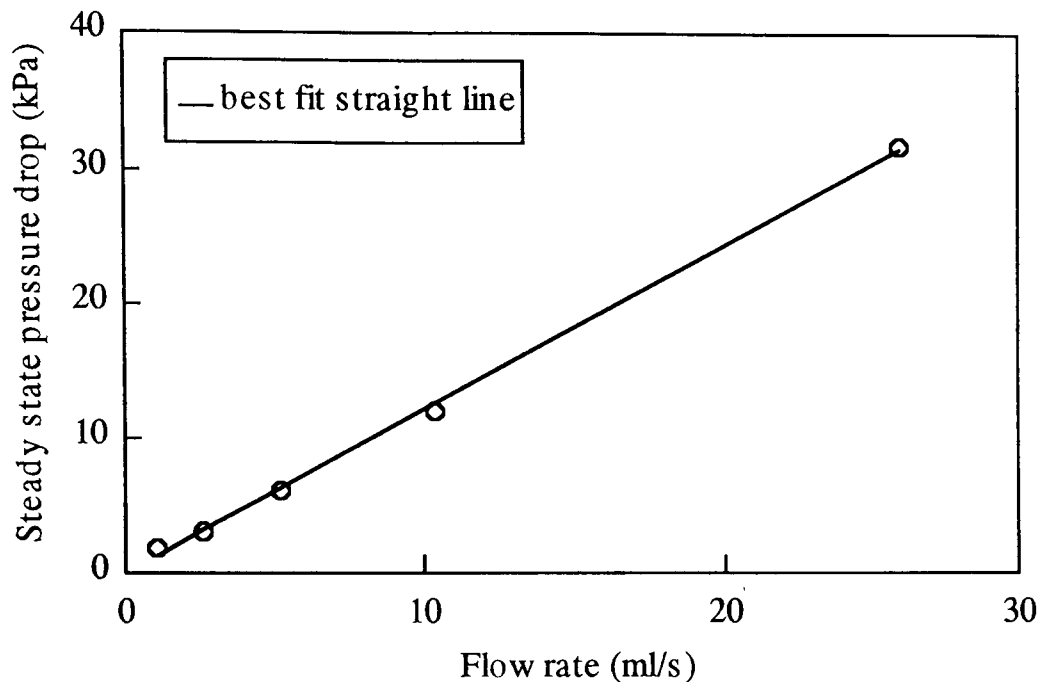
Veil formulation: 30% reclaimed fibres.

Areal density: 4x60 gm⁻².

Binder content: 15%.

Oil viscosity: 280 cP.

Recovered fibres: from SMC feed at 450°C.



The total veil sample thickness was measured under a stress of 1400 kPa by a dead weight dial gauge and was nominally 2.5 mm.

The porosity (P) of each veil sample was also calculated from the equation:

$$P = 1 - \frac{\rho_b}{\rho} \quad 6.4$$

where ρ_b is the bulk density of the veil, calculated from the areal density and the thickness, and ρ is the true density of the veil, calculated from the densities of the glass fibres and the acrylic binder and their relative proportions.

6.5.2 Results.

Figure 6.12 is a graph of permeability against porosity for the experimental veil samples.

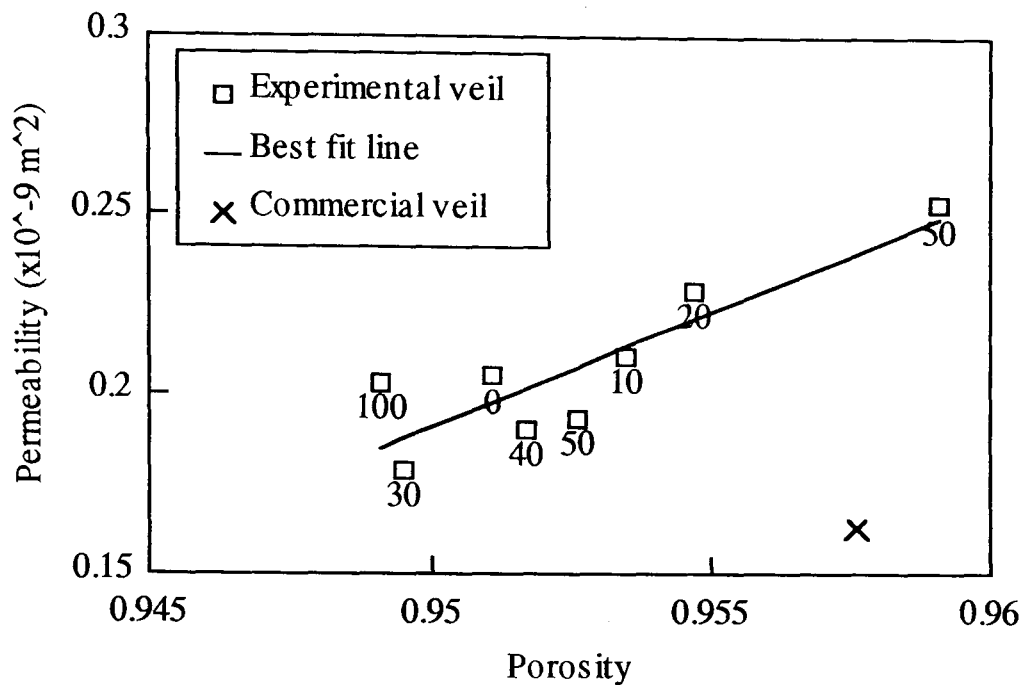
Figure 6.12 Permeability against porosity for veil incorporating reclaimed fibres. Figures represent reclaimed fibre content (%).

Binder content: 12.5 % w/w.

Areal density: 4x60 gm⁻².

Oil viscosity: 280 cP.

Recovered fibres: from SMC feed at 450°C.



6.5.3 Discussion.

It can be seen that veil permeability is independent of reclaimed fibre content but is linearly related to veil porosity in the narrow range investigated. Veil porosity is dominated by sample preparation rather than by formulation. Veil porosity is difficult to control during laboratory scale manufacture of samples but would be more easily controlled on pilot or full scale plant. The commercial veil sample has a 30% lower permeability, at the same porosity, than the experimental samples and this too is probably attributable to the positioning of the fibres as a result of the manufacturing process.

6.6 Veil as corrosion inhibitor.

Glass fibre veil materials are often used as surfacing layers on composites which are to be exposed to corrosive environments. Since the veil is formed by a random network of single glass filaments it forms a low fibre / high resin fraction layer which acts as a protective barrier. Samples of veil material containing virgin and reclaimed fibres were tested by using them as facing materials for composite plaques which were then subjected to corrosive environments. Test methods and results are described in Appendix E. No

effect of reclaimed fibre content on veil performance was measured.

6.7 Conclusions.

It has been shown that recovered fibres can be successfully processed into a veil material and that this material has useful properties. It has been established that the short fibre fraction within the recovered fibres will have a detrimental effect on the wet strength of a veil. Since the precise details of the wet strength requirements of a glass veil depend on the manufacturing process, further experimentation on a pilot scale plant is required to determine the levels of recovered fibre that would be feasible.

Use of fibres recovered at 450°C and 550°C in a veil material introduces weaker and shorter fibres into the web. The high binder contents present in these experimental veil formulations suggests that fibre strength rather than fibre length should be the main strength controlling factor in these cases. Introduction of weaker fibres leads to an approximately linear decrease in veil strength with reclaimed fibre level. The introduction of weaker fibres reclaimed at 550°C produces a greater strength decrease (66% in the case of complete replacement) than use of stronger fibres recovered at 450°C (50% in the case of complete replacement). Fibre strength values in Chapter 4 indicate that fibres reclaimed at 550°C have strengths around half those for fibres reclaimed at 450°C which in turn have strengths around half those of virgin fibres. These fibre strength relationships are carried through to the strength of the veil materials, given the large spread in the veil strength measurements.

The permeabilities of the veil samples containing reclaimed fibres are proportional to their porosities but there seems to be no influence of reclaimed fibre content. It is suggested that the preparation of the veil has a greater influence on porosity and permeability and masks any effect of the reclaimed fibres. Manufacture on a pilot plant scale would produce less variable veil formations and might highlight the effect of the recovered fibres.

Glass veils containing reclaimed fibres have been used as surfacing agents for GRP mouldings. Limited testing has shown no difference in performance to virgin fibre veil in either corrosion resistance or surface quality.

Chapter 7.

Use of recovered glass fibres in a dough moulding compound.

7.0 Introduction.

A polyester dough moulding compound (DMC) was chosen as a material in which to reuse the reclaimed glass fibres. The recovered fibres are in the form of a loose collection of entangled filaments. It was expected that fibres in this form could easily be added to a resin slurry to form a DMC without any alteration to the mixer or mixing procedure. Samples of DMC were prepared in which various levels of virgin fibre were replaced with fibres reclaimed from the fluidised bed at 450°C. The effects of the level of reclaimed reinforcement on DMC moulding properties were investigated. An experimental DMC was also prepared on a pilot plant scale and the mechanical properties measured. The results of these investigations will be reported in this chapter.

7.1 Dough moulding compounds.

Typical DMCs use polyester or phenolic resin mixed with approximately 15% w/w glass fibre bundles and 50% w/w calcium carbonate [124]. The dough is prepared in a Z-blade mixer [39] and supplied in sealed bags. DMCs are ideal for components where stiffness is more critical than strength and so represent an ideal opportunity for the reuse of the recovered glass fibres.

7.2 Laboratory trial.

Experimental DMC formulations were prepared with recovered glass fibres to investigate their effect on processing and mechanical properties.

7.2.1 Preparation of the recovered fibre.

Fibres were recovered from the SMC feed (Table 4.1) using the fluidised bed operating at a temperature of 450°C and the cyclone based fibre collection system. Most of the loose filler was removed from the recovered material by washing with a dilute detergent solution and then filtering through a 1 mm square mesh. Long fibres remained trapped on the mesh whilst the filler particles and some shorter fibres were lost.

It was assumed that any functional size on the fibres had been removed in the fluidised bed and so one batch of recovered fibres was treated with a polyester compatible silane solution (OSi Specialities product A174, gamma methacryloxypropyltrimethoxysilane) to improve the fibre to matrix bond. The required amount of washed, fibrous material was soaked in the silane solution for one hour. Some gentle agitation was required to ensure proper wet out of the fibres. After the treatment the fibres were removed, drained and dried in an oven at 85°C.

Composition of the recovered fibre material.

Analysis of the composition of the reclaimed material prepared for the DMC trials was performed by burning off organic residue, acid digesting calcium carbonate filler and washing off any remaining fillers. Three samples of washed material were dried, weighed and then heated in a furnace at 625°C for ten minutes. This treatment was calculated to remove any organic residue remaining on the fibres. The mean weight loss after heating was approximately 7%. The heated material was then placed in a small conical flask and covered with de-ionised water. 70%w/w nitric acid was added to the flask until no more gas was seen to be released. The contents of the flask were then tipped on to a 1 mm square mesh and rinsed with deionised water. The fibres tended to remain entangled whilst any remaining filler particles were washed away. Finally the remaining fibres were dried and weighed. This gave an approximate fibre level in the washed, reclaimed material of 92%. No account of contamination was taken when replacing the virgin fibres. The washed, reclaimed material was used as a 'fibre product' with an assumed density equal to that of virgin glass fibres.

7.2.2 DMC processing.

Mixing procedure.

The basic DMC formulation used is given in Table 7.1 and the total mix weight was 1000 g for each formulation. Each DMC was prepared in a 1.1 litre Winkworth Z-blade mixer. Half the resin was poured into the mixer which was then switched on and the filler was added over a 5 minute period. After the filler had been added the rest of the resin was slowly poured in. Once the mixer had been running for 25 minutes, addition of the glass fibres started and this was completed within 5 minutes. At this point the mixer was

stopped, accumulated material was scraped from the sides and the mixer lid was put on. The moulding compound was then mixed for a further three minutes before the mixer was finally stopped and the compound removed and stored in an air tight container.

Table 7.1 Experimental DMC formulation.

Resin Slurry	Weight (%)
Synolac 6404 unsaturated polyester resin †	18.9
Norsodyne A 154 shrink control agent †	9.4
Omya millicarb calcium carbonate ‡	30.9
Omyalite 95T calcium carbonate ‡	7.7
Martinal trihyde ON313 aluminium hydroxide ‡	30.9
Zinc stearate N mould release ‡	1.8
Trigonox C organic peroxide *	0.4
Fibre Reinforcement	
Chopped strand glass 254, 6 mm ‡	total volume fraction
450°C recovered fibres, 4.7 mm weight average length	

†Cray Valley Ltd.

‡Croxtton and Garry Ltd.

*Akzo Nobel Chemicals Ltd.

Moulding procedure.

A circular cavity hardened steel mould 300 mm in diameter was used to produce mouldings for physical testing. The mould was coated in a proprietary mould release agent before it was heated to 150°C. The experimental moulding compounds were divided into three 300 g charges. One charge was placed in the centre of the tool which was closed by a 150 tonne Bradley and Turton hydraulic press. A pressure of 14 MPa was applied to the moulding for 2 minutes in which time the moulding compound cured. A plaque of nominal thickness 2 mm was ejected from the mould by directing a compressed air jet over the upper surface of the moulding. All samples were post cured at 85°C for 24 hours before testing. No attempt was made to optimise the mixing procedure for the reclaimed fibre.

7.2.3 DMC testing.

The experimental DMC mouldings were tested using procedures based on BS 2782. Five samples 250 mm long by 25 mm wide were tested in tension at 2 mm min⁻¹ test speed with an Instron 1195 testing machine. Sample extension was measured over a 50 mm gauge length using an Instron extensometer. Five samples, 40 mm by 25 mm, were tested for flexural strength and modulus on the same machine at a speed of 1 mm min⁻¹. Sample deflection was equated to crosshead displacement. For Charpy impact measurement, ten samples 80 mm by 10 mm were tested on an Avery Denison pendulum type tester with a 2.7 J hammer and an impact speed of 3.46 ms⁻¹. Two samples of the control formulation were prepared, moulded and tested to indicate the variability in the test results attributable to processing.

Figures 7.1, 7.2, 7.3, 7.4, 7.5 and 7.7 show mean values (with 95% confidence limits) for the measured properties.

Figure 7.1 Effect of reclaimed fibre content on tensile strength.

Virgin fibres: 6 mm chopped strand.

Reclaimed fibres: from SMC moulding, 450°C.

Fibre volume fraction: 13%.

Process: DMC compression moulding.

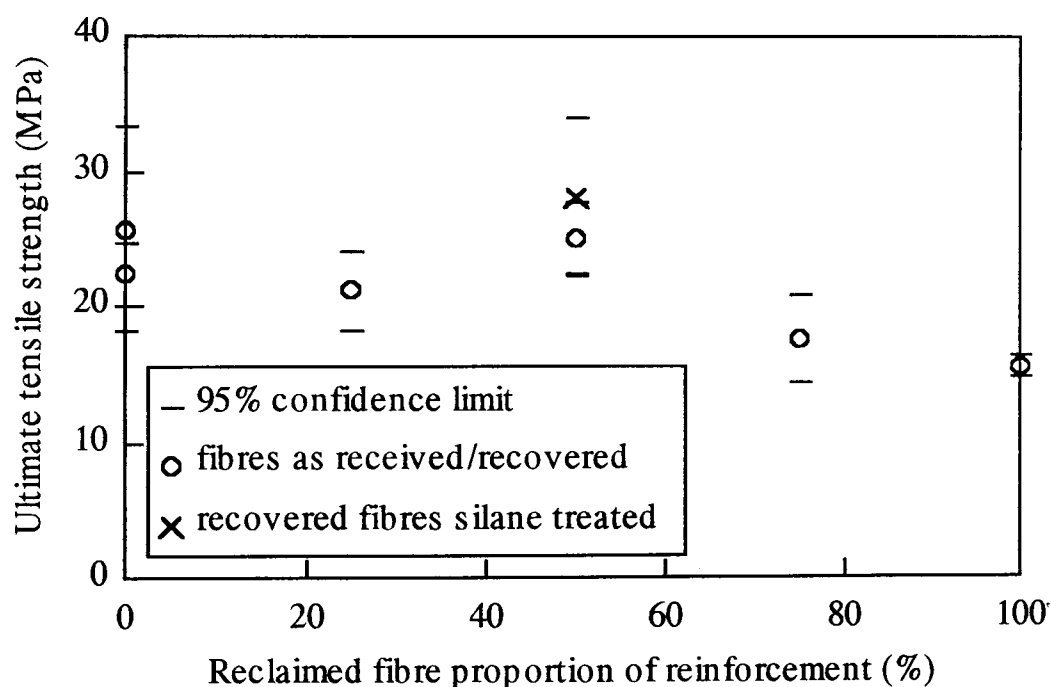


Figure 7.2 Effect of reclaimed fibre content on flexural strength.
 Virgin fibres: 6 mm chopped strand.
 Reclaimed fibres: from SMC moulding, 450°C.
 Fibre volume fraction: 13%.
 Process: DMC compression moulding.

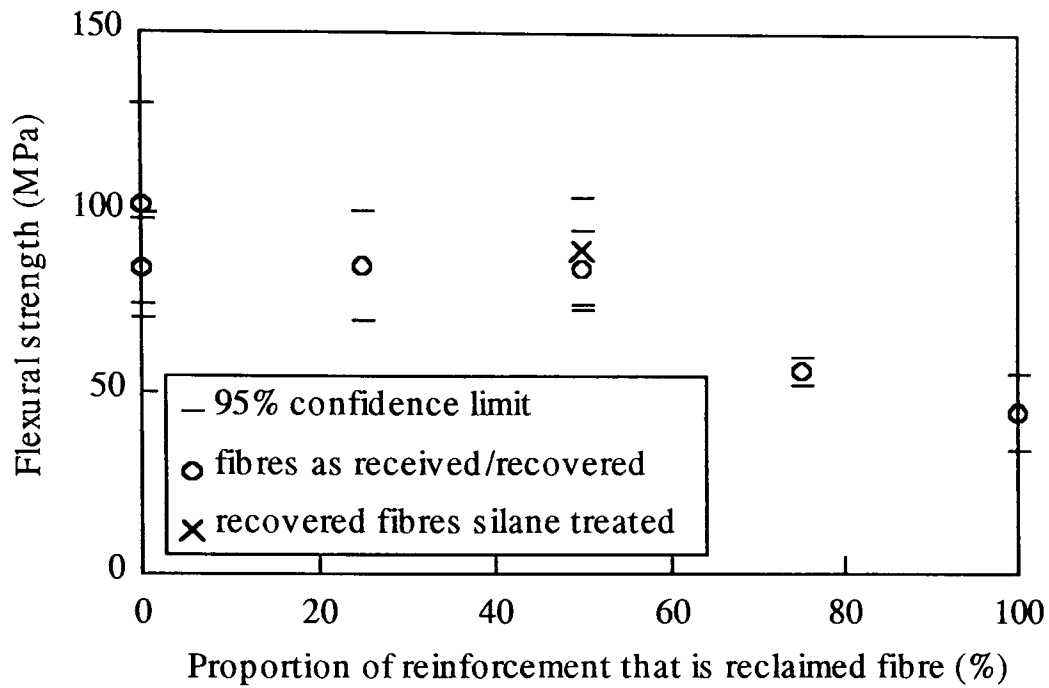


Figure 7.3 Effect of reclaimed fibre content on tensile modulus.
 Virgin fibres: 6 mm chopped strand.
 Reclaimed fibres: from SMC moulding, 450°C.
 Fibre volume fraction: 13%.
 Process: DMC compression moulding.

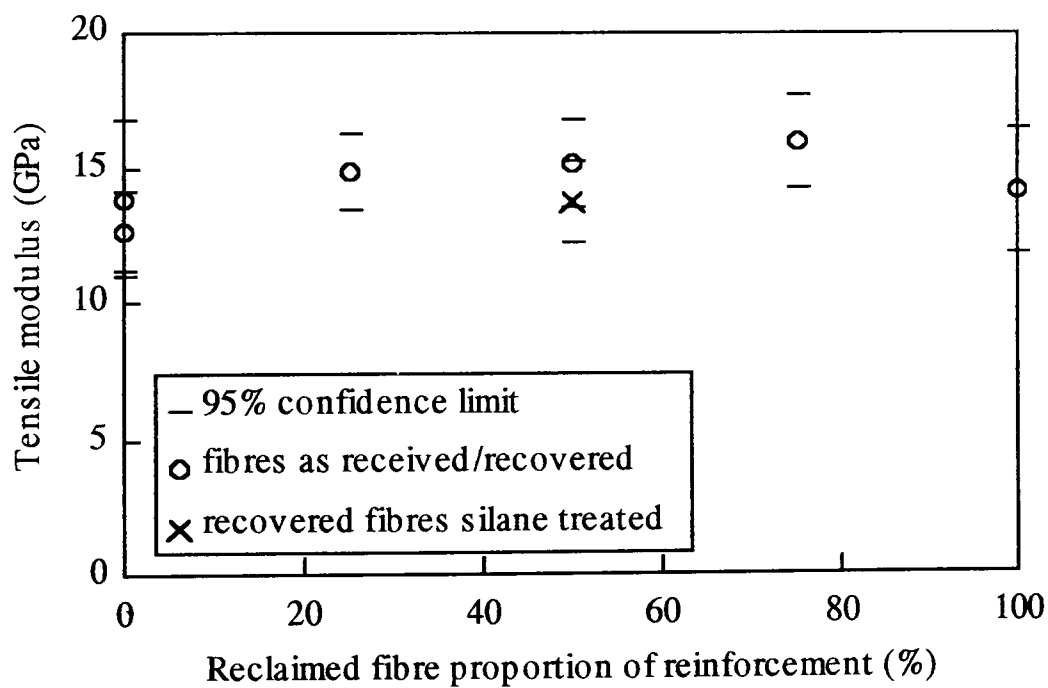


Figure 7.4 Effect of reclaimed fibre content on flexural modulus.
 Virgin fibres: 6 mm chopped strand.
 Reclaimed fibres: from SMC moulding, 450°C.
 Fibre volume fraction: 13%.
 Process: DMC compression moulding.

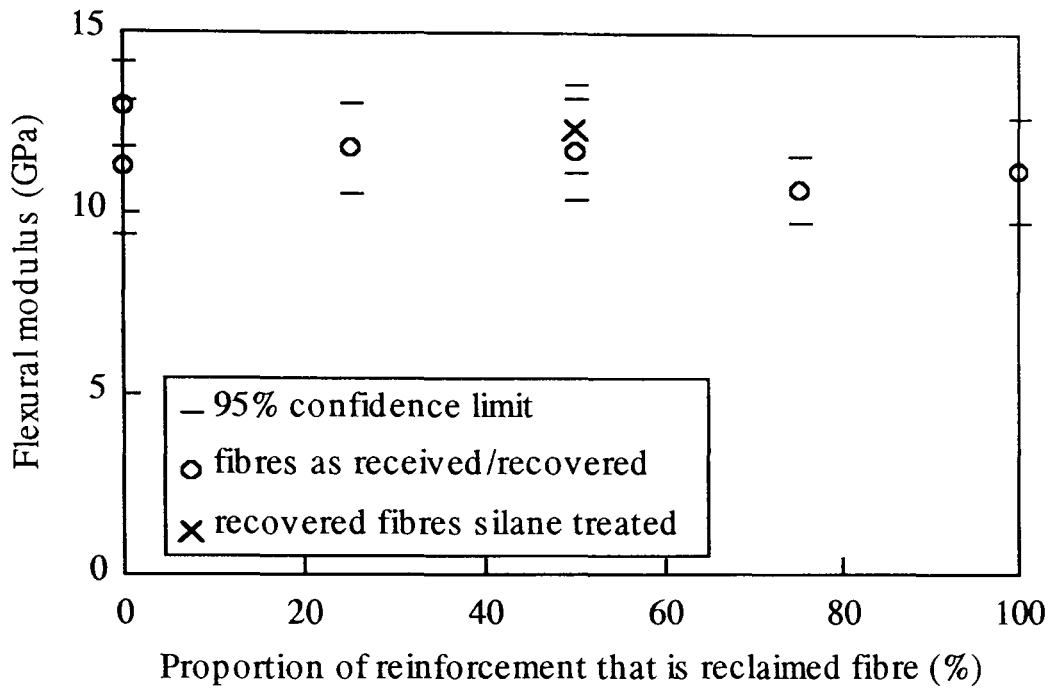


Figure 7.5 Effect of reclaimed fibre content on impact strength.
 Virgin fibres: 6 mm chopped strand.
 Reclaimed fibres: from SMC moulding, 450°C.
 Fibre volume fraction: 13%.
 Process: DMC compression moulding.

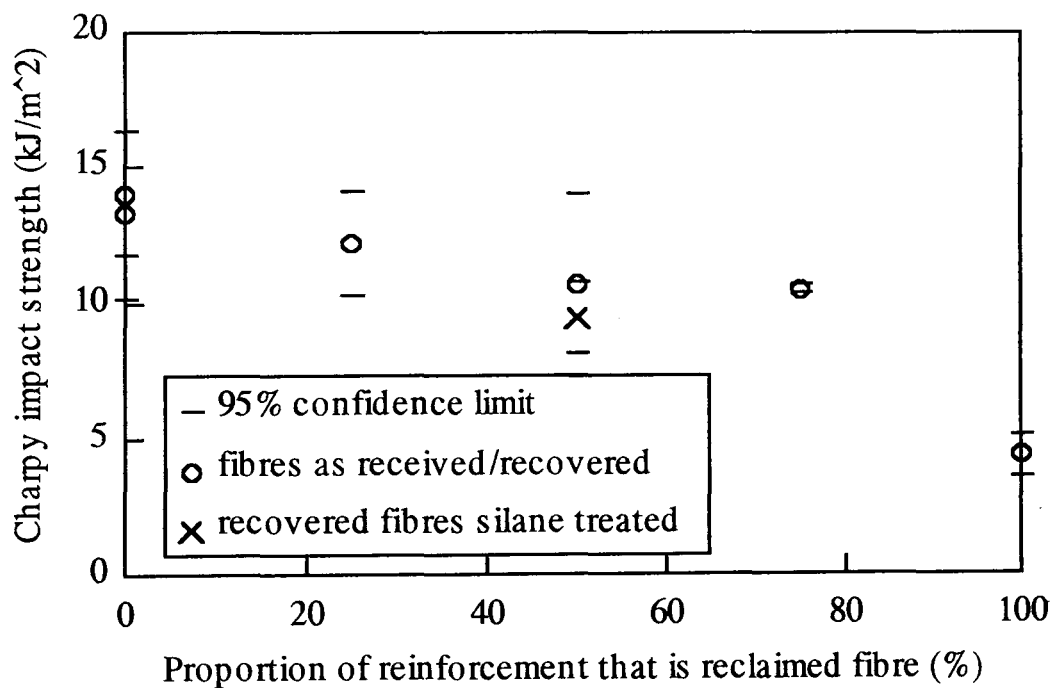


Figure 7.6 Stress as a function of strain for a DMC moulding containing only virgin glass fibres.

Virgin fibres: 6 mm chopped strand.

Fibre volume fraction: 13%.

Process: DMC compression moulding.

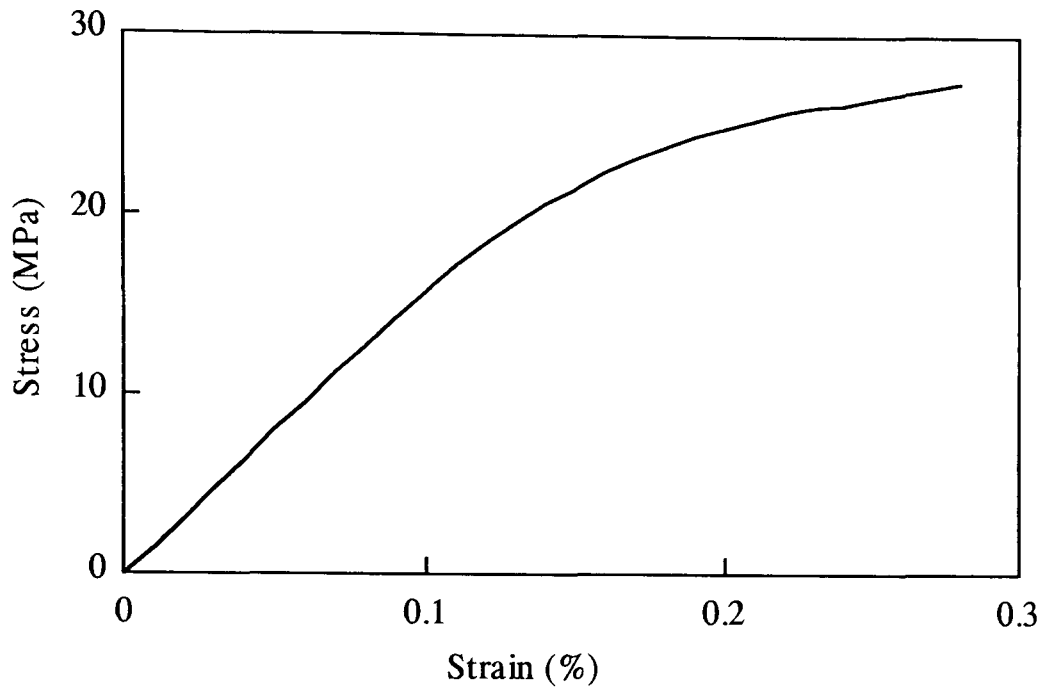


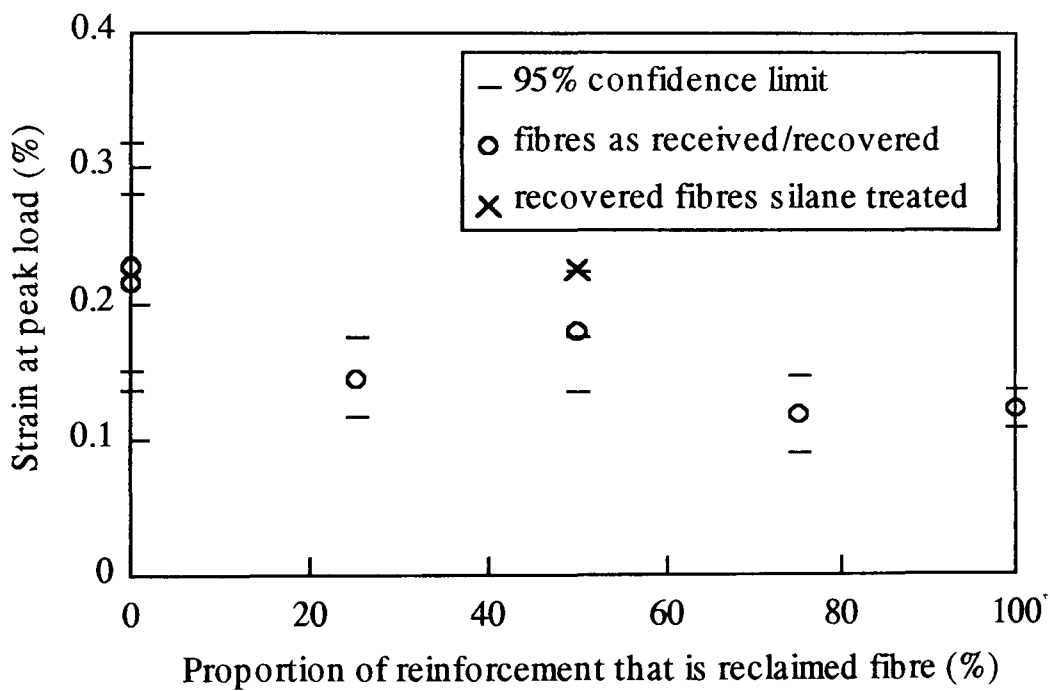
Figure 7.7 Effect of reclaimed fibre content on strain at peak load.

Virgin fibres: 6 mm chopped strand.

Reclaimed fibres: from SMC moulding, 450°C.

Fibre volume fraction: 13%.

Process: DMC compression moulding.



7.2.4 Discussion.

No effect of reclaimed fibre content on moulding tensile strength is seen for replacement levels of up to 50%. Beyond 50% a decrease in tensile strength can be seen (Figure 7.1). A similar trend is evident for the flexural strengths of the samples (Figure 7.2). In contrast to these observations, no detrimental effect of reclaimed fibre content is seen for the Young's modulus (Figure 7.3) or the flexural modulus (Figure 7.4). Data presented in Figure 7.5 show that impact strength is only significantly diminished by reclaimed fibre levels of over 50%. The typical stress against strain curve for a DMC moulding consists of an initial linear part followed by modulus degradation as the damage progresses (Figure 7.6). Failures within these different parts of the stress against strain curve lead to wide confidence limits for the strain at peak load (Figure 7.7). For the samples containing 75% and 100% recovered fibre, all the samples broke in the linear part of the curve and so the strains at peak load are low and have little variation.

For all the measured properties the confidence limits can differ from the mean value by as much as 20% so that the effects of using weaker, recovered fibres are not noticeable until quite large replacement levels are reached. The effects on tensile and flexural strength and strain at peak load are probably due to using weaker fibres but the shorter fibre lengths present in the recovered fibres and the fact that only 92% of the recovered material is fibre will also be responsible for the deterioration in properties. Results presented in Chapter 5 suggested that the stiffness of a composite material, of fibre volume fraction 0.25, is only reduced by 10% by the use of recovered fibres. This may account for the negligible effect of using recovered fibres on the DMC tensile and flexural moduli.

Resizing the recovered fibres had no significant effect on any of the DMC properties.

The recovered glass fibres processed in a similar manner to the virgin fibres but produced a moulding compound with less bulk. This is probably due to the improved packing of the short glass fibres in the recovered material. The surface appearance of the mouldings was affected by the use of the recovered fibres. Some pigment carried over from the original SMC mouldings caused a darkening of the moulding, which was white when virgin fibres were used.

7.3 Pilot plant trial.

The results of the investigations into the effects of using reclaimed fibres in a DMC were encouraging and a larger scale trial was organized at the premises of BIP Ltd. The aims were to investigate the processing of the reclaimed fibre on a larger scale, to confirm the effect of reclaimed fibres on the properties of a DMC moulding and to produce enough material for injection moulding trials with the view to producing a demonstrator component. A 50% replacement level of reclaimed fibres for virgin fibres was chosen as this was the replacement level at which an effect on moulding strength became significant in the initial trials.

7.3.1 Method.

Two 17 kg batches of a production grade DMC were prepared. Detailed formulation details are proprietary and will not be given here but the matrix was a polyester system, the filler was based on aluminium hydroxide with a black pigment and the total glass content was 18% by weight. The first batch prepared was a control DMC containing only virgin 6 mm fibres. The second batch prepared was an experimental DMC in which half of the virgin glass was replaced by fibres recovered from the FW pipe with a fluidised bed temperature of 450°C and the rotating screen collection system. Using the method described in section 7.2.1, this fibrous material was found to contain 90% by weight of fibre.

Test plaques of nominal thickness 3.5 mm were produced by BIP operators using compression moulding. These were tested as described above.

7.3.2 Results.

Results of the mechanical testing are shown in Figures 7.8, 7.9 and 7.10.

Figure 7.8 Flexural and tensile strengths of DMC mouldings.
Total fibre content: 18% w/w.
Reclaimed fibre source: FW pipe, 450°C.
Process: compression moulding.

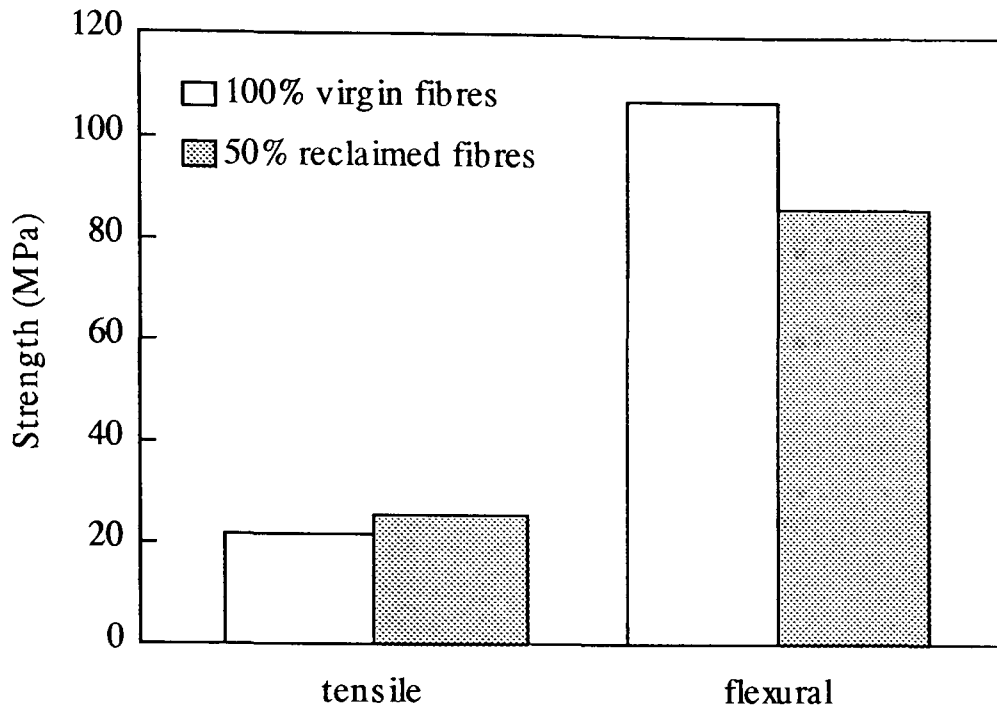


Figure 7.9 Flexural and tensile moduli of DMC mouldings.
Total fibre content: 18% w/w.
Reclaimed fibre source: FW pipe, 450°C.
Process: compression moulding.

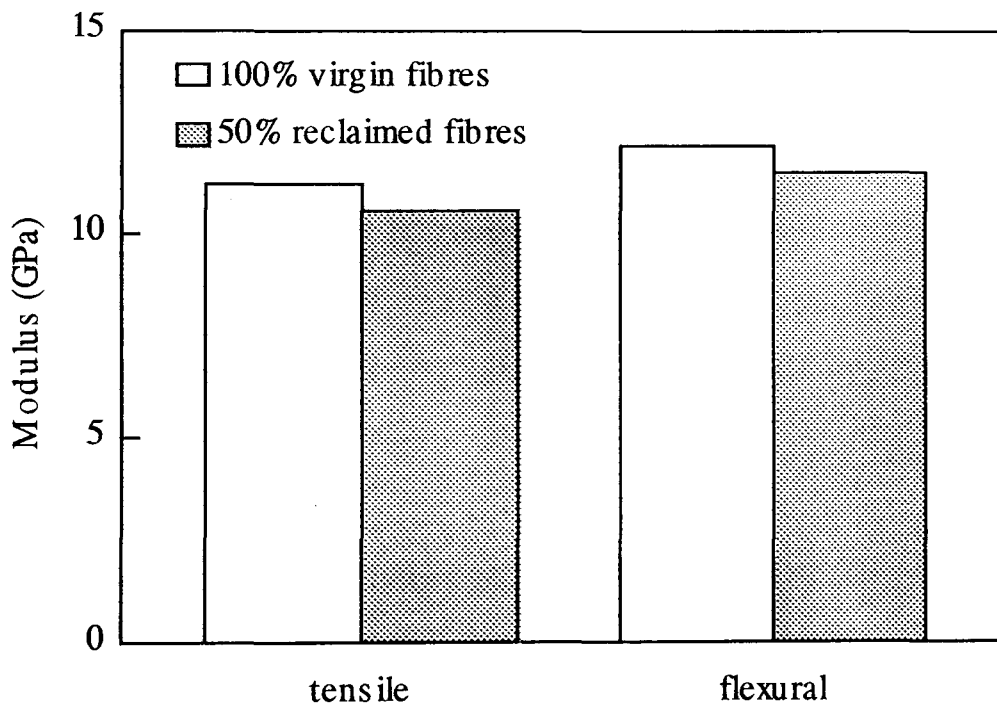


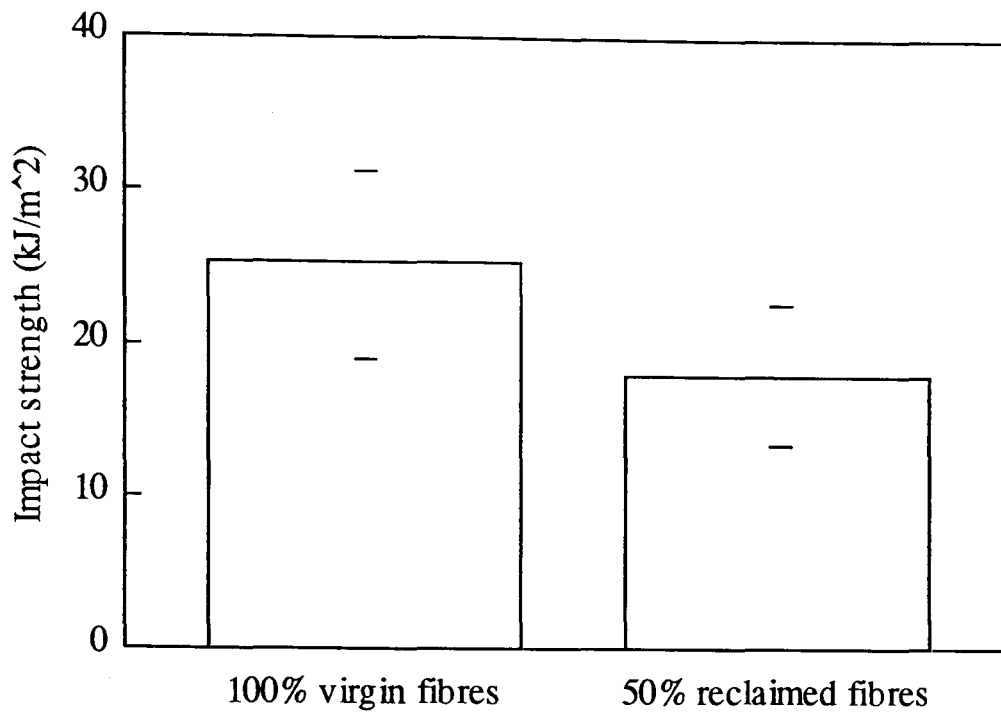
Figure 7.10 Charpy impact strength of DMC mouldings.

Total fibre content: 18% w/w.

Reclaimed fibre source: FW pipe, 450°C.

Process: compression moulding.

Experimental formulation: 50% virgin, 50% reclaimed fibres.



7.3.3 Discussion.

The results of the laboratory scale trial have been confirmed. No significant effect of the recovered fibres on any of the measured properties was found.

BIP personnel were asked for comments on the processability of the recovered fibres. They stated that feeding of the reclaimed glass into the mixer was slow because of its bulk but that it was then quickly absorbed into the mix by the action of the blades. The black pigment masked any discolouration which might have been produced by the recovered fibres and moulding appearance which was good. No fibre bundles or dry fibre patches were visible on the moulding surfaces.

DMC mouldings are often used for electrical switchgear. In these applications the ability of the component to withstand high voltage sparking and the flow of current through its body or over its surface is critical. For the experimental formulation mouldings, arc resistance, measured at BIP Ltd. using ASTM D495-73 as 195 seconds, and insulation resistance, measured at BIP Ltd. using BS 2782 method 204C IEC 167 as $12.0 \log_{10}$ ohm,

were both found to be normal. A headlamp body was successfully injection moulded on commercial plant at BIP Ltd. using the DMC containing 50% reclaimed fibres. No problems with processing were reported.

7.4 Conclusions.

Within experimental uncertainties, 50% of the virgin fibre in the DMC under investigation can be replaced by the fibrous material recovered from SMC feed by the fluidised bed at 450°C without any significant effect on the measured properties. With increasing replacement levels, flexural and tensile stiffness remain unaffected but tensile and flexural strengths, strain at peak load and Charpy impact strength start to fall. These effects compare well with those presented in Chapter 5. Any effects of silane coating the recovered fibres, at this level of fibre replacement, are insignificant.

It has been shown that recovered glass fibres can be incorporated into a DMC at a replacement level of 50% on a pilot plant scale without affecting the main properties of mouldings subsequently made from it. Preparation of the DMC could be achieved using standard equipment and mixing schedules and moulding performance was indistinguishable from that of a control formulation using either compression or injection moulding techniques.

Manufacture of a dough moulding compound is energy intensive. Most of this energy is put into the system to wet out the fibres and the fillers [39]. This leads to fibre degradation which can lead to a reduction in the ultimate mechanical properties of a moulded component. Since the recovered fibres are already filamentised to a large degree it might be possible to alter the mixing procedure to take advantage of the initial state of the recovered fibres.

Fibres recovered from scrap composites using the fluidised bed process can be recompounded into a DMC with little effect on mechanical properties, and by replacing the virgin glass fibre they can command a high price. This should be compared with the effect of replacing filler with ground composite scrap (Figures 2.1 and 2.2) where little value is generated and properties are degraded.

Chapter 8

Conclusions and Further Work.

8.0 Introduction.

The aim of this chapter is to summarize the conclusions of the work presented in this thesis and to highlight some areas of this research which would benefit from further investigation.

8.1 Conclusions.

A fluidised bed process for recovering fibrous reinforcement from thermoset composite materials has been briefly described. An initial investigation into the effect of heat on the reinforcement potential of a glass cloth was followed by an experimental investigation into the effect of fluidised bed processing on the properties of recovered glass and carbon fibres. The information gathered about the length, strength and Young's modulus of the recovered fibres was used to predict their reinforcement potential in a thermoset composite laminate and these predictions were compared to measured properties of laminates reinforced with recovered fibres. Two uses for the recycled glass fibres were investigated, a veil material and a dough moulding compound.

Conclusions are presented in the order in which the work is arranged in this thesis.

8.1.1 Heat treated glass cloth as reinforcement in a thermoset composite.

Samples of woven E-glass cloth were heated for up to 60 minutes at temperatures of up to 625°C. These samples were then used as reinforcement in polyester based laminates. It was found that heat treatment reduces the reinforcing potential of E-glass cloth. The degree of strength reduction is both time and temperature dependent but after 20 minutes of heat treatment there is little or no further strength reduction. A strength loss of 25% was measured after heating at 375°C for twenty minutes. No gain in strength was noted after silane coating the heat treated cloth in this case. A strength loss of 50% was measured after heating at 500°C for twenty minutes. A 25% gain in strength was noted after silane coating the heat treated cloth. A strength loss of 75% was measured after

heating at 625°C for twenty minutes. No gain in strength was noted after silane coating the heat treated cloth. No effect of the reinforcement heat treatment on the initial tangent modulus of the laminates was measured. It was concluded that the strengths of the glass fibres were degraded by heating but that the modulus was unchanged.

8.1.2 Properties of recycled glass fibres.

Glass fibres were recovered from a number of thermoset composite materials to investigate the effect of processing conditions on the recovered fibre properties. It was found that glass fibres recovered at 450°C retain half the strength of virgin fibres but as the fluidised bed temperature is increased, weaker glass fibres are recovered. Carbon fibres are less severely degraded by processing. The distribution of lengths of the recovered fibres depends on the form of the scrap composite material and the feed preparation details. Composites with a high fibre volume fraction tend to produce an increased number of small fibres when processed. Fibres have been recovered with number average lengths of approximately 3 mm and weight average lengths of approximately 5 mm. Over the range of processing temperatures investigated, glass and carbon fibre modulus was found to be unaffected by the recovery process. Weakened glass fibres can be restrengthened by a chemical ion exchange treatment. An increase of 16% in the Weibull scale parameter was measured as the result of an unoptimised ion exchange procedure.

8.1.3 Reinforcement potential of recycled glass fibres.

Recovered and virgin glass fibres and recovered carbon fibres were used as reinforcement in an epoxy resin laminate. The mechanical properties of the laminates were measured and compared to predicted results. The following conclusions were drawn. No significant reduction in the modulus of the laminates containing reclaimed glass fibres was measured. From theoretical considerations it was found that a reduction, accounted for by the significant number of short fibres which provide ineffective reinforcement, should be expected but this was masked by experimental scatter. The reduction in the strengths of the laminates containing reclaimed fibres is accounted for by the lower strength of the recovered fibres and theory predicts that strength is largely unaffected by the lengths of the recovered fibres. The measured laminate properties are in close agreement with the predicted properties and provide evidence that the measured fibre properties are reliable.

8.1.4 Use of recycled glass fibres in a veil material.

A glass veil was identified as an appropriate application for the recovered glass fibres since a veil material contains monofilaments and the strength of the veil is not generally critical to its performance. An initial investigation into the processing of the recovered fibres showed that recovered glass fibres can be dispersed and formed into a veil material using identical processing conditions to those required to form a veil from virgin WCS. However, virgin fibres cannot be successfully dispersed in the presence of reclaimed fibres. Some properties of glass veil containing recovered fibres were measured. The effect of replacing virgin fibres with reclaimed fibres in a benchmark veil product is to reduce the wet and dry strengths of the veil. The reduction in wet strength is due to the increased number of short fibres. The dry strength reduction is difficult to determine exactly since there is a large variation in the results of the strength test results but it seems likely that it is directly proportional to the level of virgin fibre replacement and the strength of the reclaimed fibres. Veil permeability is not affected by the use of recovered fibres but is related to the porosity of the veil sample. Veil containing recovered fibre can be successfully used as a surfacing agent for composite materials, where it prevents fibre print through and can form the basis of a corrosion resistant resin layer.

As part of the RRECOM project [23], an initial assessment of the economic viability of the fluidised bed process for recovering reinforcing fibres from scrap thermoset composites was made. This was achieved by defining the philosophy of the commercial process, designing and costing a suitable plant, estimating the profitability and then optimising the plant capacity following conventional chemical engineering practices. It was found that break even would be achieved at a scrap capacity of approximately 9,000 tonnes per year, assuming the recovered fibres could be sold at 80% of the price of virgin fibres. This is higher than existing industrial capacity, 2,000 to 6,000 tonnes per year [21], and this level of scrap could not be readily collected for processing at the present time.

It seems unlikely that veil manufacturers would be prepared to purchase recovered fibres for use in surfacing veils unless the quality and consistency of the fibres could be guaranteed. With a mix of contaminated feeds this might be difficult to ensure. A more

easily accessible market might be for veils used to provide dimensional stability to wall and floor coverings or in roofing shingles. In this application appearance is less critical. The price at which the recovered fibres could be sold into this market would depend on their effect on veil properties and ease of processing.

8.1.5 Use of recycled glass fibres in a dough moulding compound.

Glass fibres recovered at 450°C were used as replacement for virgin fibres in a dough moulding compound. The mechanical properties of plates compression moulded from the experimental dough moulding compounds were investigated. It was found that up to 50% of the glass fibres in a DMC can be replaced by fibres recovered at 450°C with little effect on any of the mechanical properties of the moulded plate. At replacement levels in excess of this the modulus of the plate is unaffected but both the tensile, flexural and impact strengths starts to decrease. At a replacement level of 50% it was found that applying a functional size to the recovered fibres had no effect on moulding properties. A DMC containing recovered fibres was prepared on a pilot scale using standard DMC preparation plant. The resulting material was successfully compression or injection moulded. A demonstrator component was injection moulded from a DMC containing 50% recovered fibres. These results show that the recovered fibres have a higher value than regrind because they can be used to replace up to 50% of the virgin fibres.

Given a future level of thermoset composites usage where there is adequate waste available to make fluidised bed recovery worthwhile, the use of recovered fibres in a DMC would seem to be economically attractive. Relatively large replacement levels (50%) are possible with little or no effect on moulding properties and so large savings for the manufacturer are possible at relatively high recovered fibre prices. Recovered fibres could more easily demand a price of 80% of that of virgin fibres in this application than when used in veil.

8.2 Original aspects of this investigation.

Novel aspects of the work presented in this thesis are:

- determination of the effects of heat treatment on the reinforcing efficiency of glass cloth.
- measurement of the strength, Young's modulus and length distribution of glass and

carbon fibres recovered from thermoset composites using a thermal fluidised bed process.

- confirmation of the reinforcing efficiency of recovered glass and carbon fibres.
- demonstration of the reuse of thermally recovered glass fibres in a veil.
- demonstration of the reuse of thermally recovered glass fibres in a dough moulding compound.

8.3 Further work.

The following suggestions for areas requiring further investigation are made.

8.3.1 Properties of recycled glass fibres.

The preparation of the composite feed material has not been fully investigated. Optimisation of the feed material preparation to give the shortest fluidised bed processing time, so maximising recovered fibre strength, and the greatest recovered fibre lengths will improve the quality of the recovered fibre product. The results presented in this thesis should be broadened by investigations into the properties of fibres recovered from a wider range of composite materials. This should include injection moulded products where the recovered fibre length is likely to be much less than that for the materials already investigated and the properties of fibres recovered from mixed composite materials and ASR.

8.3.2 Reinforcement potential of recycled glass fibres.

It would be worthwhile to investigate fibre alignment techniques as a method of producing a high fibre volume fraction recovered fibre sheet material to be sold into the reinforced plastics market. In such a case, further investigations into the merits of resizing recovered fibres would be needed. Can the fibre reinforcement potential be increased? Will the increased cost be recouped? This line of enquiry might be more appropriate for recovered carbon fibres than glass fibres.

8.3.3 Use of recycled glass fibres in a veil material.

Further investigations can only sensibly proceed with the manufacture of a veil material with an appreciable reclaimed fibre content on a pilot veil machine. This would enable

large amounts of consistent product to be produced. One of the primary concerns should be to quantify the effect of the short fibre length fraction of recovered fibres on the veil wet strength. Full characterisation of the veil material including investigations into areas of reuse and an economic analysis would then also be possible.

8.3.4 Use of recycled glass fibres in a dough moulding compound.

Extended production trials are required followed by extensive testing of the materials. These trials should concentrate on the effect of the recovered fibres on compounding, processing and final moulding properties, especially from the point of view of consistency. Further studies could investigate the effect of recovered fibres on the surface finish of a DMC moulding and the effect of subsequent recycling cycles.

8.3.5 Properties of recycled carbon fibres.

High quality carbon fibres were recovered from scrap CFRP using the fluidised bed processing rig. Further work to characterise the recovered fibres and investigate their reuse should include optimization of the processing conditions for recycling carbon fibres where the combined effects of fluidising velocity and bed temperature should be quantified. Some measurement of the fibre length distribution of the recovered fibres and an investigation of the value of resizing the fibres would help to quantify their reinforcement potential. Other possible applications for the reuse of recovered carbon fibres, possibly including use in a veil, carbon - carbon composites or as replacement for milled carbon fibres in electromagnetic field screening applications should be investigated. Finally, carbon fibre scrap often arises in offcuts of cured and uncured prepreg and the processing of this form of material should be investigated.

References

1. Anonymous, *Statistics Handbook*, . 1996, British Plastics Federation: London.
2. Henshaw, J.M., W. Han, and A.D. Owens, *Overview of recycling issues for composite materials*. *Journal of Thermoplastic Composite Materials*, 1996. **9**(1): p. 4-20.
3. Buggy, M., L. Farragher, and W. Madden. *Recycling of composite materials*. in *Advances in Materials and Processing Technologies*. 1993. Dublin.
4. Unser, J.F. and T. Staley. *Advanced composites recycling*. in *41st International SAMPE symposium*. 1996: SAMPE.
5. Jost, K., *Sheet molding composite recycling*. *Automotive Engineering*, 1995. **103**(8): p. 40-41.
6. Graham, W.D., *Recycling glass reinforced composites: the value of glass fibres*. *Polymer recycling*, 1995. **1**(4): p. 87-97.
7. Gordon, J.E., *The New Science of Strong Materials*. 2nd ed. 1976, London: Penguin Books. 287.
8. Owen, M.J., *RTM Applications*, 1995, University of Nottingham, unpublished.
9. Anonymous, *Owens Corning composites applications: auto*, 1998, Owens-Corning: [http:// www.owenscorning.com:80/owens/composites/applications/transport/auto.html](http://www.owenscorning.com:80/owens/composites/applications/transport/auto.html).
10. Anonymous, *Automotive shredder residue. Three recovery choices*. *Automotive Engineering*, 1994. **102**(8): p. 29-31.
11. Poston, I.E. *Recycling of auto shredder residue*. in *Avanced Composites Conference*. 1995. Dearborn, Michigan, USA: ESD, The Engineering Society.
12. Anonymous, *The CARE group*. 1997: <http://www.wcshome.demon.co.uk/care.htm>.
13. Zuern, J., Gueldenpfennig, M., Loehr, R., Melchiorre, M., *Recycling of instrument panels made from composites*. *Kunststoffe Plast Europe*, 1994. **84**(3): p. 40-42.
14. Cucuras, C.N., Flax, A. M., Graham, W. D., Hartt, G. N., *Recycling of thermoset automotive components*. SAE (Society of Automotive Engineers)

- Transactions, 1991. **100**(Sect 5): p. 437-452.
15. Belzowski, B.M. and M.S. Flynn. *Automotive structural composites: the recycling barrier*. in *Advanced Composites Conference*. 1995. Dearborn, Michigan, USA: ESD, The Engineering Society.
 16. Wickersham, M.S. *The option of source reduction*. in *Annual Technical Conference*. 1996. Indianapolis: Soc of Plastics Engineers, Brookfield, CT, USA.
 17. Anonymous, *Waste management*, . 1997, Environmental Data Services Ltd.: London. p. 13.
 18. Anonymous, *Ad valorem landfill tax gets a panning*. ENDS Report, 1995(246): p. 23.
 19. Anonymous, *Commision proposes directive on environmentally friendly handling of end of life vehicles*, . 1997, European Union: <http://www.europa.eu.int>.
 20. Steenkamer, D.A. and J.L. Sullivan, *Recycled content in polymer matrix composites through the use of A- glass fibers*. *Polymer Composites*, 1997. **18**(3): p. 300-312.
 21. Schaefer, P. and A.G. Plowgian. *SMC recycling: an update - ERCOM's experience in production and application*. in *49th Annual Conference, Composites Institute*. 1994: Society of the Plastics Industry.
 22. Brooke, L., *Arise, SMC recycling!* Chilton's Automotive Industries, 1994. **174**(9): p. 64-66.
 23. RRECOM, *Recycling and REcovery from COMposite Materials*. LINK Structural Composites Programme, 1994. Ref. no. IL 12/2/126.
 24. Bevis, M.J., Bream, C., Hornsby, P. R., Taverdi, K., Williams, K., *Comminution and re-use of thermosetting plastics waste*. in *Composites '96, 20th International British Plastics Federation Composites Congress*. 1996: BPF.
 25. Day, M., J.D. Cooney, and Z. Shen, *Pyrolysis of automobile shredder residue: an analysis of the products of a commercial screw kiln process*. *Journal of Analytical and Applied Pyrolysis*, 1996. **37**(1): p. 49-67.
 26. Ushikoshi, K., N. Komatsu, and M. Sugino, *Recycling of CFRP by pyrolysis method*. *Zairyo/Journal of the Society of Materials Science, Japan*, 1995. **44**(499): p. 428-431.
 27. Hanson, D.G. *Recovery of Fiberglass Reinforcement and Additive Materials from*

- Scrap Circuit Board Laminates*. in *46th Annual Conference*. 1991: Composites Institute, The Society of the Plastics Industry.
28. Allred, R.E. *Recycling process for scrap composites and prepregs*. in *International SAMPE Symposium and Exhibition (Proceedings)*. 1996.
 29. Pickering, S.J. and M. Benson. *Recovery of Material and Energy from Thermosetting Plastics*. in *ECCM6 - Conference on Recycling Concepts and Procedures*. 1993. Bordeaux: European Association for Composite Materials.
 30. Fenwick, N.J. and S.J. Pickering. *Using waste material to reduce emissions - combustion of glass reinforced plastic with coal in a fluidized bed*. in *Engineering for Profit from Waste*. 1994. London: Institute of Mechanical Engineers.
 31. Bradley, J.C., W.D. Graham, and R. Forster. *Solvent separation: a method for recycling uncured SMC*. in *49th Annual Conference, Composites Institute*. 1994: Society of the Plastics Industry.
 32. Johnson, M.S., C.D. Rudd, and D.J. Hill, *Cycle time reductions in resin transfer moulding using microwave preheating*. Proceedings of the Institution of Mechanical Engineers, Part B: Journal of Engineering Manufacture, 1995. **209**(B6): p. 443-453.
 33. Kendall, K.N.,Rudd, C. D., Owen, M. J., Middleton, V., *Characterization of the resin transfer moulding process*. Composites Manufacturing, 1992. **3**(4): p. 235-249.
 34. Owen, M.J., Middleton, V., Rudd, C. D., Scott, F. N., Hutcheon, K. F., Revill, I. D., *Materials behaviour in resin transfer moulding (RTM) for volume manufacture*. Plastics and Rubber Processing and Applications, 1989. **12**(4): p. 221-225.
 35. Owen, M.J., Rudd, C. D., Middleton, V., Kendall, K. N., Revill, I. D. *Resin transfer moulding (RTM) for automotive components*. in *American Society of Mechanical Engineers, Petroleum Division (Publication) PD*. 1991. 14th annual Energy-Sources Technology Conference and Exhibition Houston: ASME, New York, NY, USA.
 36. Rudd, C.D. and K.N. Kendall, *Towards a manufacturing technology for high-volume production of composite components*. Proceedings of the Institution of Mechanical Engineers, Part B: Journal of Engineering Manufacture, 1992.

- 206(B2): p. 77-91.
37. Benson, M., *Disposal of thermosetting resins*, in *Department of Mechanical Engineering*. 1993, University of Nottingham: Nottingham. p. 187.
 38. Anonymous, *Owens Corning reinforcing mats and veil*, . 1998, Owens-Corning: <http://www.owenscorning.com:80/owens/composites/lineup/mats/veils.html>.
 39. Burns, R. and D. Pennington. *Study Of Glass Fibre Degradation and Its Control During the Mixing Of DMC'S*. in *Reinf Plast Congress*. 1978. Brighton, Sussex: British Plastics Federation.
 40. Owen, M.J., D.H. Thomas, and M.S. Found. *Flow, Fibre Orientation and Mechanical Property Relationships In Polyester DMC*. in *Society of the Plastics Industry, Reinforced Plastics/Composites Institute, Annual Conference*. 1978. Washington, DC: SPI, New York, NY.
 41. Chu, J. and J.L. Sullivan, *Recyclability of a continuous E-glass fiber reinforced polycarbonate composite*. *Polymer Composites*, 1996. 17(4): p. 556-567.
 42. Butler, K. *Recycling of molded SMC and BMC materials*. in *46th Annual Conference, SPI*. 1991: SPI.
 43. Jutte, R.B. and W.D. Graham, *Recycling SMC scrap as a reinforcement*. *Plastics Engineering*, 1991. 47(5): p. 13-14, 16.
 44. Petterson, J. and P. Nilsson, *Recycling of SMC and BMC in Standard Process Equipment*. *Journal of Thermoplastic Composite Materials*, 1994. 7(January): p. 56-63.
 45. Kitamura, T. *Market development for recycling thermoset in Japan*. in *49th Annual Conference, Composites Institute*. 1994: Society of the Plastics Industry.
 46. Darrah, B. *Recycling composites in Canada: an update*. in *49th Annual Conference, Composites Institute*. 1994: Society of the Plastics Industry.
 47. Priest, S.M. *Thermoset composites recycling: use of recycled fiber from SMC as reinforcement in an RTM material*. in *Advanced Composites Conference*. 1995. Dearborn, Michigan, USA: ESD, The Engineering Society.
 48. Cardew, W., *Filler material price list*, . 1995, Croxton + Garry Ltd.
 49. Lubin, G., *Handbook of Composites*, in *Handbook of Composites*, G. Lubin, Editor. 1982, Van Nostrand Reinhold: New York. p. 138-140.
 50. Sridhar, M.K., *Fibre reinforcements for composites*. *Defence Science Journal*,

1993. 43(4): p. 365-368.
51. Zachariassen, W.H., *Journal of the American Chemistry Society*, 1932. 54: p. 3841.
 52. Loewenstein, K.L., *The manufacturing technology of continuous glass fibres*. 1 ed. 1973, Amsterdam: Elsevier Scientific Publishing Company. 272.
 53. Griffith, A.A., *The phenomena of rupture and flow in solids*. *Philosophical Transactions of the Royal Society*, 1920. 221A(October): p. 163-198.
 54. Otto, W.H., *Relationship of tensile strength of glass fibers to diameter*. *Journal of the American Ceramic Society*, 1955. 38(3): p. 122-124.
 55. Thomas, W.F., *An Investigation into the Factors Likely to Affect the Strength and Properties of Glass Fibres*. *Physics and Chemistry of Glasses*, 1960. 1(1): p. 4-18.
 56. Bartenev, G.M. and L.K. Izmailova, *Nature of the high strength of glass fibers*. *Soviet Physics - Solid State*, 1964. 6(4): p. 920-927.
 57. Metcalfe, A.G. and G.K. Schmitz, *Effect of length on the strength of glass fibres*. *ASTM Proceedings*, 1964. 64: p. 1075-1093.
 58. Weibull, W., *A Statistical Distribution Function of Wide Applicability*. *Journal of Applied Mechanics*, 1951. 18: p. 293-297.
 59. Sugarman, B., *Strength of Glass (A Review)*. *Journal of Materials Science*, 1967. 2: p. 275-283.
 60. Hull, D., *An introduction to composite materials*. Cambridge solid state science series. 1981: Cambridge university press. 246.
 61. Mackenzie, J.D. and J. Wakaki, *Effects of ion exchange on the Young's modulus of glass*. *Journal of Non-Crystalline Solids*, 1980. 38 & 39: p. 385-390.
 62. Sakka, S., *Effects of Reheating on Strength of Glass Fibers*. *Bulletin of the Institute of Chemical Research*, 1957. 34: p. 316-320.
 63. Hara, M., *Some aspects of strength characteristics of glass*. *Glastechnische Berichte*, 1988. 61(7): p. 191-196.
 64. Brearley, W. and D.G. Holloway, *The Effect of Heat Treatment on the Breaking Strength of Glass*. *Physics and Chemistry of Glasses*., 1963. 4(3): p. 69-75.
 65. Cameron, N.M., *Effect of Prior Heat Treatment on the Strength of Glass Fibers Measured at Room Temperature*. *Journal of the American Ceramic Society - Discussions and Notes*, 1965(July): p. 385.

66. Ward, J.B., B. Sugarman, and C. Symmers, *Studies on the chemical strengthening of soda-lime-silica glass*. Glass Technology, 1965. 6(3): p. 90-97.
67. Piggott, M.R. and J.C. Yokom, *The Weakening of Silica Fibres by Heat Treatment*. Glass Technology, 1968. 9(6): p. 172-175.
68. Cameron, N.M., *The Effect of Environment and Temperature on the Strength of E-glass Fibres. Part 2. Heating and Ageing*. Glass Technology, 1968. 9(5): p. 121-130.
69. Anonymous, *Glass fibre yarn and fabrics*, , Clark-Schwebel.
70. Bryant, M. *Glass Fabrics Production - An Overview*. in *Nepcon West '92*. 1992. Anaheim, CA, USA: Cahner Exposition Group.
71. Adams, R.G., S.J. Milletari, and A. Roth. *The Influence of Ion Exchange Strengthening on the Performance of Finished Fiberglass Fabrics in Composites*. in *26th Annual Technical Conference*. 1971: Society of Plastics Engineers.
72. Jarvela, P.K., *Bending Strength and Static Fatigue Of Glass Fibre In Different Atmospheres By Fibre Loop Test*. Journal of Materials Science, 1984. 19(8): p. 2481-2487.
73. Das, B., B.D. Tucker, and J.C. Watson, *Acid corrosion analysis of fibre glass*. Journal of Materials Science, 1991. 26: p. 6606-6612.
74. Edwards, H. and N.P. Evans. *Method For the Production Of High Quality Aligned Short Fibre Mats and Their Composites*. in *Adv in Compos Mater, Proc of the Int Conf on Compos Mater, 3rd,*. 1980. Paris, France: Pergamon Press.
75. Murty, K.N. and G.F. Modlen, *Experimental Characterization of the Alignment of Short Fibers During Flow*. Polymer Engineering and Science, 1977. 17(12): p. 848-853.
76. Salariya, A.K. and J.F.T. Pittman, *Preparation Of Aligned Discontinuous Fiber Pre-Pregs By Deposition From a Suspension*. Polymer Engineering and Science, 1980. 20(12): p. 787-797.
77. Bagg, G.E.G., M.E.N. Evans, and A.W.H. Pryde, *The Glycerine Process for the Alignment of Fibres and Whiskers*. Composites, 1969(December): p. 97-100.
78. Vyakarnam, M.N. and L.T. Drzal. *High speed process for the production of aligned discontinuous fiber structural composites using electric fields*. in *Advanced Composites Conference*. 1995. Dearborn, Michigan, USA: ESD, The Engineering

- Society.
79. Bangert, L.H. and P.M. Sagdeo, *On Fiber Alignment Using Fluid-Dynamic Forces*. Textile Research Journal, 1977. **47**(12): p. 773-780.
 80. Soh, S.K. and E. Kordyban. *Oriented fiber preforms with slurry process*. in *Advanced Composites Conference*. 1995. Dearborn, Michigan, USA: ESD, The Engineering Society.
 81. Osterholtz, F.D. and E.R. Pohl, *Kinetics of the hydrolysis and condensation of organofunctional alkoxysilanes: a review*. Journal of Adhesion Science Technology, 1992. **6**(1): p. 127-149.
 82. Sterman, S. and J.G. Marsden. *Silane coupling agents as 'integral blends' in resin-filler systems*. in *18th Annual Technical and Management Conference*. 1963. Chicago: The Society of the Plastics Industry.
 83. Gomez, J.A. and J.A. Kilgour. *The effect of silane structure on glass fiber performance in reinforced composites*. in *49th Annual Conference, Composites Institute*. 1994. Cincinnati, OH: The Society of the Plastics Industry Inc.
 84. Gomez, J.A. and J. A.Kilgour. *The effect of temperature on silane coupling agent performance at the glass fiber/resin interface*. in *48th Annual Conference, Composites Institute*. 1993. Cincinnati, OH: The Society of the Plastics Industry.
 85. Nagae, S. and Y. Otsuka, *Effect of sizing agent on corrosion of glass fibres in water*. Journal of Materials Science Letters, 1994. **13**(20): p. 1482-1483.
 86. Gomez, J.A. and J.A. Kilgour, *The effect of glass fiber surface coatings on fiber strength and the distribution of flaws*, . 1993, OSi Specialities Inc.: Tarrytown, NY.
 87. Bromley, J. *Gas evolution processes during the formation of carbon fibres*. in *1st International Conference on Carbon Fibres*. 1971. London: The Plastics Institute.
 88. Watt, W. and J. Green. *The pyrolysis of polyacrylonitrile*. in *1st International Conference on Carbon Fibres*. 1971. London: The Plastics Institute.
 89. Huxley, D.V., *What is carbon fibre?*, in *Carbon Fibres*, W.F. Waller, Editor. 1970, Morgan-Grampian (Publishers) Ltd: London. p. 8-11.
 90. Adams, R.G., *Ion exchange of glass fibres*, . 1968, J. P. Stevens & Co., Inc., New York: USA.
 91. Thomason, J.L. and M.A. Vlug, *Influence of fibre length and concentration on the*

- properties of glass fibre-reinforced polypropylene: 1. Tensile and flexural modulus.* Composites - Part A: Applied Science and Manufacturing, 1996. 27(6): p. 477-484.
92. Fenwick, N.J., *Recycling of composite materials using fluidised bed processes*, in *Department of Mechanical Engineering*. 1996, University of Nottingham: Nottingham. p. 122.
 93. Pickering, S.J., Kelly, R.M., Kennerley, J.R., Rudd, C.D., Fenwick, N.J., *A fluidised bed process for the recovery of glass fibres from scrap thermoset composites*. paper in preparation, 1998.
 94. Lawes Agricultural Trust, *Genstat 5*. 1994: Rothamstead Experimental Station.
 95. Yin, Y., Binner, J. G. P., Cross, T. E., Marshall, S. J., *Oxidation behaviour of carbon fibres*. Journal of Materials Science, 1994. 29(8): p. 2250-2254.
 96. Cox, H.L., *The elasticity and strength of paper and other fibrous materials*. British Journal of Applied Physics, 1952. 3(March): p. 72-79.
 97. DT-Open Layers Imaging, PassThru and Save Application, version 1.0.
 98. Aphelion Image Understanding, version 2.2 . 1997, AAI: Amherst.
 99. Clarke, A.R., N.C. Davidson, and G.A. Archenhold, *Microstructural characterisation of aligned fibre composites*, in *Flow-Induced Alignment in Composite Materials*, T.D.P.a.D.C. Guell, Editor. 1997, Woodhead Publishing Ltd. p. 263.
 100. Pickering, S.J., Rudd, C.D., Kelly R. M., Kennerley, J.R., *RRECOM Progress Report 9*, . 1997, University of Nottingham: Nottingham.
 101. Biddulph, R.H., M.G. Bader, and A. Buxton, *Simple apparatus for measuring the tensile strength of single fibres*. Measurement Science & Technology, 1994. 5(1): p. 9-11.
 102. Dwight, D.W., *Personal Communication*, . 1996, Owens Corning Science and Technology Center, Granville, Ohio.
 103. Anonymous, *Textile fibers for industry*, . 1994, Owens-Corning Fiberglas Corporation: Toledo.
 104. Suh, S.J. and H.J. Eun, *Small mass measurement by optical glass fibre elastic cantilever*. Measurement Science and Technology, 1990. 1: p. 556-560.
 105. Brown, D.K. and W.M. Phillips. *Effects of heat treatment on carbon fibers*. in

- National SAMPE Symposium and Exhibition (Proceedings)*. 1990. International SAMPE Symposium and Exhibition - Advanced Materials: the Challenge for the Next Decade. Part 2 Anaheim: SAMPE, Covina, CA, USA.
106. Dhami, T.L., L.M. Manocha, and O.P. Bahl, *Oxidation behaviour of pitch based carbon fibers*. Carbon, 1991. **29**(1): p. 51-60.
 107. Dorey, G., *Carbon Fibres and Their Applications*. Journal of Physics D: Applied Physics, 1987. **20**(3): p. 245-256.
 108. Hughes, J.D.H., *Evaluation Of Current Carbon Fibres*. Journal of Physics D: Applied Physics, 1987. **20**(3): p. 276-285.
 109. Marshall, P. and J. Price, *Topography of carbon fibre surfaces*. Composites, 1991. **22**(5): p. 388-393.
 110. Haynes, W.M. and T.L. Tolbert, *Determination of the graphite fiber content of plastic composites*. Journal of Composite Materials, 1969. **3**(October): p. 709 - 712.
 111. Gibson, A.G. and D.J. Payne, *Flexural and impact strength improvement in injection moulded SMC*. Composites, 1989. **20**(2): p. 151-158.
 112. Thomason, J.L., Vlug, M. A., Schipper, G., Krikort, H., *Influence of fibre length and concentration on the properties of glass fibre-reinforced polypropylene: Part 3. Strength and strain at failure*. Composites - Part A: Applied Science and Manufacturing, 1996. **27**(11): p. 1075-1084.
 113. Krenchel, H., *Fibre reinforcement*, in *Laboratory of structural research*. 1964, Technical University of Denmark: Copenhagen.
 114. Pollard, A., *GKN epoxy resin properties*, . 1997, GKN Technology Ltd.
 115. Kelly, A. and W.R. Tyson, *Tensile properties of fibre-reinforced metals: copper/tungsten and copper/molybdenum*. Journal of the Mechanics and Physics of Solids, 1965. **13**: p. 329-350.
 116. Johnson, R.W. and M.D. Landon. *Simulation and optimization of a slurry based fiberglass preform manufacturing process*. in *Advanced Composites Conference*. 1995. Dearborn, Michigan, USA: ESD, The Engineering Society.
 117. Soh, S.K. *Slurry process for preform manufacture*. in *Advanced Composites Conference*. 1994. Dearborn, Michigan, USA: ESD, The engineering society.
 118. Tang, L., L. Li, X. Yi, Z. Pan., *Aqueous powder slurry manufacture of*

- continuous fiber reinforced polyethylene composite*. Polymer Composites, 1997. **18**(2): p. 223-231.
119. Wallace, P.L., *Radlite: powder to parts manufacture of automotive components*. Composites Manufacturing, 1990. **1**(2): p. 109-111.
120. Brandenburg, K.L., *Critical process variables in the white water system that affect glass fiber dispersion*. Tappi Journal, 1993. **76**(7): p. 145-148.
121. Kallmes, O. and H. Corte, I. *The Statistical Geometry of an Ideal Two Dimensional Fiber Network*. Tappi, 1960. **43**(9): p. 737-752.
122. Seth, R.S., *The effect of fiber length and coarseness on the tensile strength of wet webs: a statistical geometry explanation*. Tappi Journal, 1995. **78**(3): p. 99-102.
123. Scheidegger, A.E., *The physics of flow through porous media*. 3rd ed. Vol. 1. 1974, Toronto: University of Toronto Press. 353.
124. Thomas, K. and D. Dawson, *Effects Of Materials and Processing On DMC Injection Mouldings*. Plastics and Rubber Processing and Applications, 1985. **5**(4): p. 293-300.
125. Timoshenko, S., D.H. Young, and W. Weaver, *Transverse vibrations of prismatic beams*, in *Vibration problems in engineering*. 1974, John Wiley & Sons Inc. p. 415-431.

Appendix A

University of Nottingham system for measuring fibre lengths.

This appendix describes the Aphelion macro used as part of the Nottingham system to analyse the digital images of recovered fibres described in Chapter 4. The calibration of the system and some tests comparing the Nottingham system with the Leeds University IRC system [99] are also presented.

A.1 Macro Listing.

The following Aphelion script macro was used to analyse images of recovered glass fibres.

```
Sub main
  dim members() as single          ' Edgels members of fibre edges
  dim moments() as double         ' Edgel min, MAX, etc
  dim indexes() as long           ' Index of an edgel
  dim vector() as single          ' General result vector
  Dim f As String

  fibres = AphImgNew("Fibres")
  smoothed = AphImgNew("Smoothed")
  ridges = AphImgNew("Ridges")

  distance = 20                    ' Distance parameter for edgel neighbours
  MinChainLength = 1
  MaxLinkLength = 20.0             ' Chain formation parameters - 1,20.0, 0.25
  MaxAngle = 0.25

  'Open fibreimage
  f$ = OpenFilename$("Open Picture", "Image Files:*.TIF")
  If f$ < > "" Then
    AphImgRead fibres, f$
  End If

  'Make EDGES
  AphImgLowPass3x3 fibres, smoothed
  AphImgRidgeValleyEdges smoothed, ridges, 1, 20.000000
  AphImgFree smoothed
  AphImgCopy ridges, AphImgNew("Image 0")
  AphImgFrame AphImg("Image 0")
  AphImgNot AphImg("Image 0"), AphImg("Image 0")
  AphImgMask ridges, AphImg("Image 0"), ridges
```

```

AphImgFree AphImg("Image 0")

'Make the first EDGES object set
AphImgEdgesToEdgels ridges, AphObjNew("EDGES"), "EDGEL"
AphEdgelNeighbors AphObj("EDGES"), "EDGEL", "NEIGHBORS", distance
AphObjRemoveOverlay ridges, AphObj("EDGES"), "EDGEL"

'Count to find how many edgels we have, to control While loop
AphObjGetIndexList AphObj("EDGES"), indexes
lo = LBound(indexes)
hi = UBound(indexes)
AphImgDisableRoi ridges, 0      'Must disable whole image ROI
fibre = 0

While hi > 200                  'Altered to take into account dust particles
  'Find the strongest remaining edgel
  AphObjMoments AphObj("EDGES"), "MAGNITUDE", moments
  'Make a single chain (fibre) to include the brightest edgel
  fibre = fibre + 1
  f$ = "FIBRE" + Cstr(fibre)
  AphEdgelNeighbors AphObj("EDGES"), "EDGEL", "NEIGHBORS", distance
  AphEdgelsToChains AphObj("EDGES"), AphObjNew(f$), 1, moments(1),
  MinChainLength, MaxLinkLength, MaxAngle
  'AphObjFree AphObj("EDGES")
  AphObjSpatialAttributeToRegions AphObj(f$), "CHAIN", "REGION", 1.0000, 0
  colour = fibre mod 6
  AphObjDraw fibres, AphObj(f$), "REGION", colour, 0, 0
  'Add the new fibre to the FIBRE object set ...
  if fibre =1 then AphObjCopy AphObj(f$), AphObjNew("FIBRES") else
  AphObjAppend AphObj("FIBRES"), AphObj(f$), AphObj("FIBRES"), 0

  'Make a ROI from the new fibre
  AphImgDisableRoi ridges, 0      'Must disable whole image ROI
  AphImgAddRoi ridges, AphObjGetAttributeR( AphObj(f$), 1, "REGION")
  'AphImgDisableRoi ridges, 0      'Must disable whole image ROI
  'And zero fill the region as an ROI on the edge image
  AphImgFill ridges, 0.000000
  AphImgResetRoi ridges
  'Make new EDGES from masked image
  AphImgEdgesToEdgels ridges, AphObjNew("EDGES"), "EDGEL"
  AphObjRemoveOverlay ridges, AphObj("EDGES"), "EDGEL"
  'Count the objects in it
  AphObjGetIndexList AphObj("EDGES"), indexes
  lo = LBound(indexes)
  hi = UBound(indexes)
  'Delete the temporary fibre object
  AphObjFree AphObj(f$)
Wend

```

```

'Get rid of non-fibres ...
AphRegionShape AphObj("FIBRES"), "REGION"
'If compactness > 0.5, object is not a fibre ...
AphObjFilter AphObj("FIBRES"), AphObj("FIBRES"), "COMPACTNESS", 0.000000,
0.500000

'm$ = "high bound " + Cstr(hi) + "Max i " + Cstr(edgel)
'MsgBox m$, 0, "Aphelion Macro Message"
End Sub

```

The Aphelion macro reads in the digital image and performs a standard smoothing operation on it to remove any high frequency noise. The macro then detects ridges corresponding to the centre lines of the fibres and converts these to a number of edge elements which have an intensity and a direction. Once the set of all edge elements has been constructed the macro finds the strongest element in the image and attempts to join it to neighbours of similar magnitude and direction. Operator controlled parameters in the image analysis macro limit how close in orientation and separation two elements have to be to be considered as belonging to the same fibre. Once the appropriate elements have been joined they are bounded by a region of interest (ROI) and removed from the image. The subroutine in the macro then starts again with the strongest remaining edge element. This procedure builds up a set of ROIs, one for each fibre, and the positions and lengths of the ROIs are stored in an object set. The lengths of the ROIs correspond to the lengths of the fibres.

A.2 Limitations of the Nottingham system.

The macro can deal with crossing fibres and fibres with slight curvature but there is a chance of splicing fibres together that cross at shallow angles. In a crowded field, as each fibre is identified and removed this can leave gaps in remaining fibres and this increases the chances of a fibre being split into two or more pieces. Any fibre coming within 5 pixels of the edge of the image is removed as there is a chance that it extends beyond the image boundaries and so its true length cannot be measured. The relatively small size of the field of view means that long fibres are more likely to be ignored and so the measured distribution is biased away from long fibres.

Glass fibres illuminated in the dish act as sources of light due to internal reflections and

refractions. This means that light coming from the fibre edges is diffuse and this gives the impression that the fibres have a greater diameter than they actually have. Images of 13 μm diameter fibres are approximately 3 pixels wide which corresponds to a diameter of 150 μm using the magnification of the image capture system calculated in Section A.3. Dust and filler contamination can also be seen in the fibre images and is removed by screening out any items which have an aspect ratio (length divided by diameter) of less than 2. This puts a lower limit to the length of fibre that can be measured by this system at approximately 300 μm .

A.3 Calibration of the Nottingham system.

In order to assess the accuracy of the fibre length measurements made by the Aphelion software a sample of fibres of known length was prepared and analysed.

Method.

A sample of 6 mm chopped strand (CS) 254 supplied by Croxton and Garry Ltd. was heated in a furnace at 450°C for 30 minutes to remove the sizing. These fibres were then manually dispersed in a petri dish and an image was obtained and analysed using the Nottingham fibre length measurement system. The dimensions of the fibre image were measured with a steel rule for calibration. Conversion of fibre lengths expressed as pixels to true lengths was carried out using this factor. The conversion factor was measured as 0.048 mm pixel⁻¹.

Results.

Results of the analysis of the lengths of the 6 mm fibres are given in Table A.1 where average length, L_n , is defined as:

$$L_n = \frac{\sum N_i L_i}{\sum N_i} \quad \text{A.1}$$

where N_i is the number of fibres of length L_i and weight average fibre length L_w is defined as:

$$L_w = \frac{\sum N_i L_i^2}{\sum N_i L_i} \quad \text{A.2}$$

A histogram of the length distribution is shown in Figure A.1.

Figure A.1.

Length distribution of 6 mm chopped strand fibres measured by the Nottingham system.

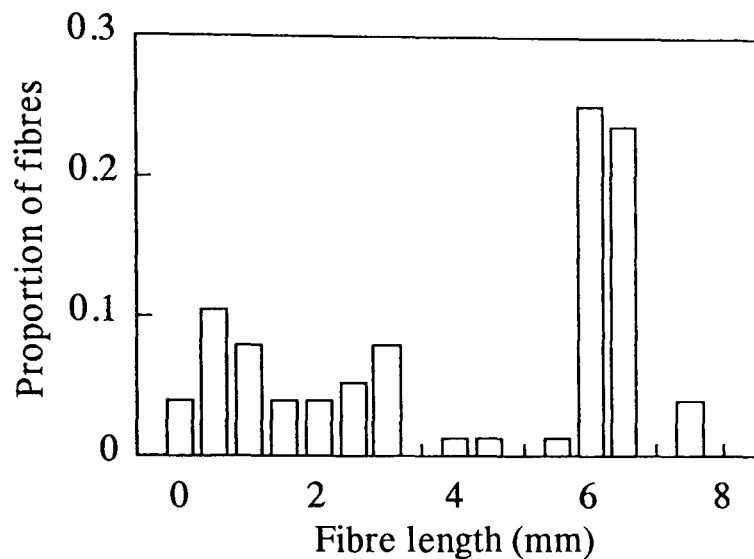


Table A.1 Calculated lengths for 6 mm fibre sample.

L_n (mm)	L_w (mm)	modal length (mm)
4.41	5.82	6.25

Discussion.

Fibres described as 6 mm in length were measured with a travelling microscope and were found to have lengths of 6.3 mm (nominally ¼ inch). The Nottingham system correctly measured this as the modal, or most common, length (Table A.1). The two average lengths (number average and weight average) were less than 6.3 mm and this was due to some shorter fibre lengths being measured. Fibres in the sample which were broken during the dispersion process, fibres which were incorrectly measured because the image analysis macro did not identify them properly and some contaminating particles were responsible for the shorter measured lengths. In addition, some slightly longer lengths were also measured which was due to the image analysis macro splicing parts of two separate fibres together.

A.4 Comparison of Leeds and Nottingham systems.

Samples of fibres recovered from the SMC feed at 450°C and the FW pipe feed at the

same temperature were analysed with both the Nottingham system and the Leeds system. The Leeds system was used to provide a benchmark against which to test the Nottingham system.

University of Leeds IRC system.

A sample prepared for analysis by the Nottingham system is placed on a microcomputer controlled translating stage under a high powered microscope. The translating stage is moved accurately in such a way that a high magnification composite image of the entire dish is built up from individual sub-images spliced together by dedicated image analysis software. This software then tracks fibres across adjacent sub-images and calculates their lengths. Crossing fibres are measured successfully but fibres with significant curvature have to be removed from the dish and analysed separately. No significantly curved fibres were present in any of the recovered fibre samples investigated during the work presented in this thesis. Fibres with lengths less than 20 μm can be measured using the Leeds system, due to the high magnification available from the microscope.

Results.

The lengths measured with both systems are compared in Table A.2 to indicate the variability between each measurement system. A 400 μm lower length (limit of the Nottingham system) was used in the calculations of the average fibre lengths for the two sets of measurements so that a meaningful comparison could be drawn. The fibre length distributions measured by the Leeds system are shown in Figures A.3 and A.5 and those measured with the Nottingham system in Figures A.2 and A.4.

Table A.2 Comparison of fibre length measurements made by Nottingham and Leeds systems for fibres recovered from SMC and FW pipe feed at 450°C.

Dish	Leeds			Nottingham		
	L_n (mm)	L_w (mm)	N	L_n (mm)	L_w (mm)	N
SMC	3.22	4.72	1082	3.31	5.55	355
FW pipe	2.00	4.18	3688	2.07	3.47	500

Figure A.2. Length distribution of recovered fibres.

Fibre source: SMC.

Fluidised bed temperature: 450°C.

Collection system: cyclone.

Measurement system: Nottingham.

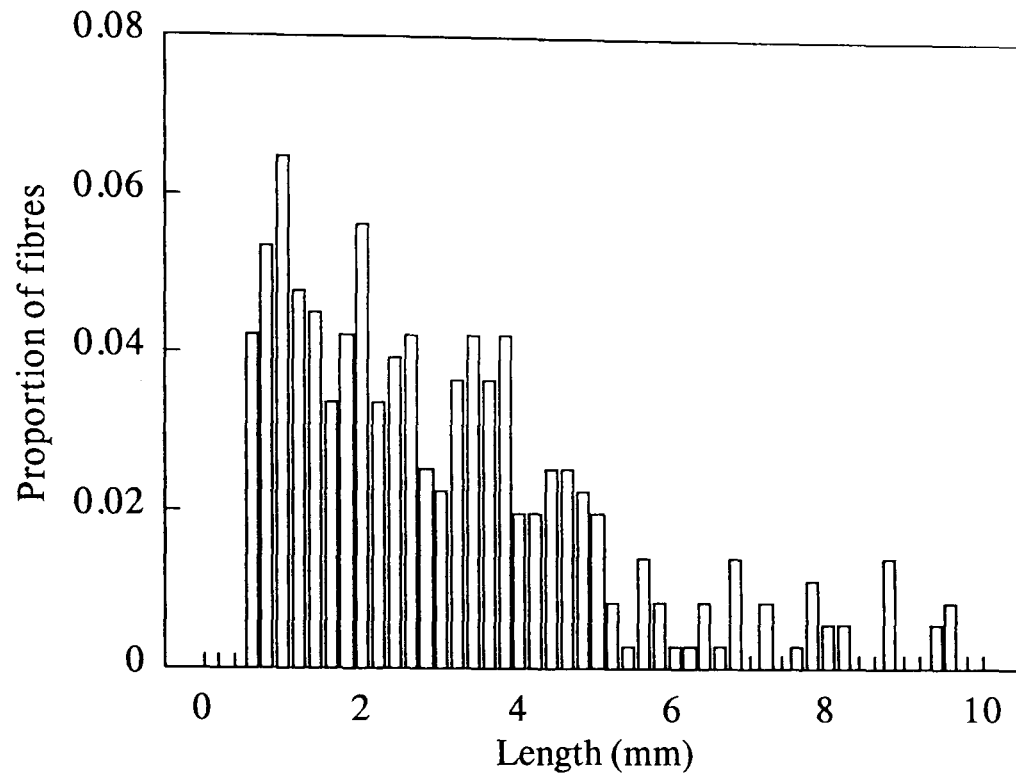


Figure A.3. Length distribution of recovered fibres.

Fibre source: SMC.

Fluidised bed temperature: 450°C.

Collection system: cyclone.

Measurement system: Leeds.

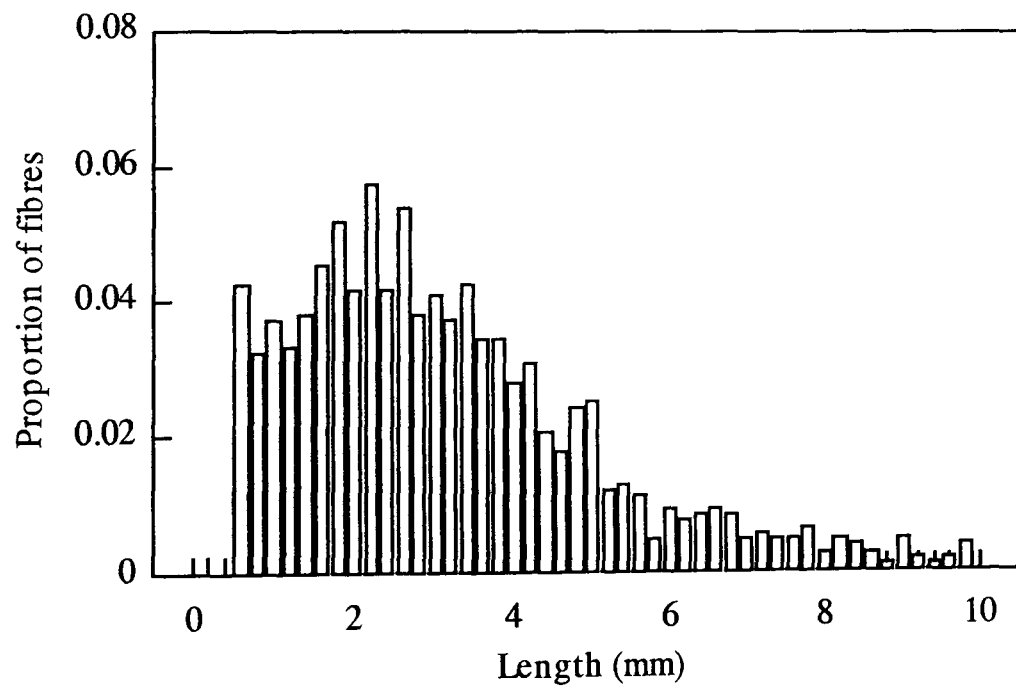


Figure A.4. Length distribution of recovered fibres.

Fibre source: FW pipe.

Fluidised bed temperature: 450°C.

Collection system: rotating screen.

Measurement system: Nottingham.

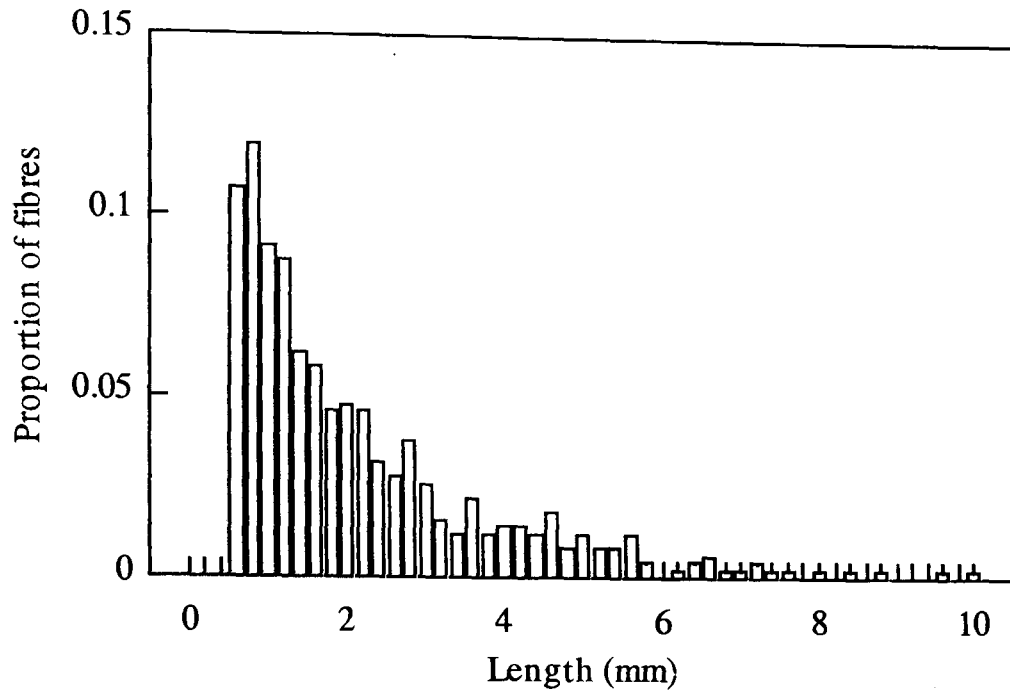


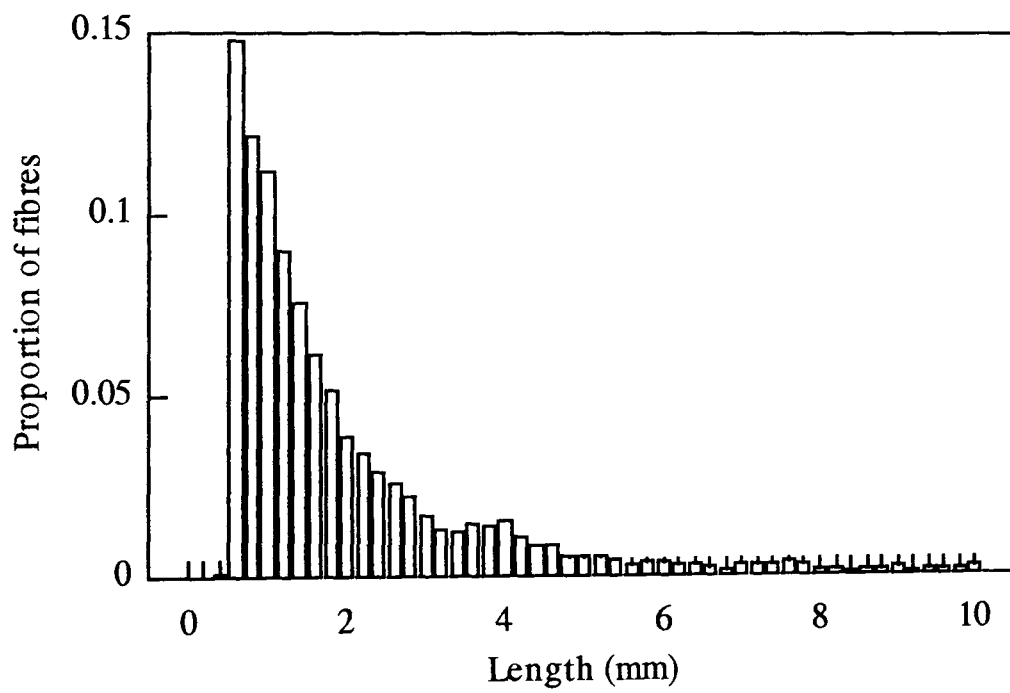
Figure A.5. Length distribution of recovered fibres.

Fibre source: FW pipe.

Fluidised bed temperature: 450°C.

Collection system: rotating screen.

Measurement system: Leeds.



Discussion.

It can be seen from Table A.2 that there is good agreement between number average length measurements made with the two systems. There is a greater difference between weight average lengths measured by the two systems. This is possibly because the Nottingham system is more likely to splice unconnected fibres and split whole fibres. The Nottingham system counted fewer fibres in each dish because the field of view was smaller than that of the Leeds system. The shapes of the fibre length distributions are similar for the two systems (Figures A.2, A.3, A.4 and A.5).

Analysis of the lengths of fibres recovered from the SMC measured by the University of Leeds system which can measure fibres with lengths as short as 20 μm shows that as many as 15% of the fibres have lengths less than 400 μm but these fibres only constitute approximately 1.5% of the mass of the sample. It is likely that contamination could account for some of the short fibres measured. The Nottingham system cannot measure these fibres without increasing the magnification of the system, which would decrease the number of long fibres measured.

Correctly identified fibres are accurately measured by the Aphelion image analysis software. Unfortunately, not all fibres are correctly identified. Control parameters within the analysis macro can be adjusted to improve the fibre detection reliability. The macro was optimized for the images captured by the Nottingham system. These results suggest that the Nottingham system for measuring fibre length distributions gives accurate information about the shapes of the fibre length distributions and useful information about the lengths of the recovered fibres.

Appendix B

Calculation of composite void contents and fibre volume fractions.

B.1 Composite density.

The density of a glass fibre reinforced composite can be measured at room temperature using a 50 cm³ glass density bottle. It can be shown that:

$$\rho_c = \frac{m_2 - m_1}{v_b \left[1 - \frac{m_3 - m_2}{m_4 - m_1} \right]} \quad \text{B.1}$$

where,

ρ_c is the sample density (g cm⁻³)

m_1 is the dry mass of the bottle plus lid (g),

m_2 is the mass of the bottle plus lid plus sample (g),

m_3 is the mass of the bottle plus lid plus sample plus water (g),

m_4 is the mass of the bottle plus lid plus water only (g),

v_b is the volume of the density bottle (50 cm³).

B.2 Composite fibre volume fraction.

The fibre volume fraction of a glass reinforced composite can be measured by burning off the polymer at 625°C for 30 minutes. It can be shown that:

$$V_f = \frac{\rho_c}{\rho_f} \left[\frac{M_3 - M_1}{M_2 - M_1} \right] \quad \text{B.2}$$

where,

V_f is the volume fraction of fibre within the composite,

M_1 is the mass of the specimen tray (g),

M_2 is the mass of the specimen tray plus the sample (g),

M_3 is the mass of the specimen tray plus the clean fibre after heat treatment (g),

ρ_f is the fibre density (g cm⁻³).

B.3 Composite void volume fraction.

Similarly, the void content of the composite can be calculated from the measurements made to calculate the fibre volume fraction. It can be shown that:

$$V_v = 1 - \frac{\rho_c}{M_2 - M_1} \left[\frac{M_3 - M_1}{\rho_f} + \frac{M_3 - M_2}{\rho_m} \right] \quad \text{B.3}$$

where,

V_v is the void content of the composite material,

ρ_m is the density of the matrix (g cm^{-3})

and the other variables have been previously defined.

Appendix C

Publications.

Kennerley, J.R., Fenwick, N.J., Pickering, S.J. and Rudd, C.D.,

The tensile properties of a thermoset composite using heat cleaned glass fibres as reinforcement. Advanced Composites Letters, 1995. 4(4): p. 105-109.

Kennerley, J.R., Fenwick, N.J., Pickering, S.J. and Rudd, C.D.,

Tensile properties of thermoset composites incorporating heat cleaned glass fibres. in *4th International Conference on Automated Composites - ICAC 95.* 1995. Nottingham, England: The Institute of Materials.

Kennerley, J.R., Fenwick, N.J., Pickering, S.J. and Rudd, C.D.,

The properties of glass fibres recycled from the thermal processing of scrap thermoset composites. in *Annual Technical Conference.* 1996. Indianapolis: Soc of Plastics Engineers, Brookfield, CT, USA.

Kennerley, J.R., Fenwick, N.J., Pickering, S.J. and Rudd, C.D.,

The properties of glass fibers recycled from the thermal processing of scrap thermoset composites. Journal of Vinyl and Additive Technology, 1997. 3(1): p. 58-63.

Kennerley, J.R. Kelly, R.M., Fenwick, N.J., Pickering, S.J. and Rudd, C.D.,

The reuse of glass fibres recovered from scrap composites using a fluidised bed process. in *Fifth International Conference on Automated Composites.* 1997. Glasgow, UK: The Institute of Materials.

Kennerley, J.R., Fenwick, N. J., Pickering, S.J. and Rudd, C.D.,

Recycling glass fibres from scrap composites using a fluidised bed process. in *ESD Advanced Composites Conference.* 1997. Detroit, MI: ESD The Engineering Society.

Appendix D

Cantilever method for measuring the Young's modulus of a fibre.

A cantilever method was used to compare the Young's modulus of the recovered fibres with that of virgin fibres. This appendix describes the theory on which the method is based and details of the test method.

D.1 Cantilever theory.

Timoshenko [125] gives a derivation of the equation governing the transverse vibrational motion of a prismatic beam. The relationship between the resonant frequency of vibration (f_i) and beam length (L), density (ρ), moment of inertia of the cross section with respect to the neutral axis of the beam (I), cross sectional area (A) and Young's modulus (E) is:

$$f_i = a \frac{k_i^2}{2\pi} \quad \text{D.1}$$

where the values of k_i for a beam with one end fixed and the other end free are given by the roots of Equation D.2 (see Table D.1):

$$\cos(k_i L) \cosh(k_i L) = -1 \quad \text{D.2}$$

and where:

$$a = \left(\frac{EI}{\rho A}\right)^{\frac{1}{2}}. \quad \text{D.3}$$

For a beam of constant circular cross section, radius r :

$$I = \frac{\pi r^4}{4} \quad \text{D.4}$$

and

$$A = \pi r^2. \quad \text{D.5}$$

Substituting Equations D.3, D.4 and D.5 into Equation D.1 and rearranging gives the

following expression for the Young's modulus of the beam:

$$E = \frac{(2\pi f_i)^2 4 L^4 \rho}{(k_i L)^4 r^2} \quad \text{D.6}$$

Table D.1 First four roots of Equation D.2 governing the vibration of a cantilever beam. The subscripts 1,2,3 and 4 refer to the modes of oscillation.

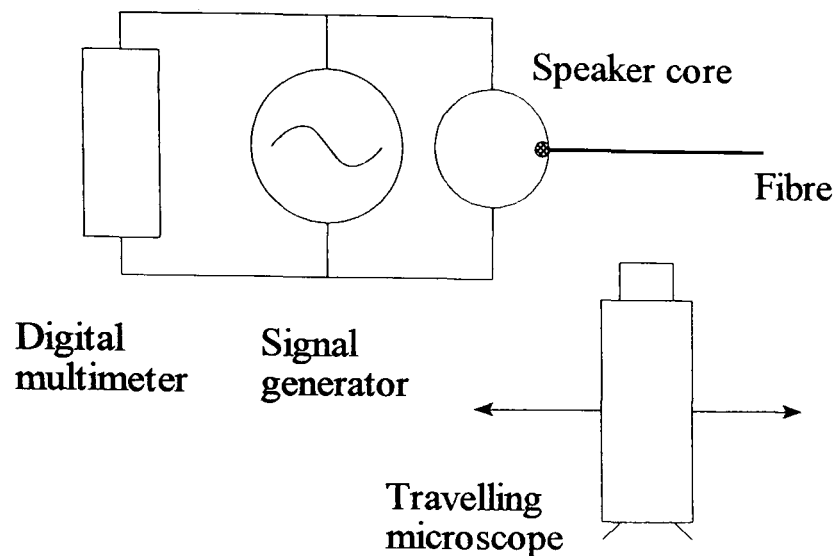
k_1L	1.875
k_2L	4.694
k_3L	7.855
k_4L	10.996

Assumptions made in the derivation of Equation D.6 are that the fibres have constant circular cross section; that there is no contamination on the surface of the fibres; that no damping of the fibres occurs during vibration. An additional assumption made is that the density of the fibres does not change during the recovery process.

Method.

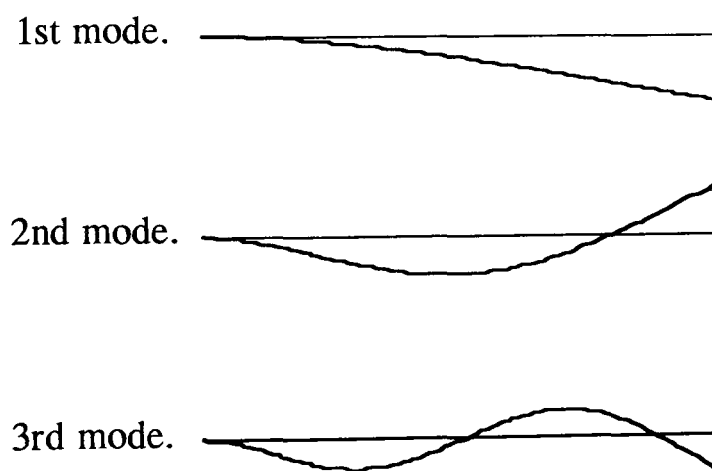
Five 15 mm long fibres were taken from the sample. One fibre was then bonded to the core of a 8 Ω , 0.25 W, 55 mm diameter loudspeaker with cyanoacrylate adhesive such that at least 10 mm, and more commonly 15 mm, of the fibre protruded horizontally over the edge of the speaker core (Figure D.1). Part of the speaker diaphragm was cut away to allow free vertical movement of the fibre.

Figure D.1 Experimental apparatus for determining the Young's modulus of a fibre by a vibrational method.



The loudspeaker was driven by a sinusoidal signal (variable up to 0.4 V in magnitude) from a Farnell LFM4 sine square oscillator (10 Hz - 1 MHz) signal generator. This caused the fibre to vibrate at the speaker frequency and this frequency was determined by connecting an Iso-Tech IDM 203 digital multi-meter across the speaker terminals.

Figure D.2 Resonant mode shapes of vibrating fibre.



The free end of the fibre was observed through a Precision Tool and Measurement Company Limited vernier travelling microscope, model number 13, as the frequency of

the driving signal was gradually increased from approximately 10 Hz. A resonant frequency of the fibre was indicated by a sudden increase in amplitude at the free end of the fibre and the appearance of well defined nodes along the length of the fibre. The number of nodes was counted to determine which resonant mode was being observed (Figure D.2). The frequency of the forcing signal at resonance was recorded and then the signal frequency was increased to find the next resonant mode. When the last visible mode had been observed and the resonant frequency recorded the forcing frequency was reduced and the resonant frequencies recorded as the signal frequency was returned to its starting value. This scan up and down the frequency spectrum was repeated and the resonant frequencies recorded again.

The first resonant mode could not be precisely identified as it coincided with a resonant mode of vibration of the speaker mounting and so modes two to six were used to calculate the Young's modulus of the fibres under test.

Fibre length was measured with the same travelling microscope used to view the vibrations of the fibre under test. Fibre diameter was measured, prior to mounting on the speaker core, using the method used for single fibre strength testing described in Section 4.3.2 and density was assumed to be constant and was taken from literature as 2560 kg/m³ for E-glass [60] and 1770 kg/m³ for Toray T300B carbon fibres (taken from the material data sheet).

Appendix E

Veil as a surfacing agent.

Veil containing recovered glass fibres was used to form the surface of a composite plate. The corrosion resistance and surface quality of the plates were then assessed.

E.1 Veil as corrosion inhibitor.

Method.

Samples of two veil formulations of nominal areal density 70 gm^{-2} and nominal acrylic binder content of 20% by weight were made. The first sample contained only 18 mm WCS fibres and the second contained only fibres recovered from FW pipe at 450°C using the rotating screen recovery system.

One layer of veil was impregnated with a Cray Valley general purpose isophthalic polyester laminating resin to give a resin:glass weight ratio of 20:1. This was then backed by two layers of 450 gm^{-2} chopped strand mat with a resin:glass ratio of 2.5:1. The resultant laminates were exposed to 20% sulphuric acid solutions for one month at temperatures of 40°C and 65°C .

Results.

A visual inspection of the exposed face of the test plates was carried out. For both veil samples, fibres close to the surface had been exposed by the treatment at 65°C but no blisters were visible on any of the samples. The recovered fibre veil appeared to have performed no differently to the virgin fibre veil at either treatment temperature.

Discussion.

Since most of the corrosion protection is provided by the resin held at the surface of the test plate by the veil material it is not surprising that little difference in the performance of the two veil formulations should be seen. However, since the surface layer is the most critical part of a structure such as a chemical tank it is unlikely that anyone would want to take the risk of replacing virgin fibre veil by recovered fibre veil for only a small cost

saving. However, reclaimed fibre veil could be used to provide protection from the weather to GRP mouldings where, in this case, failure would not be critical.

E.2 Veil as a composite surface enhancer.

Composite materials can have rough surface finishes due to reinforcing fibre bundles protruding through the resin to become visible on the material surface. One way around this is to use a gel coat backed by a glass veil on the composite surface to mask the reinforcing fibres.

Method.

Laminates were produced, in a carefully controlled way at Cray Valley Ltd., with a gel coat backed by samples of veil material described in section E.1. The surface roughness of these samples was measured using a Mitutoyo Surftest and compared to a sample with the gel coat but without a veil layer.

Results.

The results of the surface roughness measurements are given in Table E.1.

Table E.1 Surface roughness measurements on experimental plates.

	no veil present	virgin fibre veil	reclaimed fibre veil
Ra (microns)	0.28 (0.06)	0.09 (0.02)	0.12 (0.05)

Figures in brackets are standard deviations.

Discussion.

Surface roughness measurements indicate that the recovered fibre veil improves the surface of the laminate. No blemishes due to fibre clumps or partially burnt resin were visible through the gel coat.

Appendix F

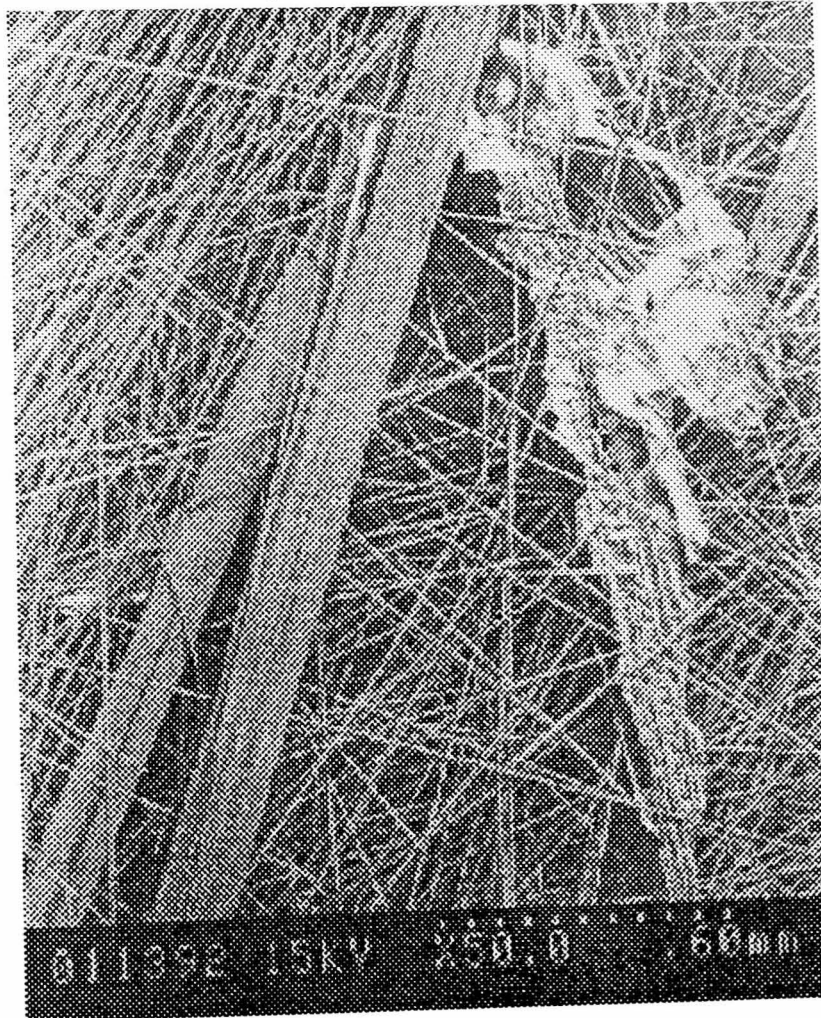
SEM and EDS analysis of recovered carbon fibres.

Samples of carbon fibres recovered from the filament wound carbon propshaft (Table 4.1) at a processing temperature of 450°C were analysed at GKN Technology Ltd. Scanning electron microscopy (SEM) and energy dispersive X-ray spectral (EDS) analysis techniques were used. The results were compared to those for virgin carbon fibres.

F.1 SEM micrographs of recovered carbon fibres.

Figure F.1

SEM of carbon fibres recovered at 450°C. Matrix material is clearly visible.



Scanning electron micrographs (Figure F.1) reveal that there is some particulate matter on the surface of the recovered carbon fibres and that discrete bundles or tows have

survived the milling and thermal processing stages of the recycling process. Detailed examination reveals that the surface residues are either particulate matter or partially combusted matrix material. Processing at a higher bed temperature would improve the removal of the matrix material. Since the feed material was an unfilled material, it is likely that the particulate matter on the fibre surfaces is residue from previous processing of filled, glass reinforced thermoset composites. Processing CFRP in a dedicated fluidised bed would reduce the level of this sort of contamination.

F.2 EDS traces of recovered carbon fibre surfaces.

EDS examination of the carbon fibres recovered from the filament wound carbon propshaft at 450°C confirms the conclusions drawn from the SEM analysis. Elements such as aluminium, silicon, sulphur and calcium are present in significant amounts on the recovered fibres (Figure F.3) but not pristine carbon fibres (Figure F.2). These elements are found in typical glass reinforced thermoset composite fillers such as calcium carbonate and aluminium trihydroxide and in the fluidised bed sand.

Figure F.2

Energy dispersive X-ray spectrum for pristine Akzo carbon fibre tow.

The carbon peak is off the scale.

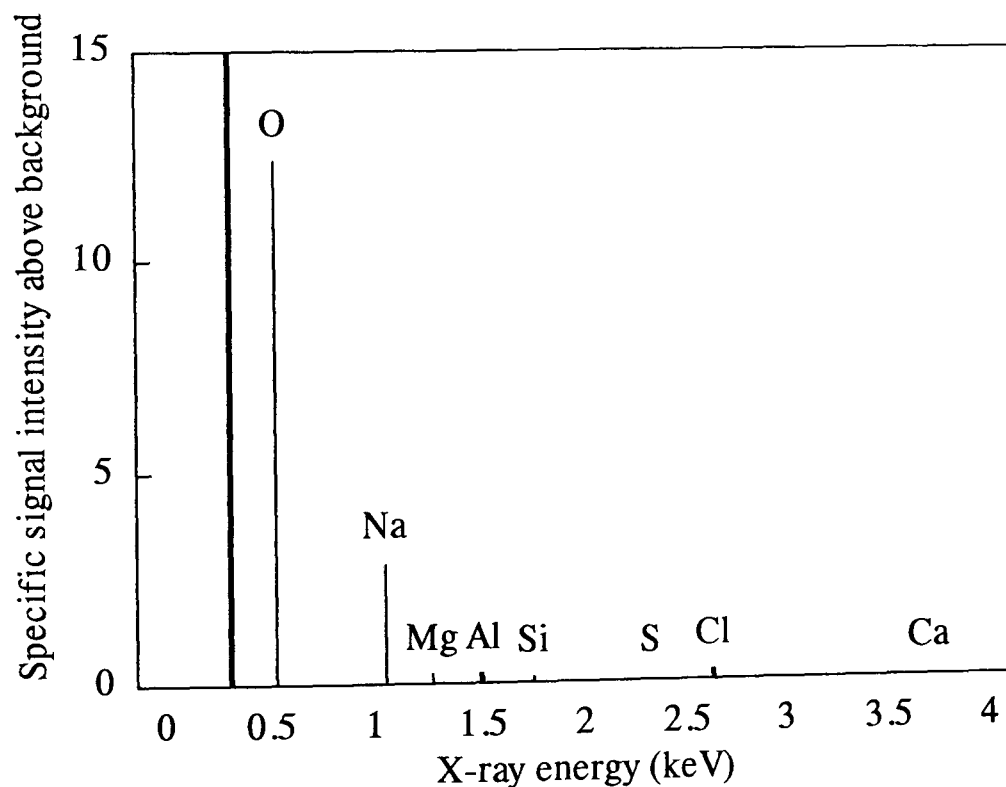


Figure F.3

Energy dispersive X-ray spectrum for carbon fibres recovered from filament wound propshaft at 450°C. The carbon peak is off the scale.

